THE PHYSICAL REVIEW

VOLUME 47 Second Series NUMBER 6

MARCH 15, 1935

Published for the

AMERICAN PHYSICAL SOCIETY

by the

AMERICAN INSTITUTE OF PHYSICS

Incorporated

LANCASTER, PA., AND NEW YORK, N. Y.

...ICAN PHYSICAL SOCIETY

OFFICERS OF THE SOCIETY

...D, *President*
...s Hopkins University
..., Maryland

...ERMANN, *Secretary*
...bia University
...k, New York

...TATE, *Editor*
...ity of Minnesota
...polis, Minnesota

F. K. RICHTMYER, *Vice President*
Cornell University
Ithaca, New York

G. B. PEGRAM, *Treasurer*
Columbia University
New York, New York

L. B. LOEB, *Local Secretary for the Pacific Coast*
University of California
Berkeley, California

THE PHYSICAL REVIEW

BOARD OF EDITORS

...T. TATE, *Editor* J. W. BUCHTA, *Assistant Editor*

Associate Editors

...BARROW — A. ELLETT — W. V. HOUSTON
...BRIARD — L. A. TURNER — R. S. MULLIKEN
...RIARE — G. E. UHLENBECK — I. I. RABI

...PHYSICAL REVIEW, which was established ... is a journal of experimental and ... physics. It is published for the American Physical Society by the American Institute of Physics Incorporated. There are two volumes annually with twelve issues in each volume.

...publication should be submitted to ... University of Minnesota, Minneapolis, ...

...correspondence concerning papers in the ..., should be addressed to the Editorial ...an Institute of Physics, 11 East 38th ..., New York.

...n United States and Possessions and ... Foreign, $16.50. Subscriptions and orders ... should be addressed to Prince and ..., Lancaster, Pennsylvania, or to the Amer... of Physics, 11 East 38th Street, New York.

...s not accepted for the *Physical Review* but ... to the *Review of Scientific Instruments ... News and Views*, a companion publication of ..., and a medium through which the field of physics can be reached most effectively. Rates and other information will be furnished on request to the Editorial Secretary.

Changes of address and complaints of failure to receive the *Physical Review*, in the case of members of the American Physical Society, should be addressed to the Treasurer; in the case of other subscribers, to the Editorial Secretary. New copies can be sent free in response to complaints of non-delivery only if notice of non-delivery is received within three months of date of issue.

The Physical Review is published semi-monthly at Prince and Lemon Streets, Lancaster, Pennsylvania.

Entered at the Post Office at Lancaster, Pennsylvania, as second class matter.

Acceptance for mailing at special rate of postage provided for in section 1103, Act of October 3, 1917, authorized September 4, 1926.

THE
PHYSICAL REVIEW
A Journal of Experimental and Theoretical Physics
VOL. 47, NO. 6 MARCH 15, 1935 SECOND SERIES

The Variation with Altitude of the Production of Bursts of Cosmic-Ray Ionization*†

C. G. MONTGOMERY AND D. D. MONTGOMERY, *Bartol Research Foundation of the Franklin Institute*

(Received January 29, 1935)

The rate of occurrence of bursts of ionization from 140 pounds of lead shot was measured in a fifty liter, Dowmetal ionization chamber, filled with nitrogen at 14.5 atmospheres pressure, at four elevations between sea level and the summit of Pike's Peak (4300 meters). The ionization chamber was so designed as to minimize the random fluctuations of the cosmic-ray ionization. The increase in the rate of occurrence with elevation was found to be very large, and increasingly greater at higher elevations. The rates of occurrence of all sizes of bursts greater than 1.5×10^6 ions in the chamber increased with elevation in the same manner. The results are discussed in the light of W. F. G. Swann's theory.

THE occurrence of large bursts of ionization in a closed vessel, first noticed by G. Hoffmann[1] in 1927, has since been the object of many investigations. Of vital importance to the understanding of this phenomenon is the question of the nature of the radiation which produces it. The most direct attack upon this question would appear to involve a study of the variation of the rate of occurrence of these bursts with altitude. As part of the general program of investigation at the Bartol Research Foundation concerning burst production, observations have been made at four elevations—at Pike's Peak (4300 m), at Glen Cove (3500 m), at Colorado Springs (1860 m) and at Swarthmore (61 m), the same apparatus being used in all cases.

The bursts of ionization were observed in a fifty liter, spherical chamber cast of Dowmetal. The chamber was made gas tight by means of a close-fitting internal shell of aluminum and was filled with commercial nitrogen to a pressure of 14.5 atmospheres. The electrodes were a series of concentric, spherical shells spaced at an average distance of five centimeters. The change of potential of the electrodes when a burst occurred was measured by a vacuum tube electrometer. Fig. 1 shows the circuit diagram of the apparatus. The galvanometer used had a sensitivity of approximately fifty megohms and a period of three seconds. The voltage sensitivity of the whole apparatus was about 1700 mm/volt, and the charge sensitivity 5×10^5 ions/mm. During the observations the sensitivity was determined at frequent intervals by the application of a known voltage to the control grid of the vacuum tube by means of the dry cell and potentiometer unit in the control box (resistances R_2 and R_3 in Fig. 1.

The observations at Pike's Peak and at Glen Cove were taken visually; those at Colorado Springs and at Swarthmore by photographic registration. The galvanometer spot was allowed to fall upon a horizontal slit placed in front of a moving strip of photographic paper. Fig. 2 shows a section of such a record, taken at

* This work was supported by a grant from the American Philosophical Society.

† A preliminary report was made at the Pittsburgh Meeting of the American Physical Society, December 28–29, 1934.

[1] G. Hoffmann, International Conference on Physics, London, October, 1934.

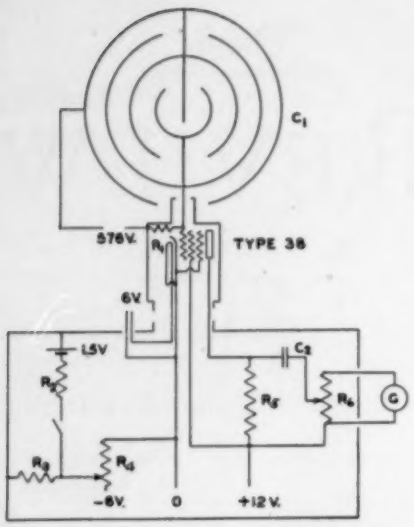

FIG. 1. Circuit diagram of the vacuum tube electrometer.

$R_1 = 4\times10^{10}$ ohms
$R_2 = 100$ "
$R_3 = 1$ "
$R_4 = 400$ "
$R_5 = 10^9$ ohms
$R_6 = 18{,}000$ "
$C_1 = 1.23\times10^{-10}$ farad
$C_2 = 8\times10^{-4}$ "

Swarthmore. The upper trace on the paper was taken with no lead above the chamber, and a burst of ionization is indicated by a downward deflection. The lower trace was taken with 140 pounds of lead above the chamber. Here the galvanometer leads have been reversed, and a burst is indicated by an upward deflection. The lead, in the form of shot, was contained in seven heavy canvas bags which were tied onto the top of the sphere. The thickness was not uniform, but its average may be estimated to be equivalent to four centimeters of solid lead. Only bursts of ionization greater than 1.5×10^6 ions were measured.

The smallest size of burst which can be measured with reasonable certainty in an ionization chamber depends upon the magnitude of the statistical fluctuations in the ionization of the cosmic rays passing through the chamber. Let t be the time interval during which a burst of ionization is observed, i.e., the time of collection of the ions. Let r represent the standard deviation of the ionization during unit time. Then the standard deviation in the ionization occurring in the time t is $rt^{\frac{1}{2}}$. The rate of occurrence of a fluctuation of size S ions or greater is given by

$$[1/t(2\pi)^{\frac{1}{2}}]\int_y^\infty e^{-y^2/2}dy \quad \text{where} \quad y=S/rt^{\frac{1}{2}}.$$

The value of r, if it cannot be conveniently measured, may be estimated in the following way. If the cosmic radiation consisted of single, unrelated rays passing through the chamber at random, at the rate of N per second, then r would be $IN^{\frac{1}{2}}$, where I is the average ionization produced by one ray. Since it is known that groups of two and more related rays occur frequently, this value for r must be multiplied by a corrective factor. This factor may be estimated from the cloud-chamber observations of C. D. Anderson[2] to be about 1.5 at sea level. It is greater than this at higher elevations. Any other fluctuations present, such as those caused by alpha-particles, must, of course, be taken into account also. It is to be noted that the rate of occurrence of large fluctuations may be much reduced by reducing the value of t.

In the chamber employed for these observations the collecting time was reduced to a minimum value by reducing the spacing of the electrodes (to 5 cm), by applying a relatively high potential (574 volts) and by using only as high a pressure (14.5 atmos.) as was necessary to eliminate the fluctuations of the alpha-particle ionization. By these means, the value of t was reduced to 0.5 second. If one chooses for the value of N, 2.5×10^{-2} per cm^2 per second;[3] for the mean path of a ray through the sphere, two-thirds of the diameter; for the specific ionization, 60 ions per centimeter;[4] a saturation of 72 percent as estimated from the data of I. S. Bowen;[5] and a pressure of 14.5 atmospheres; the standard deviation in the ionization in the interval of 0.5 second at sea level is 1.3×10^5 ions.[6] It is more difficult to estimate the size of the fluctuations at Pike's Peak. However, the ratio of the fluctuations in a chamber at Pasadena to those at an elevation of 14,700 feet on the magnetic equator has been reported by Evans and Neher.[2] Because of the presence of the magnetically deflected rays at Pike's Peak, the standard deviation in the ionization there will be

[2] C. D. Anderson, Phys. Rev. **44**, 406 (1933). See also R. Evans and V. Neher, Phys. Rev. **45**, 144 (1934).
[3] J. C. Street and R. H. Woodward, Phys. Rev. **46**, 1029 (1934).
[4] W. F. G. Swann, Phys. Rev. **44**, 961 (1933).
[5] I. S. Bowen, Phys. Rev. **41**, 29 (1932).
[6] This also involves the assumption that every ionizing ray has sufficient penetrating power to travel across the chamber through the electrodes.

TABLE I.

Size in ions	Rate of occurrence (per hour). Swarthmore	Pike's Peak
5×10^5	0.4	260
10^6	<0.004	1.1
1.5×10^6	<0.004	<0.004

somewhat larger than that computed from this ratio. Table I gives the rates of occurrence of fluctuations larger than a given size at Swarthmore and at Pike's Peak. It is to be noticed that the fluctuations are well below the chosen lower limit of size of bursts measured, namely, 1.5×10^6 ions.

OBSERVATIONS AND RESULTS

At each of the four stations where observations were taken, an effort was made to have as little material as possible over the apparatus. At Swarthmore, the observations were taken in a building with a thin wooden roof, on the roof of the Bartol Research Foundation Laboratory. In Colorado Springs, the apparatus was placed under a large skylight on the top floor of Palmer Hall at Colorado College. At Glen Cove, the apparatus was located on the first floor of a

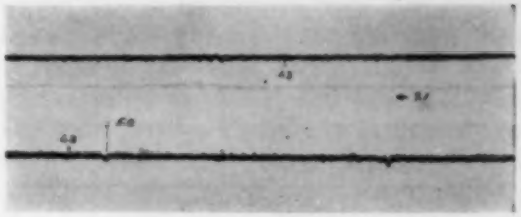

FIG. 2. Sample of photographic record. Lower trace with lead, upper trace without lead. Sizes of bursts in millions of ions.

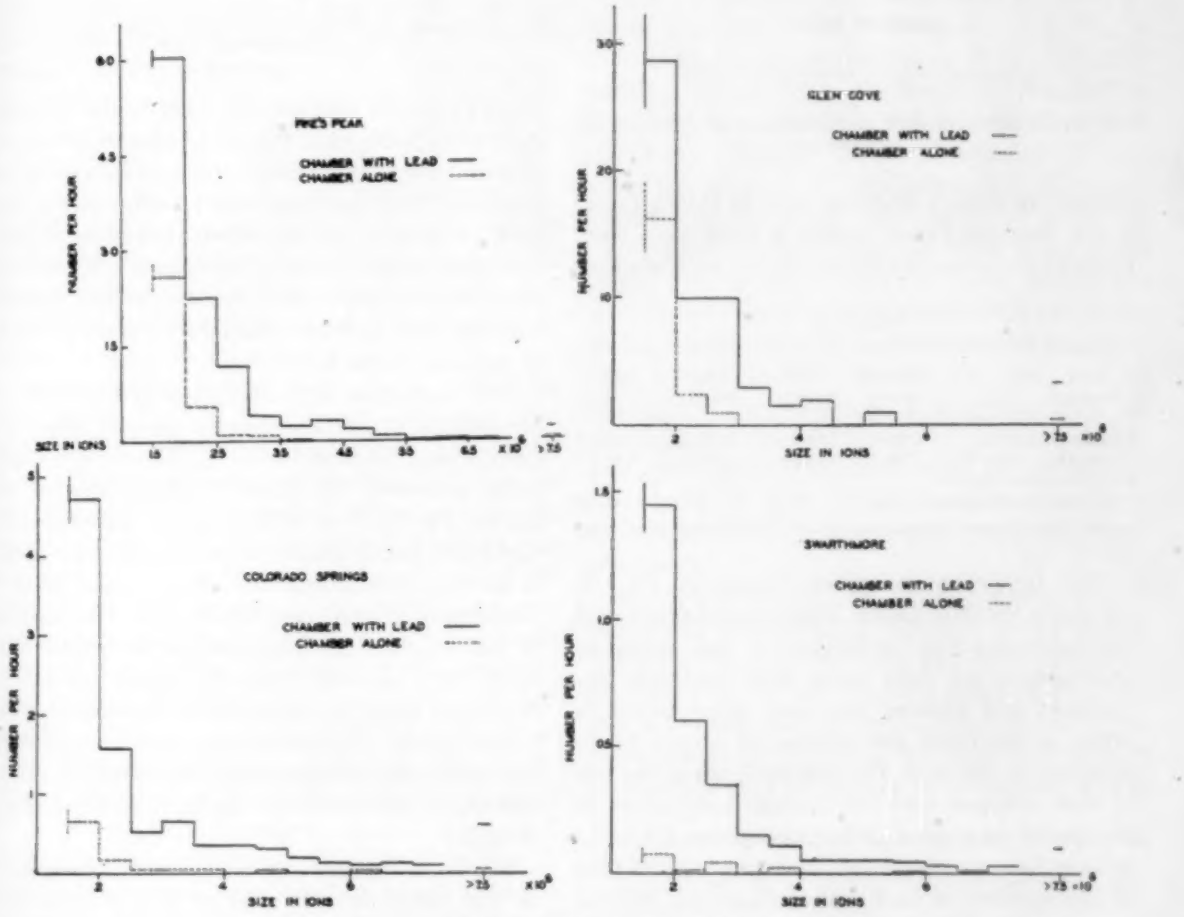

FIG. 3. Frequency distributions of bursts at the four elevations.

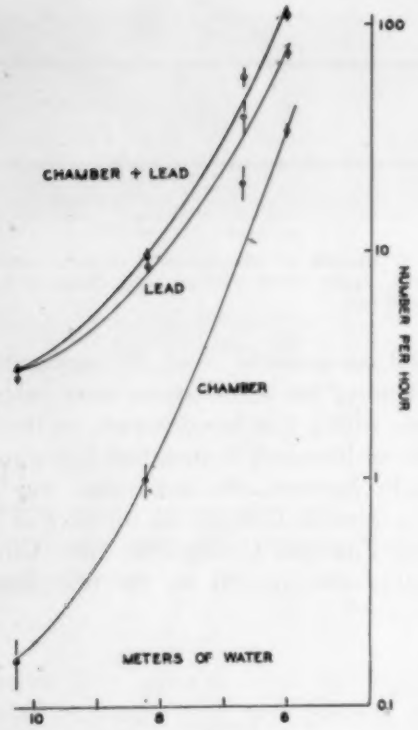

FIG. 4. Variation of rate of occurrence of bursts with altitude.

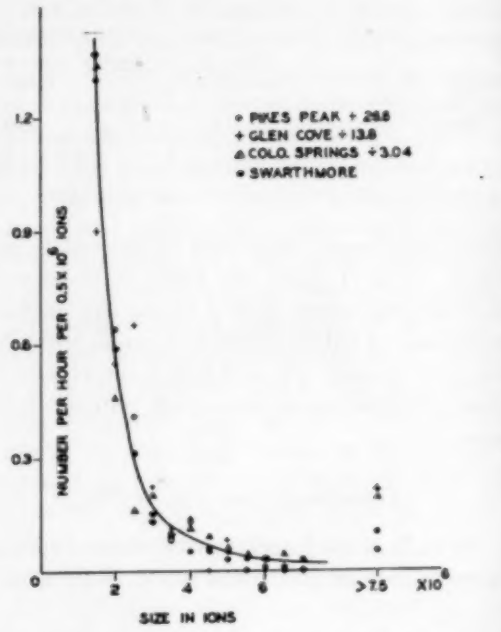

FIG. 5. Frequency distribution of bursts from lead reduced to a common total rate.

wooden, two story building, and at Pike's Peak, in the Summit House under a sheet iron roof. Table II gives the elevation data for each station.

TABLE II.

Station	Swarth-more	Colo. Springs	Glen Cove	Pike's Peak
Elevation (m)	61	1860	3500	4300
Barometer (mm Hg)	756	607	494	445
Depth below top of atmos. (m of water)	10.27	8.25	6.73	6.04

The frequency polygons shown in Fig. 3, represent the data taken. The difference between the corresponding ordinates of the polygons representing the data taken with lead over the chamber and without the lead, respectively, is taken to represent the number of bursts which originate in the lead. The vertical lines at the left of each polygon give the standard deviation in the rate of occurrence of bursts between 1.5 and 2 million ions as computed from the square root of the number of such bursts observed. All the bursts greater than 7.5 million ions have been classed together and are indicated to the extreme right of each diagram. Bursts greater than twenty million ions would throw the galvanometer off scale, and their size could not be determined, but their occurrence was recorded. It is to be noticed that, although at sea level the bursts without lead present form only a small fraction of the number with the lead, at Pike's Peak they represent about 31 percent of the total.

The variation with elevation of the rate of occurrence of all the bursts greater than 1.5 million ions is given in Fig. 4. The vertical lines again represent the standard deviations of the points. The increase with elevation is surprisingly rapid and much greater than the increase either in the total intensity of the cosmic radiation or in the softest known component of it. The number of bursts with no lead present increases even faster with altitude than the bursts from lead. However, since an appreciable fraction of these bursts might originate in the surrounding walls and roofs, this increase might be ascribed almost entirely to differences in the surroundings of the chamber.

For lead, the increase with elevation seems to be the same for all sizes of bursts measured. This may be seen from Fig. 5. Here the fre-

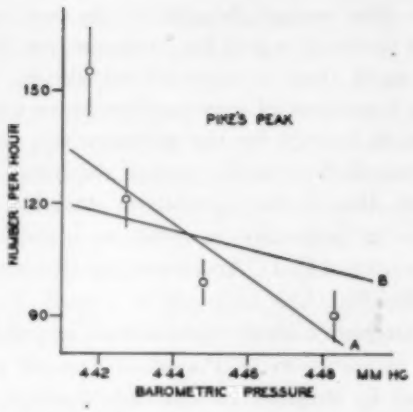

FIG. 6. Barometer effect for bursts with lead on chamber at Pike's Peak. Line *A* is least squares fit, line *B* estimated from variation of rate of occurrence of bursts with elevation.

quencies for each size of burst at each elevation are divided by the ratio between the total rate of occurrence of bursts at that elevation and that at Swarthmore, and plotted against the size of burst, the rate for each interval of size being plotted at the beginning of that interval. The smooth curve is drawn through the mean of the Swarthmore, Colorado Springs and Pike's Peak points. Within the accuracy of their determination, all the points are seen to fit this smooth curve. Using the assumptions already stated under the discussion of fluctuations, the number of rays which would be needed to produce the ionizations observed in these experiments is about 51 rays per million ions.

There is an independent check upon the variation in the rate of occurrence of bursts with elevation reported here. The Pike's Peak data were taken during such a time that the change in the number of bursts with barometric pressure could be estimated. Fig. 6 shows the results of this analysis. The line *A* is the best fit, by least squares, to the four points representing rates of occurrence of bursts greater than 1.5 million ions which occurred when lead was over the chamber. The slope of this line is -7.1 bursts per hour per mm Hg, with a probable error of 2.3 in the same units. The slope of the curve for lead chamber in Fig. 4, at the elevation of Pike's Peak, also gives a value for this "barometer effect," *viz.*, -2.7 bursts per hour per mm Hg. Line *B* in Fig. 6 represents this estimate. The agreement between the two values is fair considering the paucity of relevant data, the difference being just less than twice the probable error of the first value. From the slope of the same curve (Fig. 4) at the Swarthmore point, a barometer effect of about 0.5 percent per mm Hg may be estimated. This cannot be reconciled with the value 5 percent per mm Hg reported by Steinke, Gastell and Nie,[7] but is not in disagreement with experiments of the authors which showed the effect to be less than 1 percent at Swarthmore.

DISCUSSION

The number of bursts which occur at any elevation should be proportional to the number of burst-producing rays I multiplied by the probability p that such a ray will produce a burst. The observed variation with elevation may be the result of a change in either or both of these quantities.

If we assume that p is independent of the depth below the top of the atmosphere, then Fig. 4 represents the absorption curve of the radiation which produces bursts. We see that this radiation is not exponentially absorbed, but the absorption coefficient, defined as the derivative of the logarithm of the function at the point considered, varies from about 1.8 per meter of water at Pike's Peak to about 0.4 per meter of water at sea level. The actual values of these absorption coefficients will vary considerably with the shape of the curve that is drawn through the points in Fig. 4 and hence express only the general character of the variation. This "component" of the cosmic radiation, however, cannot produce any appreciable ionization, since all the ionization, even at very high elevations, has been accounted for by previously reported components.[8]

On the other hand, the variation with elevation may all be caused by a variation in the probability p. This point of view has been developed by W. F. G. Swann.[9] Swann assumes that the number of nonionizing corpuscular cosmic rays is independent of elevation, but that their energy decreases by the production of showers of rays as

[7] E. G. Steinke, A. Gastell and H. Nie, Naturwiss. **51**, 898 (1933).
[8] I. S. Bowen, R. A. Millikan and V. Neher, Phys. Rev. **44**, 250 (1933).
[9] W. F. G. Swann, Phys. Rev. **46**, 828 (1934).

they pass through the atmosphere. It is the ionization produced by these showers that is measured in an ionization chamber. The ionization increases with altitude because the number of showers increases with the energy of the primary rays. The number of showers produced in air may be expressed as $N_{air}=f(E)$, where E is the energy of the primary rays. The number of showers which will be produced in lead will be represented by $N_{Pb}=F(E)$, which may be quite a different function of E from $f(E)$. It is N_{Pb} which is measured in these experiments. The data are fairly well represented by the assumption that $F(E)\propto f^2(E)$ This agreement is illustrated in Table III.

TABLE III.

Station	Swarthmore	Colo. Springs	Glen Cove	Pike's Peak
Relative ionization[9]	1	1.80	3.51	4.78
Relative ionization squared	1	3.24	12.3	22.8
Relative No. of bursts	1	3.04	13.8	26.6

Thus the observations seem to have a simple interpretation from the point of view of Swann's theory. The actual details of the mechanism of burst production may be, of course, much more complicated than is represented above. There may be a number of intermediate steps between the loss of energy by the primary ray and the formation of the ionizing rays of the burst as, for example, the shower producing photons which seem to be necessary in order to interpret the photographs of C. D. Anderson and Blackett and Occhialini.[10]

The authors wish to express their appreciation of the cooperation of President Davies and of Dr. Paul E. Boucher of Colorado College. They are also indebted to Mr. Benjamin Stewart and to Mr. Orrie Stewart of Colorado Springs, who provided space for the apparatus on Pike's Peak and at Glen Cove. To Dr. W. F. G. Swann, without whose helpful advice and continued support of the project these experiments could not have been carried out, the authors are deeply grateful.

[10] See, for example, P. M. S. Blackett, International Conference on Physics, London, October, 1934.

MARCH 15, 1935 PHYSICAL REVIEW VOLUME 47

On the North-South Asymmetry of Cosmic Radiation

G. LEMAITRE, M. S. VALLARTA AND L. BOUCKAERT, *University of Louvain and Massachusetts Institute of Technology*

(Received January 28, 1935)

The development of the theory of the latitude and azimuthal effects is reviewed and the significance of Johnson's experiments on the north-south asymmetry is brought out. Störmer's critical remarks are commented on with reference to Lemaitre and Vallarta's paper and to recent papers by Lemaitre and by Bouckaert.

THE theory of the latitude and azimuthal effects of cosmic radiation[1] developed by Lemaitre and Vallarta has now been sufficiently carried through by Bouckaert to lead to precise results for sufficiently high energies ($x_0>0.414$ in the energy units defined by Eq. (12) in (I)) and low geomagnetic latitudes. For these energies the allowed cone (*not* a circular cone) has been calculated by Bouckaert except for angles close to the horizon. His results (III) are reproduced in Fig. 1, drawn for positive particles, which gives the orthogonal projection on the horizontal plane of the trace of the cone on the unit sphere, for energies $x_0=0.45$, 0.5, 0.6 and 0.7 and geomagnetic latitudes $\lambda=0°$, 10° and 20°. For positive particles, which alone will be considered for the moment, the cone at the equator opens from the west and is symmetrical with respect to the east-west vertical plane. As the latitude increases the eastern boundary of the cone of a given energy moves towards the east and markedly shifts towards the south. As a conse-

[1] G. Lemaitre and M. S. Vallarta, Phys. Rev. **43**, 87 (1933); G. Lemaitre, Ann. de la Soc. Sci. de Bruxelles **A54**, 162 (1934); L. Bouckaert, Ann. de la Soc. Sci. de Bruxelles **A54**, 174 (1934). These papers will be referred to here as (I), (II), (III), respectively.

quence one must expect in the northern hemisphere, as already pointed out in our first paper (I), a greater intensity from the south than from the north. Using Bouckaert's formulae we may calculate the cone for $\lambda = 29°$ and sufficiently high energies, but since at this latitude the convergence of his series expansions becomes doubtful we must await the results of further investigations now under way at this Institute with the help of Bush's differential analyzer. There is scarcely any doubt that the north-south asymmetry at $\lambda = 29°$ will be much more marked than that at $\lambda = 20°$; however it will be necessary to include a discussion of some energy values below the critical value $x_0 = 0.414$. As Lemaitre (II) has shown, in this energy range the principal part of the cone is surrounded by an infinite number of narrow bands extending clear over to Störmer's limiting circular cone defined by his equation for $\sin\theta$ with $\gamma_1 = 1$ (I, Eq. 14). As we have shown, by Liouville's theorem[2] the intensity in the principal part of the cone and in each band is exactly the same, but because of the narrowness and number of these bands, for practical purposes the intensity tapers off from the principal cone to the forbidden region. In the language of optics the principal part of the cone is a fully lighted region surrounded by penumbra. The contribution of the penumbra is probably negligible; estimates of it may be given later.

The theoretical prediction of the southern effect has been recently confirmed experimentally by Johnson[3] who as a result of measurements made in Mexico at 29° geomagnetic latitude, with the method of triple coincidences, has reported a greater intensity from the south than from the north. The ratio of the difference to the mean value of the south and north intensities

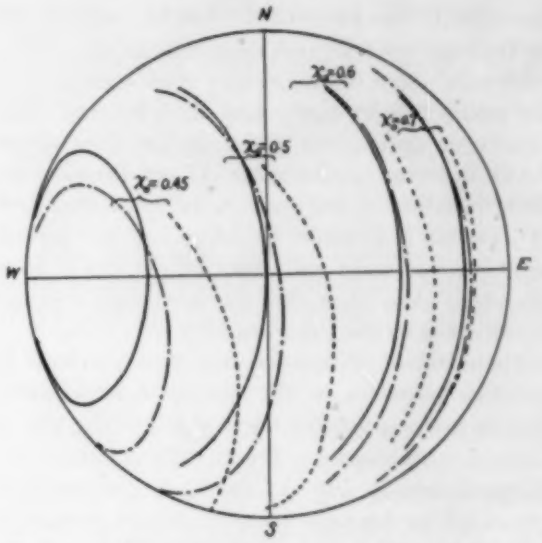

FIG. 1. Orthogonal projection on horizontal plane at observation point of traces of cones on unit sphere. Positive particles, northern hemisphere. ——— $\lambda = 0°$; — — — $\lambda = 10°$; - - - - - $\lambda = 20°$.

plotted as a function of zenith angle (reference 3, Fig. 1) has a minimum at about 40°. This minimum seems to be due to a secondary effect due to absorption in the atmosphere and will be discussed in connection with similar anomalies observed in the east-west effect in a forthcoming paper by Vallarta and Schremp.

To account for his experimental findings Johnson invokes a "shadow effect" due to certain trajectories being stopped by other regions of the earth. Such a shadow effect has been considered by Lemaitre (II) and has led to a distinction between two kinds of orbits which can be on the surface of the cone at a given point, for a particular energy and a given value of γ_1. The orbits of the first kind are orbits which do not vary continuously with respect to infinitely small changes of the derivatives at the given point. Lemaitre has proved from general theorems on the existence and continuity of integrals of differential equations that orbits of the first kind must be periodic or asymptotic to periodic orbits. The orbits of the second kind do not involve discontinuity with respect to the final conditions. They fix the limit of orbits which would intersect the earth before reaching the given point. These orbits of the second kind must be tangent to the earth before reaching the given point so that for small changes of the

[2] Paper (I). Liouville's theorem has been applied independently to the present problem by E. Fermi and B. Rossi, Rend. della R. Accad. Naz. dei Lincei **17**, 346 (1933). It has been discussed at length by W. F. G. Swann, Phys. Rev. **44**, 224 (1933). A simple proof that the intensity is the same in all allowed directions, independent of Liouville's theorem, has been given by W. F. G. Swann, by B. Rossi, Ricerca Scientifica **1**, 569 (1934) and by G. Lemaitre (II). This application of Liouville's theorem has been criticized by C. Störmer, Publ. Univ. Obs. Oslo No. 10 (1934) and Phys. Rev. **45**, 835 (1934). However, in the latter paper he seems to agree with W. F. G. Swann that our result is correct for an infinitely thin tube of orbits which, since this tube can be arbitrarily chosen, is all that is needed for our application of Liouville's theorem.

[3] T. H. Johnson, Phys. Rev. **47**, 91 (1935).

direction at that point either they are intercepted by the earth or they just escape its surface. They exist only when the trajectory after approaching the earth recedes again and then returns. This can occur only when x_0 is smaller than about 0.414. Both the approximate (I) and Bouckaert's determination of the cone make use only of orbits of the first kind, as orbits of the second kind do not exist for energies $x_0 \geq 0.45$. It is therefore clear that the southern effect is not mainly due to the "shadow effect."

Hitherto our discussion has been confined to positive particles in the northern hemisphere. For negative particles the cones are the mirror images, with respect to the meridian plane, of the cones drawn in Fig. 1, therefore the southern effect will be the same for positive as for negative particles, while the east-west effect will be reversed. Therefore the north-south asymmetry depends on the sum of the positive and negative intensities while the east-west asymmetry depends on their difference. This opens a possibility for determining the percentage of magnetically deflectable particles of either sign. In this connection one must not overlook that primary positives and negatives, if the latter exist, would presumably be of different kinds and would have different laws of absorption. In the southern hemisphere the cones drawn in Fig. 1 would be their mirror images with respect to the east-west vertical plane, and the southern excess observed in the northern hemisphere should be replaced by a northern excess, irrespective of the particles' sign. Experiments are already planned for the purpose of testing this conclusion.

We take advantage of this opportunity to make a few remarks on our first paper (I). This paper was avowedly not written as a complete and final treatment of the problem, but rather was intended, first, as an outline of a general method of attack and, second, as a report of an approximate theory for the interpretation of experimental results. Papers (II) and (III) are further developments along the same line of attack which, although representing a real advance, must be continued still further. Although Störmer[4] prefers other methods of attack the statement of his problem is precisely the same as the statement of ours.

We first wish to note that the limiting value of γ_1 for which Störmer's periodic orbits disappear and which we had estimated in our first paper (I) to be 0.783 has been more accurately calculated by Lemaitre[5] who finds the value 0.78856.

As we have pointed out above, Störmer's limit for $\gamma_1 = 1$ is reached for energies $x_0 < 0.414$ by the region of penumbra. On the other hand, our limit $\gamma_1 = 0.78856$ is an absolute lower limit which is not reached for every value of x_0. Störmer[6] has studied the orbits reaching the pole and has shown that for $\gamma_1 < 0.9312$ all these orbits come from infinity. Therefore for infinitely small values of x_0 our upper limit is raised from 0.78856 to 0.9312 and takes intermediate values for values of γ_1 in this interval. Therefore our curves (I) for small energies are somewhat steeper than there drawn.

We also note the following errata in our first paper (I), most of which have been pointed out by Störmer in the *Physical Review*.[2]

p. 88, Section III, 4th line, read "west" instead of "east";

p. 89, Eq. (7) delete factor 1/2;

p. 89, Eq. (9) change sign before integral in numerator;

p. 89, Section IV, 24th and 28th lines, read "Eq. (10)" instead of "Eq. (9)";

p. 89, Eq. (18) p. 90, Table I and p. 90, 2nd line, read "$C/4\gamma_1^2$" instead of "C";

p. 90, Table I, 4th col., 1st line, read "1" instead of "0".

[4] Reference 2, and further Publ. Univ. Obs. Oslo No. 12, (1934); Astrophysica Norvegica **1**, 1 (1934).

[5] G. Lemaitre, Ann. de la Soc. Sci. de Bruxelles **A54**, 194 (1934).

[6] C. Störmer, Terr. Mag. and Atm. Elec. **37**, 375 (1932).

Frequency and Magnitude of Cosmic-Ray Bursts as a Function of Elevation

RALPH D. BENNETT, GORDON S. BROWN AND HENRY A. RAHMEL, *Massachusetts Institute of Technology*

(Received January 29, 1935)

Measurements of the magnitude and frequency of cosmic-ray bursts have been made at elevations of 185, 1620, 3240 and 4300 meters above sea level for periods of time ranging from 189 to 336 hours, using one of the new cosmic-ray intensity meters of the Carnegie Institution. Only bursts releasing more than 10^7 ion pairs are considered. The rather meager data which could be collected in these short times of observation indicate that: (1) Burst-frequency decreases with burst magnitude in a way which can be represented by a series of exponentials. (2) These large bursts contribute only a small fraction of the total ionization. (3) The magnitude of the largest burst observed increases rapidly with altitude, one observed at 4300 meters elevation exceeding 10^9 ion pairs or 3×10^{10} electron volts of energy released in the chamber.

INTRODUCTION

DURING the past summer the first of the new cosmic-ray intensity meters[1] being built at the University of Chicago under the direction of Professor A. H. Compton and under the sponsorship of the Carnegie Institution of Washington, was taken to Colorado for a field test at different altitudes. Observations were made on the University of Denver campus at 1620 meters elevation, at Echo Lake at 3240 meters elevation and at the summit of Mt. Evans at 4300 meters elevation.

The field test of the instrument showed it to be sound in principle and sufficiently rugged to perform perfectly under the most adverse conditions. During the course of the field tests records extending over some eight hundred hours were accumulated, and to these through the cooperation of Drs. E. O. Wollan and R. L. Doan of the University of Chicago, we have been able to add over 250 hours of observations made at Chicago, 185 meters elevation, giving us data at four levels. From these records we have made a study of bursts of ionization (Hoffmann Stösse), investigating their frequency, magnitude and other properties in relation to barometric pressure and mean intensity of ionization.

CRITERIA FOR RECOGNIZING BURSTS

Fig. 1 shows a section of record for the period 10:00 P.M., July 23, to 5:00 A.M., July 24, taken with the instrument operating at the summit of Mt. Evans, elevation 4300 meters. The transverse lines on the record represent intervals of one hour, and the longitudinal lines are millimeters deflection. The smooth white line is a record of barometric pressure, and the jagged black line indicates the position of the electrometer needle and hence the variation of cosmic-ray intensity above and below the mean value to which the compensation mechanism is set. At the end of each hour the electrometer is automatically reset to an arbitrary zero and every four hours its sensitivity is measured, although the sensitivity dots are not easily perceived in this reproduction. Several bursts of ionization are shown in the record of Fig. 1. The one at 10:30 P.M. corresponds to more than 765×10^6 ions and sent the indicator off scale when the sensitivity and zero were set at optimum values for average observing. Those of the cluster between 2:00 A.M. and 5:00 A.M. range in magnitude from 46×10^6 to 102×10^6 ions.

The first step in a study of the recorded bursts is to set up criteria for distinguishing between true bursts and statistical variations which may have the appearance of bursts. The traces of the bursts possess several general characteristics which help to distinguish them, such as direction of deflection of the indicator, initial and average steepness of the deflection, duration and magnitude of the deflection.

After selecting the bursts on this basis, an estimate was made (see Appendix) of the probable number of statistical variations which had been included because they were indistinguishable from bursts. To do this, the time necessary to collect the ions from a burst was calculated and the calculation checked by measurements from the record. Next, the average number of rays traversing the chamber during

[1] Compton, Wollan and Bennett, Rev. Sci. Inst. **5**, 415 (1934).

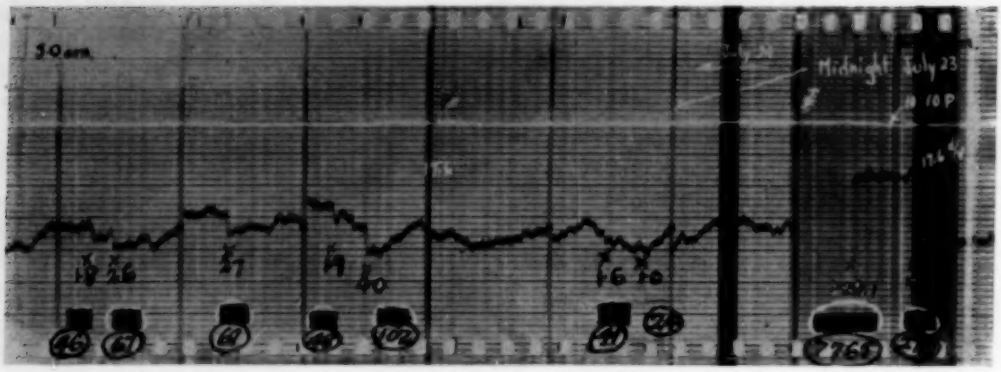

FIG. 1. Section of record for the period 10 P.M. July 23 to 5 A.M. July 24. Instrument operating at summit of Mt. Evans.

the time of collection of the ions was calculated from measurements of average ionization, assuming 135 ions per cm in air at atmospheric pressure (see Appendix). On the assumption that these rays come singly and are randomly distributed in time we have calculated the expected frequency of statistical fluctuations of magnitudes as large as the smallest of those we have included in our tabulations. In all cases the expected number of such fluctuations is negligibly small compared to the number of bursts observed.

However, a fraction of the rays will occur in groups as a result of their originating in bursts either of small numbers of tracks or so placed that only small numbers enter the chamber. Observations with cloud chambers indicate that the fraction of the rays occurring in groups is small near sea level. At other elevations the magnitude of this fraction is unknown. Hence it is not possible at present to calculate the effect of grouping on statistical fluctuations. This effect introduces some uncertainty into our values for numbers of bursts in the smaller magnitude groupings though it seems doubtful that this uncertainty is larger than that due to the small number of observations.

BURST-FREQUENCY AS A FUNCTION OF MAGNITUDE

In Fig. 2 we have grouped and plotted all the bursts observed at each of the four elevations. The minimum magnitude included at the three upper levels was 20×10^6 ions, and at the lowest level, 10×10^6 ions. The group magnitude chosen for the two upper levels was 20×10^6 ions, and for the two lower levels, 10×10^6 ions. Any other reasonable grouping leads to a similar result.

We next resorted to a smoothing process which enabled us to pass smooth curves through the block curves resulting from the grouping. This process is illustrated in detail in Fig. 3, with the data taken at the summit of Mt. Evans. The block curve I is integrated by addition to give the points of curve II indicated by the crosses.

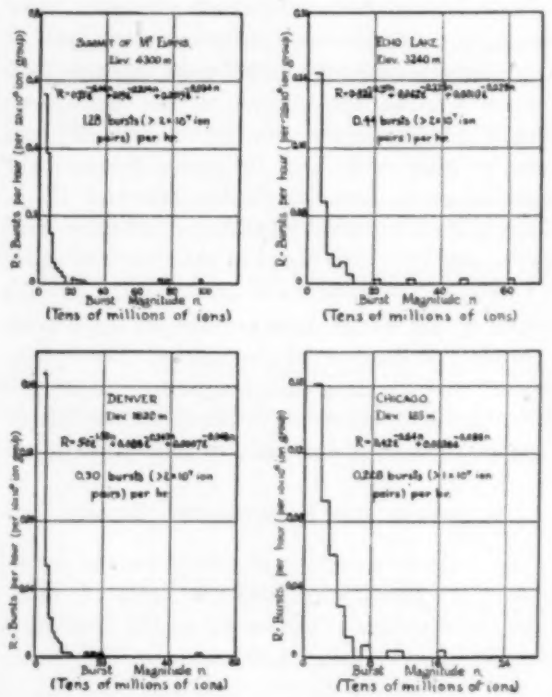
Summit of Mt Evans
Elev. 4300 m
1.28 bursts (> 2×10⁷ ion pairs) per hr
Echo Lake
Elev. 3240 m
0.44 bursts (> 2×10⁷ ion pairs) per hr
Denver
Elev. 1620 m
0.30 bursts (> 2×10⁷ ion pairs) per hr
Chicago
Elev. 185 m
0.228 bursts (> 1×10⁷ ion pairs) per hr
R= Bursts per hour (per 10⁷ ion pairs)
Burst Magnitude n
(Tens of millions of ions)

FIG. 2. Burst-frequency as a function of burst magnitude at four elevations.

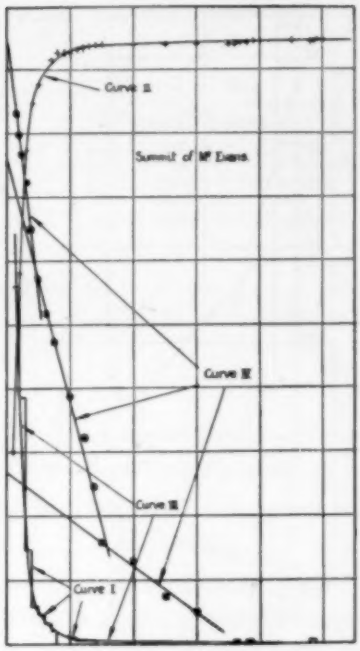

FIG. 3. Method of analysis of burst-frequency curves.

Curve II is then drawn through the crosses, and differentiated graphically to give curve III.

It was desired to obtain a mathematical expression for curve III. To do this we plotted the logarithms of the ordinates of curve III at the corresponding abscissae and obtained the points indicated as crossed circles. Three straight lines appeared to pass through these points very well, indicating that curve III might be reasonably well represented by three exponentials. We also found this to be the case at the two intermediate levels. At the lowest level the data, taken indoors, indicate only two exponentials.

From this plotting process we obtained the equations of the form

$$R = R_1 e^{-a_1 n} + R_2 e^{-a_2 n} + R_3 e^{-a_3 n} \qquad (1)$$

shown in Fig. 2 for smooth curves representing the block curves. The values of coefficients and exponents were obtained graphically by determining the coefficient and exponent of the lowest curve directly, subtracting the values obtained from this coefficient and exponent from those of curve III, replotting and similarly obtaining the slope and intercept of the next lowest curve, etc. The equations were checked by calculation of representative points, and as a whole by integration, the integral of R with respect to n leading to the total rate observed when bursts of all sizes between the smallest recorded in the block curve and infinity are included.

TABLE I. *Constants of Eq. (1) calculated from curves.*

Elevation	Coefficients R_1	R_2	R_3	Exponents a_1	a_2	a_3	Ratios of exponents a_1/a_2	a_2/a_3	a_1/a_3
4300 m	0.75	0.19	0.0015	0.46	0.204	0.034	2.25	6.0	13.5
3240 m	0.92	0.042	0.0010	0.75	0.223	0.029	3.35	7.7	25.8
1620 m	5.0	0.086	0.0007	1.5	0.343	0.048	4.37	7.1	31.2
185 m	—	0.42	0.0026	—	0.64	0.086	—	7.4	—

The coefficients and exponents obtained by the above process are given in Table I. These have been reduced in such a way that all apply to a common group magnitude of 10×10^6 ions.

On account of the relatively small number of data at our disposal it is difficult to say whether the trends indicated in the table are significant. The exponents a_1, a_2, a_3 are probably reliable to within approximately 20 percent, but we do not consider the coefficients R_1, R_2, R_3, good to within better than 100 percent. Obviously more extensive data are necessary before laws of variation of burst-frequency with burst-magnitude can be definitely established. The effect of the slate, steel and concrete roof over the apparatus at Chicago seems to have been to eliminate the group of smallest bursts.

In order to investigate the possibility that all cosmic-ray ionization phenomena might occur as a result of bursts, we have calculated the total rate of ionization contributed by bursts of all sizes from those corresponding to but one particle passing through the chamber up to bursts corresponding to an infinite number of particles, on the assumption that all burst phenomena can be represented by the three exponentials obtained above. The result is given in Table II.

The numbers of column 4 indicate that bursts in these classifications account for only an extremely small fraction of the total ionization. However, our data actually deal only with bursts of about 50 or more tracks at the lowest elevation, and about 100 or more tracks at the other elevations. It appears, therefore, that the frequency distribution of the very small bursts (showers) must be quite different. In connection with this point the data on showers given by Evans and Neher[2] were plotted in a manner

[2] Evans and Neher, Phys. Rev. **45**, 144 (1934).

TABLE II. *Calculations which show that bursts in these classifications contribute but a small fraction of the total ionization.*

ELEVATION	NO. OF IONS PER SEC. CONTRIBUTED BY BURSTS OF ALL MAGNITUDES	OBSERVED TOTAL NUMBER OF IONS PER SECOND	PERCENT OF TOTAL IONS CONTRIBUTED BY BURSTS
4300 m	0.0261×10^8	5.18×10^8	0.504
3240 m	0.0102×10^8	3.62×10^8	0.282
1620 m	0.0088×10^8	2.50×10^8	0.352
185 m	0.0036×10^8	1.55×10^8	0.245

similar to our burst data, as shown in Fig. 4. A mathematical expression representing this curve is $F=2.2e^{-2.16\tau}+0.063e^{-0.63\tau}$. In this case we have used the number of tracks τ as abscissae and the fraction of the total observed number of showers F as ordinate, the scale at the left applying to F and that at the right to $\log_{10} F$. There result again two exponentials, though these are not directly comparable with our derived exponentials because of the different scales used. The two sets of data can, however, be compared by calculating from our data the expected relative numbers of single-track, double-track, triple-track, etc., showers, using the data at the 185-meter elevation as being most nearly comparable to that obtained in cloud chambers. The ratios are given in Table III.

TABLE III.

RATIOS	CLOUD-CHAMBER DATA	EXTRAPOLATED LARGE BURST DATA
Double to single	0.113	0.99
Triple to single	0.015	0.97
Quadruple to single	0.008	0.96

The table indicates that the variation with magnitude for very small bursts (showers) of a few tracks must be very much different from that of the large bursts we have observed. These analyses seem to indicate that the relation between burst-frequency and burst magnitude can be represented by a series of many exponentials.

RELATIVE VALUES OF VARIOUS QUANTITIES

In Fig. 5 we have plotted a number of quantities as functions of barometric pressure. In order to see more easily the relative rates of

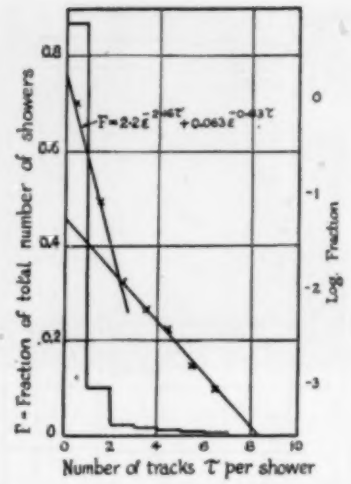

FIG. 4. Plot of data on showers given by Evans and Neher.[2]

increase of these quantities we have plotted the ratio of the magnitude at each elevation to the magnitude found at Denver. The values at Denver were taken as basic rather than those at Chicago, because at Chicago the instrument was operated under a roof, whereas at each of the other locations it was in a tent. The resulting curves indicate the following:

(1) The values of total ionization taken with the new instrument at the three upper levels plus a fourth taken especially for us outdoors at Chicago by Dr. R. L. Doan, give an absorption curve of the usual shape. The values found for ionization (per cm³ per second reduced[1] to air at 1 atmosphere) fall below those found for this latitude with the 1932 apparatus by about the amount to be expected with the increased shielding on the new machine.

(2) The total number of bursts increases at about the same rate as the total ionization up to an elevation of about 3240 meters, after which it rises much more rapidly.*

(3) The number of very large bursts, specifically bursts releasing more than 100×10^6 ion pairs within the chamber, increases much more rapidly with altitude than does the total ionization. Further, the rate of increase of this quantity also increases rapidly with elevation.

(4) The magnitude of the largest burst observed at each elevation increases at least as

* Considering only bursts greater than 20×10^6 ions.

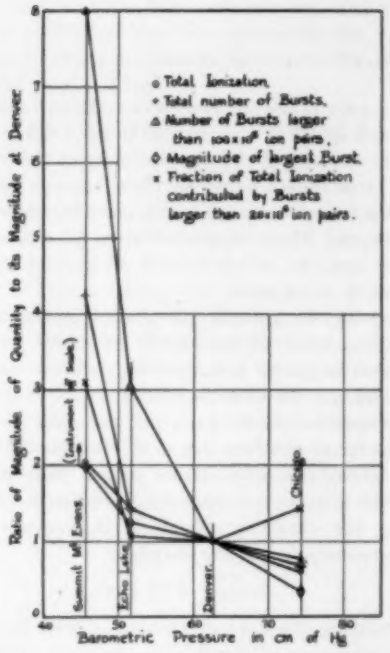
o Total Ionization.
+ Total number of Bursts.
Δ Number of Bursts larger than 100×10⁶ ion pairs.
◇ Magnitude of largest Burst.
x Fraction of Total Ionization contributed by Bursts larger than 20×10⁶ ion pairs.
Ratio of Magnitude of Quantity to its Magnitude at Denver
Summit (Instrument off scale)
Echo Lake
Denver
Chicago
Barometric Pressure in cm of Hg

FIG. 5. Plot of various quantities associated with cosmic-ray bursts as a function of barometric pressure.

fast as the total ionization. (At the summit the very large bursts threw the indicator off scale.)

(5) The fraction of the total ionization contributed by bursts greater than 20×10^6 ion pairs is not constant. This fraction is less at Denver than at Chicago, the higher value at Chicago perhaps being due to bursts originating in the roof over the instrument. This fraction increases very rapidly again above 3240 meters.

Three bursts at the 4300-meter level were of sufficient magnitude to exceed the range of the scale of the instrument at the sensitivity used. The records indicate that these bursts released 10^9 or more ion pairs. Using the value of 135 ion pairs per cm in air, some 5000 tracks would be required to produce so many ions. With 30 electron volts expended for each ion pair the energy becomes of the order of 3×10^{10} electron volts. Since the absorbing power of the argon in our chamber was equivalent to only about 2 mm of lead, whereas the shielding amounted to some 120 mm, it seems reasonable to expect that the total energy released approached 10^{12} electron volts, in agreement with the findings of others.

CONCLUSIONS

For the type of apparatus used and for bursts of magnitude greater than 20×10^6 ion pairs:

(1) The burst-frequency decreases with magnitude of burst in a way which can be represented by a series of exponentials.

(2) The total burst-frequency increases with elevation, at approximately the same rate as the total ionization up to 3000 meters, but considerably more rapidly for higher elevations.

(3) The frequency of very large bursts increases much more rapidly with elevation than the total ionization.

(4) The magnitude of the largest burst likely to be observed increases with elevation more rapidly than the total ionization.

(5) The observed bursts contribute a very small fraction of the total ionization. However, the possibility that all the ionization comes from bursts is not excluded, since the contribution of the smaller but much more frequent bursts is not included.

(6) The number of ions released in a burst is a function of the size of the chamber, those observed in the 1932 apparatus of 1/2-liter capacity amounting to a few tens of millions of ion pairs; those reported by Millikan in a chamber of 1.6 liters capacity amounting to the order of one hundred million ion pairs; those in the new instrument of volume 19.3 liters amounting to about one thousand million ion pairs. This would indicate that the physical dimensions of the instruments have not yet exceeded the physical dimensions of the bursts.

(7) The very large bursts may result either (a) from larger numbers of tracks than the number of constituent entities yet observed for any single atom, indicating the cooperation of a number of atoms; (b) from particles of greater ionizing power than those most commonly recognized in a cloud-chamber work; (c) possibly from materialization of the energy of photons into particles.

ACKNOWLEDGMENTS

It would not have been possible to carry out this work without the cooperation of many people. The Carnegie Institution of Washington supplied the instrument and its transportation. To Professor A. H. Compton we are indebted for advice and cooperation both in the experimental work and in the analysis of the results. Professor J. C. Stearns, of the University of Denver, extended to us the freedom of his laboratory and gave us most valuable advice and help. Mr. Walter Ailinger and the Mountain Parks Division of the City of Denver supplied us with men and trucks for the transportation of the heavy instrument to the mountain summit. Drs. Doan and Wollan, of the University of Chicago, have supplied us with instrument data and constants and have made a series of records for us at Chicago.

Appendix

On Distinguishing Between Bursts and Statistical Variations

Supposedly the bursts of ionization indicated on the records are produced by a large number of ionizing rays traversing the chamber in a time which is small compared with any natural period inherent in the instrument. Such natural periods in this instrument result from the period of the electrometer itself and from the time necessary for the ions to migrate to the electrodes under the influence of the collecting field. The electrometer period at the sensitivities used is of the order of one second, and negligibly small compared with the time necessary to collect the ions, as is demonstrated below. Hence, where the background of single rays (or multiples involving small numbers of rays) is large, as in this case, a sudden statistical variation in the rate of production of ions may resemble a burst when such a variation takes place in a time which is comparable with the time necessary to collect ions. This time may be calculated approximately, as follows.

The longest time involved will result when ions are produced near the inner surface of the outer sphere and have to be drawn all the way to the inner collector. It is true that as soon as the ions begin to separate, their influence begins to be felt by electrostatic induction on the inner collector, but the full change in voltage is not felt until they actually arrive at the collector. Hence this calculation gives the maximum possible time to realize the full effect of the charges. For the sake of simplicity the chamber and collector may be assumed to be concentric spheres of radii r_1 and r_2, respectively, without seriously impairing the accuracy of the result.

The field strength at any radius r is

$$E_r = Vr_1r_2/(r_2-r_1)r^2,$$

where V = total voltage between spheres; r_1 = radius of collector sphere; r_2 = radius of external sphere. Let μ = mobility of ions in cm/sec./volt/cm at 1 atmos. pressure; v_r = velocity in cm per sec. of ions at radius r; p = pressure in atmospheres.

Then

$$v_r = \mu E_r/p = dr/dt, \qquad dt = dr/v_r = pdr/\mu E_r;$$

or

$$t = \int_{r=r_1}^{r=r_2} \frac{pdr}{\mu E_r}, \qquad t = \frac{p(r_2-r_1)}{V\mu r_1 r_2}\int_{r_1}^{r_2} r^2 dr,$$

$$t = \frac{p(r_2-r_1)}{3Vr_1r_2\mu}\,(r_2^3-r_1^3) \text{ seconds.}$$

In this case $\mu = 1.37$ (*Smithsonian Tables*); $V = 250$ v; $p = 50$ atmos.; $r_2 = 17.8$ cm; $r_1 = 5.7$ cm (mean of max. and min. diameters of collector). Thus $t = 32$ seconds.

This sets an upper limit for the time necessary to collect the ions from any burst, provided of course the instrument has been in operation long enough to clear away the very large and slow ions found initially in such a chamber. In no case would it be possible to realize as long a period as this, since it would not be possible to produce a large amount of ionization right at the outside wall by means of many particles traveling in straight lines.

Records were taken for two days at Echo Lake at four times normal speed. It was possible to get a fairly accurate (5 percent) measure of the time constant of the apparatus from the large bursts found on these records, and a less accurate measure from large bursts on other records made at normal speed. These experimental values range between 14 and 23 seconds, which is well within the calculated upper limit of 32 seconds.

By knowing this period it is possible to calculate the expected frequency of statistical variations resembling bursts which might be mistaken for them in reading the records. This may be done as follows:

Let n = number of ion pairs per cm path in air at 1 atmos.; f = factor between argon at 50 atmos. and air at 1 atmos. ($f = 67.0$)[1]; nf = number of ion pairs per cm in argon at 50 atmos.; s = mean length of path of particle traversing the chamber, assuming that every particle passes completely across the chamber.

$$s = 4r_2/3 \text{ or } 23.7 \text{ cm.}$$

In calculating the average number of ions per particle, there are a number of possible choices for n ranging from 31 to 135.[2] To get the largest expected frequency of statistical bursts, one should choose the largest of these values, namely, 135. Then $nfs = 214{,}200$ ions per particle.

Let N = total number of ions produced per second on the average. Then N/nfs = average number of particles per second. In time Δt we get $x = N\Delta t/nfs$ particles and $N\Delta t$ total ions.

The probability P that in the interval of time Δt there will be collected not $N\Delta t$ ions but $(N\Delta t + B)$ ions (where B is the number of ions in an apparent burst) or that there will be not $x = N\Delta t/nfs$ particles but $(x+y) = (N\Delta t + B)/nfs$ particles is by Poisson's law[2]

$$P = x^{x+y}e^{-x}/(x+y)!.$$

By Sterling's approximation:

$$(x+y)! = [2\pi(x+y)]^{\frac{1}{2}}(x+y)^{(x+y)}e^{-(x+y)}.$$

Hence

$$P = \frac{x^{x+y}e^{-x}}{[2\pi(x+y)]^{\frac{1}{2}}(x+y)^{x+y}e^{-(x+y)}} = \frac{1}{[2\pi(x+y)]^{\frac{1}{2}}}\left(\frac{x}{x+y}\right)^{x+y}e^{y},$$

and

$$\log P = y\log e + (x+y)[\log x - \log(x+y)] - \tfrac{1}{2}\log 2\pi - \tfrac{1}{2}\log(x+y).$$

The case where a statistical variation is most likely to be mistaken for a burst occurs when reading from the records the smallest bursts where the background due to single particles and small showers is largest. The background is largest at the summit of Mt. Evans, and the smallest burst which can be conveniently read from the records is one of about ten million ions. The existence of a statistical variation of a given magnitude becomes more probable the longer the instrumental period chosen. Hence we shall take the longest period found experimentally, namely, 23 seconds. A burst of 10^7 ions is equivalent to

46.6 particles on the above assumptions, and the background of 5.18×10^{6} ions per second at the summit is equivalent to 24.1 particles per second or 555 particles in a 23-second period. Then

$$x=555, \qquad y=46.6, \qquad x+y=601.6,$$

and

$$P=1/430.$$

Hence we should get one statistical burst of 10^{7} ions in 430 periods of 23 seconds each, or about one every 2.75 hours, which is a rate comparable to that observed. However, if we consider the prevalence of statistical twenty million ion bursts we find we should expect one about every 730 hours, which would amount to about 0.25 percent of the total observed. On this basis we felt safe in including all bursts greater than 2×10^{7} ions at the three higher elevations. At Chicago the expected frequency of a statistical 10^{7} ion burst is found to be one every 42.2 hours and for a 1.5×10^{7} ion burst, one every 18,000 hours. Actually we observed 6.8 bursts between 10^{7} and 2×10^{7} ions per 42.2-hour period at this elevation, so only bursts less than 10^{7} ions were omitted at this elevation.

There is, of course, the possibility that these large fluctuations may result from instrumental accidents. The possibility of incipient arcs, as suggested by Millikan and Neher,[3] is definitely ruled out by the construction of the instrument, as has been pointed out.[4] Furthermore, bursts occur when the total voltage on the chamber is reduced to less than the ionizing potential of argon. Battery fluctuations have no effect on the recording system because of the electrostatic balance arrangement.[1] We are certain that the recording system is amply shielded against electrostatic disturbances, since frequent nearby lightning strokes, as well as corona streaming from tent poles, nearby rocks, etc., at noted times, produced no disturbance of the recording mechanism. Hence we feel justified in retaining the full numbers of bursts as read from the records and plotted in our curves.

[3] Millikan, Anderson and Neher, Phys. Rev. **45**, 141 (1934).
[4] R. D. Bennett, Phys. Rev. **45**, 491 (1934).

The Absorption Spectra of Acetylene, Ethylene and Ethane in the Far Ultraviolet

W. C. PRICE,* *Rowland Physical Laboratory, The Johns Hopkins University*

(Received January 31, 1935)

An absorption spectrum of acetylene in the region 1520A to 1050A has been found. It appears at very low pressures. The analysis was made by obtaining the spectrum of acetylene made from about 50 percent heavy water. The small isotopic shifts of many bands revealed them to be vibrationless electronic transitions. These are arranged into two Rydberg series going to the same limit which corresponds to an ionization potential of 11.35 volts. The upper levels of the two series are designated as $np\Sigma$ and $np\Pi$ levels. The excitation and ionization are from the CC bond and only vibrations affecting this bond appear. The character of the vibrations present is deduced from the magnitude of the isotopic shifts. Strong predissociation occurs around 1520A. This yields a value of about 187 Cal/mole for the strength of the triple CC bond. A similar set of bands appears in ethylene in the region 1750A to 1200A. The bands are more diffuse than those in acetylene, and only one strong Rydberg series was discovered. The limit of the series corresponds to an ionization potential of 10.41 volts. The vibrational analysis is similar to that in acetylene. The spectrum of ethane is extremely diffuse and no analysis of it could be made. It is concluded that, as in methane, all the upper states are unstable.

A GREAT deal of data has been accumulated on the acetylene molecule in the ground state. It is known that the molecule is linear and symmetrical. The five frequencies in the unexcited state have been identified correctly and the infrared and Raman spectra of this molecule have been thoroughly worked out. Until recently there has been a scarcity of reliable data on the absorption of acetylene in the ultraviolet. Kistiakowsky[1] obtained a set of bands in the region 2400–2000A but was unable to obtain a satisfactory analysis of them. The author working with a vacuum grating spectrograph has obtained an extensive system of bands extending from $\lambda = 1520 - 1050$A. The bands were obtained in absorption, the source being a Lyman continuum. The appearance of the bands is somewhat complex and it was only by taking the absorption of heavy acetylene that sufficient clues were found to enable the analysis to be made. The spectrum yields a spectroscopic value for the ionization potential of acetylene, a plausible value for the energy of the triple CC bond and gives an insight into the absorption spectra in the far ultraviolet of many other polyatomic molecules which have been investigated more recently by the author.

The vacuum spectrograph used in this work was of the grazing incidence type, the angle of incidence being about 78°. The grating was a glass one of about 2 meters radius of curvature and ruled with 30,000 lines to the inch. The dispersion varied from 2.5A/mm at 1700A to 2A/mm at 1000A. The discharge tube used for obtaining the continuum was of the type designed by Collins and Price.[2] It was operated by the discharge of a condenser of about 3μf capacity charged to a potential of 15,000 volts through a capillary of 1 mm bore. The pressure was measured by means of a Pirani hot wire gauge. The advantage of this type of gauge was that it gave a continuous record of the pressure. This is very important in taking absorption photographs since unless the pressure does remain sensibly constant throughout the exposure the absorption bands tend to be blurred. Lines in the spectrum of molecular hydrogen were used as standards.

The method of obtaining the absorption spectrum of acetylene was as follows: Tank acetylene was purified by passing it through five spiral wash bottles containing water, chromic acid, mercuric chloride in HCl, copper nitrate in nitric acid and sodium hydroxide. It was then dried over P_2O_5 and led into the back of the spectrograph through a long fine capillary. The partial pressure of acetylene was never higher than 0.1 mm Hg in the high pressure pictures, and less than 0.001 mm in the low pressure ones, the path length being about 1.5 meters. Hydrogen was used as a conducting gas in the discharge tube.

* Commonwealth Fellow.

[1] Kistiakowsky, Phys. Rev. **37**, 277 (1931).

[2] Collins and Price, Rev. Sci. Inst. **5**, 423 (1934).

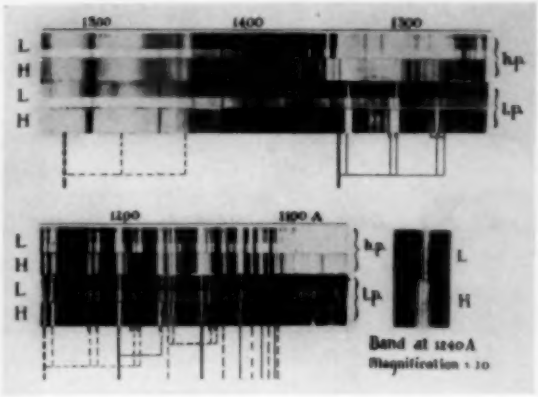

FIG. 1. The absorption spectrum of acetylene in the far ultraviolet.

As is seen from Fig. 1 a very rich absorption spectrum is obtained. It contains both diffuse and sharp bands. The bands obtained by Kistiakowsky round 2300A are sharp. The bands shown here round 1500A are very diffuse. At 1350A they are less diffuse and below this they become sharp again. Towards the shorter wavelengths they become very numerous and overlap, eventually reaching a limit at about 1050A. From this point on a continuous absorption starts. However, it becomes rapidly weaker and at about 800A the substance is again transparent. This transparency below 800A is also found for ethylene even when comparatively high pressures are used. It extends at least as far down as 150A, as observed by emission lines.

The bands can be conveniently divided into two classes.

Class I bands have a single head and are shaded towards the red. At low pressures and with very narrow slit widths (of the order of 0.001 inches) they appear as a single absorption line which is somewhat diffuse on the long wavelength side. They are, therefore, assumed to contain only P and R branches, and are designated as parallel bands.

Class II bands have two fairly sharp heads which are shaded towards the red. At low pressures they appear as a narrow absorption doublet having a separation of about 0.2A. The heads are apparently caused by the R and Q branches of the bands. A measurement of the separation of the heads gives a value for the moment of inertia of the molecule.

Taking the value of the moment of inertia of the molecule in the ground state to be 23.51×10^{-40} g cm^2 we obtain for the band at 1247A, $I = 25.00 \times 10^{-40}$ g cm^2 as compared with the value $I = 25.6 \times 10^{-40}$ g cm^2 obtained by Kistiakowsky for the bands round 2300A. The heads of the bands at shorter wavelengths have all about the same wave-number separation as that at 1247A. It thus appears that I changes considerably with the first electronic jump, the subsequent increases being comparatively small. The bands of class II are termed perpendicular bands. They contain P, Q and R branches.

Acetylene possesses five possible vibrational frequencies in both the upper and lower states. Because of the complexity of the spectrum great difficulty was experienced in trying to find these frequencies and then to assign them to the correct modes of vibration. The whole problem was, however, cleared up by obtaining the absorption of heavy acetylene which was made from a few drops of (60 percent) heavy water kindly supplied by Professor Taylor of Princeton University. A special type of generator was used for this purpose but it is not considered necessary to describe it in detail here.

The photographs for the heavy acetylene which contained about 45 percent C_2DH, 45 percent C_2H_2 and 10 percent C_2D_2 are shown in plate $I(H)$. A large number of the bands are apparently not shifted, but a closer investigation of the low pressure photographs shows that some of them suffer very small shifts. The microphotographs enlarged 20 diameters, show that the doublet at 1247A has now a third component on the short wavelength side, becoming a triplet. The increased relative intensity of the central component indicates that the long λ component of the heavy acetylene doublet overlaps the short λ component of that of light acetylene. The shift is very small, being only $0.30\text{A} \equiv 20$ wave numbers. Consequently these bands must be due to electronic transitions between the fundamental levels of the initial and final states. They suffer only a small isotopic shift due to the change in the difference of zero point energy between these two states.

light $\nu_L'' = \nu_e + \frac{1}{2}\sum\omega_L' - \frac{1}{2}\sum\omega_L''$

heavy $\nu_H'' = \nu_e + \frac{1}{2}\sum\omega_H' - \frac{1}{2}\sum\omega_H''$

$$\nu_H - \nu_L = \tfrac{1}{2}\{\sum(\omega_L'' - \omega_H'') - \sum(\omega_L' - \omega_H')\}.^*$$

'' indicates the ground state.
' indicates the excited state.

It is assumed here that ν_e does not change appreciably in going over from light to heavy acetylene. Our subsequent analysis will justify this.

As the vibration frequencies in the ground state are greater than those in the upper state, the change $(\omega_L'' - \omega_H'')$ will be greater than the change $(\omega_L' - \omega_H')$ as both depend on approximately the same mass factors. Consequently $\nu_H - \nu_L$ is positive and there will be a shift towards the violet. The magnitude of the shift will be small and it is only on account of the high dispersion of the instrument that it could be detected. Only the fundamental electronic transitions of the bands of class II could be revealed this way. The ν_0's of the parallel bands were found by the apparent absence of shift and the fact that they fitted into a certain Rydberg series. [The head of the band of C_2DH fell in a region where the corresponding band of C_2H_2 was absorbing.]

The vibration bands are shifted by larger amounts and their second members are easily detected by the doubling of their shifts, vibrations of the same type all being shifted proportionally. There are some bands of appreciable intensity to the red side of all the very strong bands. These can be interpreted as transitions from an initial transverse vibrational state. The transverse vibrations in acetylene are of such small frequencies (605 and 730 wave numbers) that they must be present in appreciable quantities at room temperatures.

Analysis of the Bands

When the ν_0's of class I bands were taken it was found that they were represented fairly closely by the following Rydberg series:

$$\nu_0^n = 92{,}076 - R/(n-0.50)^2 \quad n = 3, 4, 5 \qquad (I)$$

and those of class II by

$$\nu_0^n = 91{,}950 - R/(n-0.95)^2 \quad n = 3, 4, 5. \qquad (II)$$

An idea of the accuracy with which the bands are represented by these formulas may be obtained by inspection of Table I: (The accuracy of the measurement of the bands varies considerably depending on whether they are sharp or diffuse. If the bands are sharp their heads can be measured to within a tenth of an Angstrom unit ($\sim 10\ cm^{-1}$). The measurements on the diffuse bands have a much greater probable error.)

TABLE I. *Observed and calculated frequencies of class I and class II bands.*

	Class I				Class II		
n	Int.	Wave number		n	Int.	Wave number	
		Obs.	Calc			Obs.	Calc.
3	10 *D*	74516	74518	3	10 *DD*	65790	65838
4	10	83140	83118	4	10	80116	80153
5	10	86665	86657	5	10	85226	85260
6	10	88431	88449	6	10	87636	87647
7	8	89464	89479	7	6	88946	88952
8	obscured			8	4	89743	89742
9	6	90560	90557	9	3	90260	90257
10	4	90860	90860	10	2	90610	90610

Both the series have approximately the same limit which coincides with the region where the continuous absorption starts. As many as ten members of each can be observed and measured. The subsequent members are somewhat obscured by overlapping and accurate measurements cannot be made on them.

The bands round 2300A investigated by Kistiakowsky would fall into this scheme by putting $n = 2$ in I, but as will be shown later this is probably a mere coincidence. The fact that they are observed at extremely high pressures indicates that the transition probability corresponding to them is extremely low whereas in the case of the bands which we have observed it is at least 100,000 times as great. Further Kistiakowsky's bands have *P*, *Q* and *R* branches. If they were fitted into our scheme they would fall into a class which contains only *P* and *R* branches.

A large number of facts, which come out of the vibrational analysis, go to show that one of the valence electrons between the two carbons is excited. Thus the two series may very probably be due to the different coupling of its orbital momentum with the internuclear axis. This leads to the designation of the upper levels of class I

* In this formula the transverse frequencies have to be multiplied by two as they have two degrees of freedom.

bands as $p\Sigma$ levels and those of class II bands as $p\Pi$ levels; which is in agreement with the fact that the bands of class I contain only P and R branches, while those of class II contain P, Q and R branches. Further, G. H. Dieke[3] has calculated the differences between the energies of the $p\Sigma$ and $p\Pi$ levels for the various electronic states of helium, this being the only other molecule except N_2 for which such a large number of electronic states has been observed. As shown in Table II, there is a striking numerical agreement between the actual magnitude of these energy differences and those of helium.

TABLE II. *Comparison of energy differences of the $p\Sigma$ and $p\Pi$ levels in C_2H_2 and in He_2.*

$p\Sigma - p\Pi$	
C_2H_2	He^2
−8726	−8890
−3024	−2970
−1437	−1400
− 795	− 998 ?
− 518	?

The differences in the case of acetylene have not been corrected for zero point energy but it will be shown later that this does not alter the agreement appreciably. The differences are for the $p^3\Pi$ levels of helium.

From the limits of the Rydberg series the ionization potential of acetylene is calculated to be 11.35 electron volts probably correct to one-hundredth of an electron volt. The best and most recent determination by the methods of electron impact is due to Tate and Smith.[4] The value they give is 11.6±0.1 volts, which is in good agreement with the one given here. This is only one example of the possibility of obtaining accurate values of the I.P.'s of various molecules from their absorption spectra in the far ultraviolet. Other substances for which the author has been able to do the same thing are C_2H_4, CH_3OH, H_2CO, CH_3HCO, $(CH_3)_2CO$, O_2, CS_2, H_2S, SO_2, the methyl and ethyl halides and many others. The work on these substances is now in the process of publication.

[3] G. H. Dieke, Zeits. f. Physik **57**, 71 (1929).
[4] J. T. Tate and P. T. Smith, Phys. Rev. **39**, 270 (1932)

Rotational Structure

The dispersion of the instrument is of course not high enough to resolve the rotational structure of the bands. One important thing however could be noticed in the case of class II bands.

A close inspection of one of the vibration bands accompanying the second member of this class reveals that its R branch is very slightly wider than that of the corresponding band for C_2DH. This is in agreement with the corresponding increase in moment of inertia of the C_2DH molecule and our assignment of P, Q and R branches to these bands. (The isotopic shifts were measured between the heads of the Q branches when this was possible.)

The Analysis of the Vibrational Structure

In the bands having low values of n a great deal of vibrational structure can be observed. As many as ten vibrational transitions accompany some of the fundamental electronic transitions. For bands having higher electronic quantum numbers, however, the vibrational structure is obscured by the overlapping of the subsequent electronic transitions. The vibrational analysis is greatly simplified by the magnitudes of the isotopic shifts. The shift of the ν_0 band due to the change in zero point vibrational energy is very small (20 cm^{-1}). In the particular case of acetylene the vibrational analysis could probably be made purely from the knowledge of the actual magnitude of this shift.

Fig. 2 shows the various vibrations possible in acetylene; the values of their frequencies in the ground state are those given by Sutherland.[5]

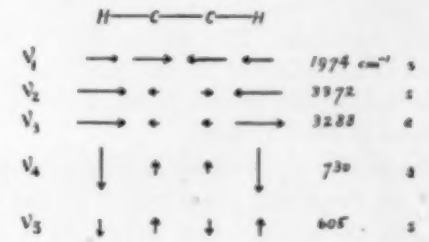

FIG. 2. Vibrations in acetylene.

[5] Sutherland, Phys. Rev. **43**, 173 (1933).

The lengths of the arrows indicate qualitatively the relative displacements of the various atoms. (This can be derived from a purely mechanical treatment of a model.) It is seen that to a rough approximation: ν_2, ν_3 and ν_4 depend mainly on the CH linking and a rough calculation shows that they are approximately diminished by 11 percent in going from C_2H_2 to C_2DH. On the other hand, ν_1 and ν_5 depend mainly on the CC linking and are diminished by only about 5 percent by this substitution. Now it is very probable if the excited electron comes from the C≡C bond, that the CH bonds and therefore the frequencies ν_2, ν_3 and ν_4 will not be appreciably affected by the excitation. However, if it comes from the CH bond these frequencies will certainly be changed considerably. The latter possibility cannot occur as even small changes in the frequencies ν_2 and ν_3 would require a much larger shift in zero point energy than the 20 wave numbers observed; e.g., a 10 percent change would give rise to a shift in zero point energy of about 80 wave numbers.

In order to find the selection rules determining which vibrational transitions should occur, we must consider the influence of two factors: In the first place the symmetry of the molecule determines a selection rule. If the symmetry of the electronic eigenfunctions of the excited state is the same as that of the normal state, the selection rules are the same as those for the infrared bands. If the symmetry is different then different selection rules of the same character apply. It is not necessary to go into this here as only the symmetrical vibrations appear and for these there is no specific selection rule in either case.

Secondly, bands which might be allowed by the symmetry considerations may be nevertheless excluded for reasons which are analogous to those leading to the Franck-Condon principle for diatomic molecules. This means that if the CH distance is not affected by the electronic transition no transitions should occur which involve vibrations in the CH bond.

An inspection of the vibration diagram indicates that if an electronic jump occurs in the C≡C bond only the symmetrical vibrations ν_1 and ν_3 can be excited, and it will be shown that this is what happens in our case. It is supported by the fact that all the bands belonging to one particular

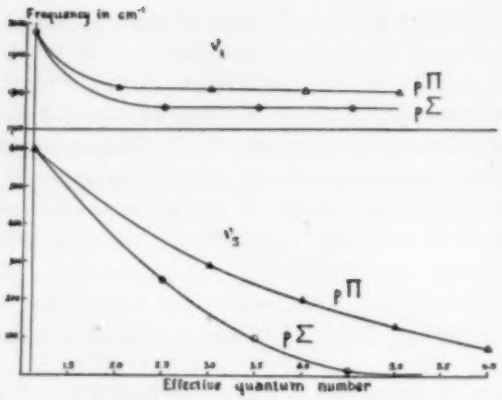

FIG. 3. Frequencies plotted against effective quantum number.

electronic transition are of the same type, i.e., they are either all parallel or all perpendicular bands. This could only happen if both vibrations are symmetrical.

The observational facts are as follows: All the bands of class I and class II are accompanied by equally strong bands, a little to the short wavelength side of them. The separation of these accompanying bands from the ν_0 band decreases rapidly in the case of class I bands to almost zero with increase in electronic quantum number. In the case of class II bands, the diminution of the frequency difference is much slower. In both cases these bands must represent vibrations of the type ν_5 superimposed on the electronic transition. They could not represent a superposition of the vibration ν_4 as the change of ν_4 from 730 cm^{-1} in the ground state to the values of the differences observed would give rise to a much greater isotopic shift in the ν_0's than that actually found. The frequency differences are plotted against the effective quantum number of the electronic state in Fig. 3. It is seen that smooth curves are obtained which can be extrapolated to 600 cm^{-1}, which is the value of ν_5 in the ground state.

THE ν_1 VIBRATION

Class I bands are accompanied also by bands lying about 1760 wave numbers to the short wavelength side. They have an observed isotopic shift of about 90 cm^{-1}. When the shift in ν_0 is taken into account the diminution in frequency difference is 110 cm^{-1}. The bands of class II are

also accompanied by a similar set of bands lying about 1810 wave numbers to the short wave-length side of each number. The total diminution of the frequency difference is 90 cm^{-1} in this case. The magnitude of the shift which corresponds to a diminution of the wave-number separation by about 5 percent makes it certain that a vibration of the type ν_1 is involved. The values of the frequency are plotted against effective quantum number in Fig. 3. It is seen that, after the first electronic jump, the value of ν_1 remains appreciably constant in both $p\Sigma$ and $p\Pi$ states; this also occurs in the corresponding bands in helium. The differences in the absolute magnitude of ν_1 in the two states can be ascribed to the difference in the relative values of the force constants. This holds also for ν_5.

In both $p\Sigma$ and $p\Pi$ states, the frequency ν_1 appears equally intense in combination with the strong ν_5 transverse vibration. The frequencies $2\nu_1$ and $2\nu_1+\nu_5$ also appear quite strongly in some of the lower band systems. They are easily identified by the doubling of the isotopic shift.

This accounts for all the strong bands. There are, however, a number of bands lying to the red side of some of the strong bands, in particular the bands at 1340A and 1247A. They can be ascribed to transitions from the vibrational levels of the ground state. The difference 605 cm^{-1}, corresponding to a vibration of the type ν_5 in the ground state, is found fairly strongly and the values $\nu_4=730$ and $2\nu_5=1210$ are found somewhat more weakly. Most of the extremely strong bands have these weaker vibrations accompanying them and this seems the most plausible explanation for such bands.

The Predissociation of the λ1500 Band

The bands observed by Kistiakowsky at about 2300A are sharp. They have been investigated still further in this laboratory by Professor G. H. Dieke, who has shown that even round 1900A they exhibit no signs of predissociation. Thus the continuous absorption reported by Kistiakowsky at about 2200 is due to impurities. The bands we have obtained are very diffuse round 1500A and even round 1300A are still slightly diffuse. Below this they are sharp.

If it is assumed that this diffuseness is caused by predissociation and further that this predissociation might be due to interaction with the normal state, then we find that the heat of dissociation of C_2H_2 into CH+CH must be slightly less than 8.1 electron volts or the energy of the triple bond is slightly less than 187 Cal./mole. This is in good agreement with the best chemical data. The value given by F. O. Rice[6] is about 200 Cal./mole, that given by R. G. W. Norrish[7] is 220 Cal./mole. However, it is generally accepted that these values are too high, and further the experiments from which they are obtained are not capable of great accuracy. In the above it is assumed that the molecule dissociates into normal CH radicals. An investigation of the energy values of excited CH shows that this must be so.

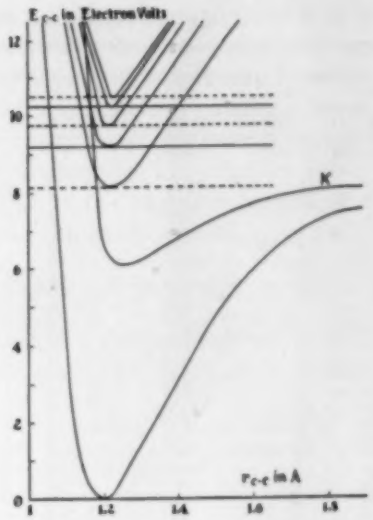

FIG. 4. Potential energy curves for the CC bond in C_2H_2

The assumptions mentioned at the beginning of the last paragraph are only justified by the resulting agreement obtained for the energy of the C≡C linking. In fact, the assumption that the excited state interacts with the normal state must be somewhat modified. This is seen from an inspection of the potential energy curves between the two carbon atoms, Fig. 4.

Approximate Morse[8] curves can be obtained for this potential in the following way. The various constants of the acetylene molecule are

[6] F. O. Rice and W. R. Johnston, J. Am. Chem. Soc. **56**, 214 (1934).
[7] R. G. W. Norrish, Trans. Faraday Soc. No. 152, 106, January, 1934.
[8] P. M. Morse, Phys. Rev. **34**, 57 (1929).

TABLE III. *Frequencies of the observed bands in C_2H_2 and their assignments.*

TYPE	INTENSITY h.p.	INTENSITY l.p.	FREQUENCY	n	ASSIGNMENT ν_1	ν_2	$(\nu_3)_0$	$(\nu_4)_0$
L	100 *DD*	50 *DD*	65790	$3\rho\Pi$	0	—	0	0
"	100 *DD*	50 *DD*	67610	"	1	—	0	0
"	100 *DD*	30 *DD*	69430	"	2	—	0	0
H p	2	0	72335	$3\rho\Sigma$	0	0	−?	
L "	4	0	73148	"	0	0	−1	−1
H "	5	1	305	"	0	0	−?	
L "	10	1	408	"	0	1	−1	−1
H "	10	1	781	"	0		−?	
L "	10	2	74020	"	0	1	−1	0
L "	10	4	510	"	0	0	0	0
" "	100	10	750	"	0	1	0	0
" "	10 *D*	1 *D*	990	"	0	2	0	0
" "	10 *D*	4 *D*	75235	"	0	3	0	0
H "	10	1	550	"	1	0	0	−1
L "	10	1	640	"	1	0	0	−1
H "	10	1	800	"	1	1	0	−1
L "	10	1	872	"	1	1	0	−1
H "	obsc.	10	76170	"	1	0	0	0
L "	10	8	266	"	1	0	0	0
H "	obsc.	10	400	"	1	1	0	0
L "	20	10	497	"	1	1	0	0
L "	5	1	77427	"	2	0	0	−1
" "	5	2	667	"	2	1	0	−1
H "	10	3	800	"	2	0	0	0
L "	10	5	008	"	2	0	0	0
H "	10	1	040	"	2	1	0	0
L "	10	1	256	"	2	1	0	0
	2	0	78790	$4\rho\Pi$	0	0	−1	−1
	3	0	79076	"	0	1	−1	−1
	3	0	400	"	0	0	−1	0
	3	0	510	"	0	0	0	−1
	3	0	662	"	0	1	−1	0
L s	50	10	80110	"	0	0	0	0
H s	50	10	130	"	0	0	0	0
H & *L s*	100	10	400	"	0	1	0	0
L "	2 *D*	0	81200	"				
L "	2 *D*	0	390	"				
L "	4	0	700	"				
*H** "	3	0	770	"	1	0	0	0
H "	10	5	830	"	1	0	0	0
L "	10	10	925	"	1	0	0	0
*H** "	3	0	82050	"	1	1	0	0

TYPE	INTENSITY h.p.	INTENSITY l.p.	FREQUENCY	n	ASSIGNMENT ν_1	ν_2	$(\nu_3)_0$	$(\nu_4)_0$
H "	5	2	110	"	1	1	0	0
L "	10	4	210	"	1	1	0	0
H "	8	2	83630	"	2	0	0	0
L "	8	2	730	"	2	0	0	0
H "	8	2	860	"	2	1	0	0
L "	8	2	84020	"	2	1	0	0
H & *L p*	50	10	83120	$4\rho\Sigma$	0	0	0	0
p	50	10	190	"	0	1	0	0
H "	30	10	760	"	1	0	0	0
*H** "				"	1	1	0	0
L "	8	2	880	"	1	0	0	0
H "				"	1	1	0	0
L "	10	7	952	"	1	1	0	0
L "	obsc.		85630	"	2	0	0	0
L s	20	10	85230	$5\rho\Pi$	0	0	0	0
H "	20	10	250	"	0	0	0	0
H & *L s*	30	10	430	"	0	1	0	0
H "	10	8	86950	"	1	0	0	0
L "	10	8	87046	"	1	0	0	0
L "	6	3	242	"	1	1	0	0
L p	50	10	86665	$5\rho\Sigma$	0	0	0	0
L "	10	5	88431	"	1	0	0	0
L "	obsc.		90205	"	2	0	0	0
L s	30	10	87635	$6\rho\Pi$	0	0	0	0
L "	2		776	"	0	1	0	0
L "	2		89447	"	1	0	0	0
L p	30	10	88430	$6\rho\Sigma$	0	0	0	0
	obsc.		90200	"	1	0	0	0
	20	8	88946	$7\rho\Pi$	0	0	0	0
	6	0	89020	"	0	1	0	0
	4	0	90760	"	1	0	0	0
	10		89464	$7\rho\Sigma$	0	0	0	0
	10	4	89743	$8\rho\Pi$	0	0	0	0
			91560	"	1	0	0	0
	10	5	90100	$8\rho\Sigma$	0	0	0	0
	8	3	90260	$9\rho\Pi$	0	0	0	0
	5	1	92085	"	1	0	0	0
	8	2	90560	$9\rho\Sigma$	0	0	0	0

defined below. The values given are those obtained by Mecke[9] for the ground state.

$$H\overset{k_1}{\text{—}}C\overset{k_2}{\text{—}}C\overset{k_1}{\text{—}}H$$
$$\quad r_{CH} \quad r_{CC} \quad r_{CH}$$

k_1 = force constant between H and C = 20 volts,
k_2 = force constant between C and C = 69 volts.
$\nu_{CH} = k_1(1/C + 1/H) = 3200\ cm^{-1}$,
$\nu_{CC} = 2k_2/C = 2100\ cm^{-1}$,
$r_{CH} = 1.08$ A $\quad r_{CC} = 1.19$A.

We can calculate the values of r_{CC} in the upper states from the corresponding moments of inertia which are obtained from the separation of the band heads. This can be done on the assumption that r_{CH} does not vary. It can only be done for the bands of class II. In these we find an increase in r_{CC} over the value in the normal state of about 0.03A, the value 1.24A remaining fairly constant for all the members of the class. This small difference in r_{CC} in the upper and lower states is in agreement with the fact that long vibrational progressions are not obtained. The bands observed by Kistiakowsky round 2300A have a somewhat larger value for r_{CC} (1.26A).

The value of ν_{CC} in the ground state is practically equal to ν_1 and for the upper state it can also be taken to be equal to the value of ν_1 found in these cases. The heats of dissociation in the upper states are unknown, but for the purpose of calculating the potential curves they can be taken to be about 7 electron volts or 160 Cal./mole (i.e., = the strength of the double CC bond). That in the lower state must be equal to the strength of the triple CC bond, and is approximately equal to 8.2 electron volts or 200 Cal./mole. It is to be stressed that these values are only taken so that rough ideas of the shape and position of the potential curves can be obtained.

The potential curves obtained in this way are shown in Fig. 4. It is seen that there is no possibility of the intersection of the potential curves of the upper and lower states and to

[9] Mecke, Zeits. f. physik. Chemie **B17**, 1 (1930).

explain the predissociation of the band at 8.1 electron volts into normal CH radicals we have to postulate the curve K. This curve must go to the heat of dissociation of the normal state. It may extend down as far as 6.1 electron volts and may possibly represent the upper state of the bands observed by Kistiakowsky round 2300A. Certainly the extremely low transition probability of these bands seem to make this a likely explanation. The possibility that the predissociation does correspond to a dissociation of the type described above must be admitted from the close agreement of the bond strength predicted this way and that obtained from chemical data. Further in the case of polyatomic molecules there are a large number of instances of photodissociation into normal radicals by means of predissociation due to interaction with the initial state, e.g., formaldehyde shows one region of predissociation around 2750A corresponding to about 105 Cal./mole which is the heat of dissociation of the CH bond; also another around 1745A or about 164 Cal./mole corresponding to the breaking of the CO bond. Similar cases occur in all ketones. In the case of a polyatomic molecule predissociation may occur over a far wider range than is found for diatomic molecules. This is due to the fact that the resulting radicals may have various amounts of vibrational and rotational energy as well as electronic energy which is the only kind present in the predissociation of a diatomic molecule. This kind of explanation accounts for the partial predissociation of the λ1350 band which is considerably removed from the main region of predissociation.

Table III giving the frequencies of the bands observed in C_2H_2 along with their assignments is appended. When the bands are clearly (a) single headed they are marked p; (b) double headed they are marked s. The v's refer to the number of quanta of the respective vibrations present $L \equiv C_2H_2$, $H \equiv C_2DH$, $H^* \equiv C_2D_2$.

The Absorption Spectrum of Ethylene

The analysis given here for acetylene has also thrown considerable light on the ultraviolet absorption spectrum of ethylene. This spectrum which starts at about 1744A was obtained in the same way as that of acetylene and at about the same pressures. In this case only one strong series was observed which may be related to the fact that the molecule is no longer linear and the orbital momentum of the excited electron cannot be resolved along the internuclear axis any more.

The ν_0^n's of the higher members of the series fit fairly well into the Rydberg series

$$\nu_0^n = 84{,}400 - R/(n+0.0)^2. \quad n = 2, 3, 4, \text{etc.}$$

The degree of accuracy with which this formula represents the bands is given in Table IV. The

Table IV. *Comparison between calculated and observed values for the separation between successive members of the absorption spectrum of ethylene.*

n	Int.	Wave number	Separation between successive members (cm⁻¹)	
			Obs.	Calc.
2	10 *D*	57360	14810	15241
3	10 *DD*	72170	5410	5334
4	8	77580	2480	2469
5	7	80060	1320	1341
6	5	81380	800	808
7	3	82180		

limit corresponds to an ionization potential of 10.41 volts which agrees fairly well with the value 10.0±? given by Kallman and Dorsch[10] as determined by the methods of electron impact.

The vibration pattern of the first electronic band is similar to that in acetylene and it is therefore assumed that the same types of vibration ν_1 and ν_5 are excited.

The frequencies and assignments of the strong bands are given in Table V. The value of ν_5 decreases to practically zero in the first few electronic states while the value of ν_1 also decreases

Table V. *Frequencies and assignments of the strong absorption bands in ethylene.*

I		ν cm⁻¹	n	ν_1	ν_5	I		ν cm⁻¹	n	ν_1	ν_5
10 *D*		57360	2	0	0	8		77580	4	0	—
10 *D*		57840	2	0	1	8		77880	4	1	—
10 *D*		58700	2	1	0	5		78170	4	2	—
10 *D*		59170	2	1	1						
8 *D*		60030	2	2	0	7		80060	5	0	—
8 *D*		60500	2	2	1	7		80290	5	1	—
6 *DD*		61370	2	3	0	obscured			5	2	—
6 *DD*		61830	2	3	1						
10 *DD*	double	72170	3	0	—	5		81380	6	0	—
" "	"	72980	3	1	—	5		81600	6	1	—
8 "	"	76370	3	2	—	4		81800	6	2	—
						3		82180	7	0	—

[10] Kallman and Dorsch, *Abhandlung für Kaiser Wilhelm Institut*, Vol. 12 (1929).

to a very small value as n becomes large. Table VI shows the values of these frequencies in the

TABLE VI. *Values of ν_1 and ν_5 frequencies.*

n	2	3	4	5	6
ν_1	1340	800	300	230	200
ν_5	480	150	—	—	—

different electronic states. The values of ν_1 and ν_5 in the ground state are assumed to be 1623 cm^{-1} and 1342 cm^{-1}.[11]

A large number of weak diffuse bands were obtained which have not been classified. Some of them undoubtedly correspond to other electronic series.

THE ABSORPTION OF ETHANE

At very low pressures (0.01 mm) the absorption of ethane consists of extremely diffuse bands starting at 1350A and going down below 1000A. The bands are far too diffuse for any analysis to be attempted. In this respect they resemble methane.[12] The low pressure bands in methane start at 1300A; at somewhat higher pressures they extend up to 1450A. Those of ethane behave in the same way and move to a limiting value of around 1500A with increase in pressure. On account of the extreme diffuseness of the bands in ethane it is assumed that as in methane all the upper electronic states are unstable.

In conclusion the author wishes to express his gratitude to Dr. G. H. Dieke for his generous help and numerous suggestions in connection with both the experimental and theoretical aspects of this work.

[11] Mecke, Zeits. f. physik. Chemie **B17**, 16A (1932).

[12] A. B. F. Duncan, J. Chem. Phys. **2**, 851 (1934).

MARCH 15, 1935 PHYSICAL REVIEW VOLUME 47

Artificial Radioactivity Produced by the Deuteron Bombardment of Nitrogen[1]

EDWIN McMILLAN AND M. STANLEY LIVINGSTON,* *Radiation Laboratory, Department of Physics, University of California*

(Received January 21, 1935)

This paper describes the work leading to the discovery and investigation of radio-oxygen, and also includes some incidental results on other nuclear disintegrations. It is shown that nitrogen bombarded with deuterons gives rise to a radioactive substance which emits positive electrons of maximum energy 1.2 mv, has a half-life of 126±5 sec., and is found by chemical analysis to be an isotope of oxygen. The nuclear cross section for the activation of nitrogen at 2 mv deuteron energy is 6×10^{-27} cm^2; that for the activation of carbon is three times as great. The neutrons expected to accompany the formation of radio-oxygen were found to be present. These results were obtained using gaseous nitrogen as a target; in some of the experiments use was made of the fact that the active product can be deposited on a metal surface by recoil.

EXPERIMENTAL ARRANGEMENT

DEUTERONS were accelerated to a kinetic energy of about 2 mv in an apparatus described elsewhere.[2] A brass tube was set into the side of this apparatus in such a position as to intercept the deuteron beam, which passed into the atmosphere through a vacuum-tight window[3] as shown in Fig. 1. The target to be

* Now at Cornell University.

[1] A preliminary report of this work was given by M. S. Livingston and E. McMillan, Phys. Rev. **46**, 437 (1934).

[2] E. O. Lawrence and M. S. Livingston, Phys. Rev. **45**, 608 (1934).

[3] The window used for admitting the deuteron beam was so satisfactory that it seems worth while to describe it in some detail. It consisted of a sheet of 0.0001" thick aluminum foil (procured from the American Platinum Works) mounted with wax on a brass plate, covered as closely as possible with one mm holes over an area of 1×1.5 cm. A wax to be used for this purpose must have a high melting point (the window becomes quite warm under the deuteron bombardment), it must flow freely when melted, and it must stick firmly to a clean metal surface when cold. These requirements are satisfied by rosin, with just enough Venice turpentine added to make it sticky, as determined by trial. The window was mounted by heating the supporting grid to a temperature above the melting point of the wax, covering it with a thin coat of wax and blowing off the excess, and then putting on the foil, touching it at one edge first and

activated was placed opposite the window. The space containing the target could be evacuated or filled with various gases during the bombardment.

For studying the activity produced in gases by deuteron bombardment, a plug shown as a dotted line in Fig. 1 was waxed into the tube, leaving a space in which the gases could be bombarded. Fig. 2 shows the gas-handling arrangement used. After evacuating the system, the activating chamber was filled with the gas to one atmosphere pressure through the line *G*.

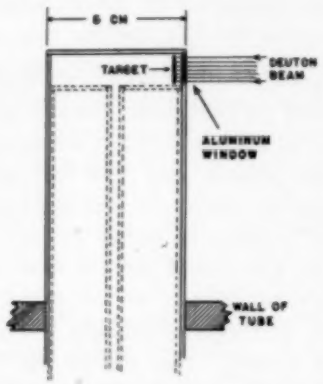

FIG. 1. Arrangement for bombarding targets outside the vacuum. A plug which may be put in to enclose a space for bombarding gases is shown by dotted lines.

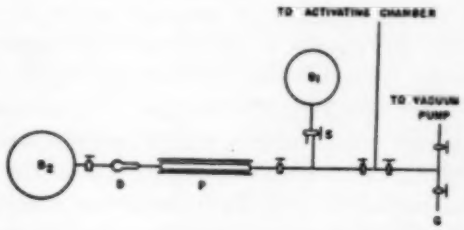

FIG. 2. Gas-handling system. *G*, line for introducing gases into the activating chamber. B_1 and B_2, bulbs for collecting activated gases before and after passage through the analyzing train consisting of the platinized asbestos tube *P* and $CaCl_2$ drying tube *D*.

When the bombardment with deuterons was completed, the activated sample was allowed to flow into the bulb B_1, whose volume was sufficiently large to collect over 90 percent of the sample. This bulb was then removed and placed beside the electroscope, which was discharged by the emitted gamma-rays. The part of the system to the left of B_1 was used for the chemical analysis, and will be described later in the paper.

Ionization Chamber Calibration

The ionization chamber used for studying the radioactivity consisted of a cylinder of dimensions 7×7 cm containing a sensitive (2×10^6 ion pairs/div.) Lauritsen type quartz fiber electroscope and provided on one side with a large window covered with 0.001 inch thick aluminum foil. From the geometry of the arrangement and the known ionization per centimeter of beta-particles one can compute roughly that, with an active target next to the window, a leak of one division corresponds to a total of 2×10^4 beta-disintegrations in the target.

For evaluating the measurements made with the gamma-rays from a gas sample contained in a bulb, a calibration of the following sort was made: An activated carbon target (which is known to give no strong gamma-rays except the "annihilation radiation" associated with the positive electrons emitted as beta-particles) was placed next to the window of the electroscope and the ionization observed. The same target was then enclosed in a box thick enough to stop all beta-particles and placed in the position of the center of the gas bulb and the ionization again observed. The ratio of the observed ionizations was 100. It was found also that the ionization produced by the target when enclosed in a box next to the window was 1/35 that produced by the bare target in the same position. This number gives a criterion for deciding whether a positron-emitter gives any appreciable gamma-rays other than the annihilation radiation.

Radioactivity Produced on Solid Targets

Carbon was the first substance to be activated after the installation of the arrangement of Fig. 1. A beam of about $\frac{1}{2}\mu$A of 2 mv deuterons emerging from the window was used, and the carbon

allowing the surface tension of the wax to pull it into place. A small leak in one hole of the window can be stopped by filling the hole with a drop of wax, applied with a hot pointed iron. A window constructed in this way has a large open area, a small stopping power (4 mm air equivalent) and can be exposed to several microamperes of ion current for long periods with no apparent damage. This seems remarkable at first sight since the wax on the back of the grid rapidly becomes carbonized and the beam in air will char paper in a few seconds, but it appears reasonable when one considers the small amount of energy lost by a high speed ion in going through the foil.

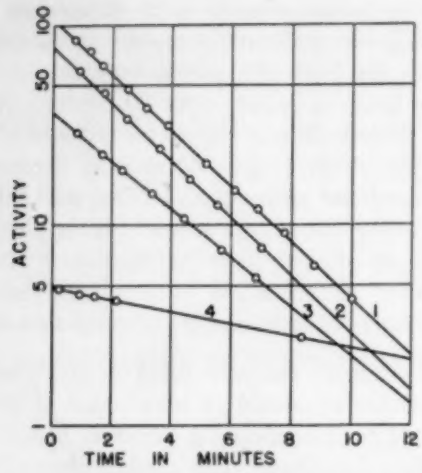

FIG. 3. Logarithmic decay curves of the activities of: 1. Platinum bombarded in air. 2. A bulb containing activated air. 3. Platinum bombarded in vacuum. 4. Platinum bombarded in CO_2. The absolute values of the activities are not represented in their correct ratios.

target was found to give, as expected,[4] a very large activity decaying with a half-life of $10' 23'' \pm 5''$. The rate of leak of the electroscope with the target next to the window of the ionization chamber, corrected to what it would be immediately after a very long exposure to $\frac{1}{2}\mu$A of deuterons,[5] was 600 divisions per second, corresponding to an activation probability of 3.6 per million deuterons striking the target. An aluminum target gave an activity with a half-life of 156 ± 5 sec. and an intensity of 50 div./sec.[6]

After this an investigation of possible contamination effects in this type of experiment was undertaken. A piece of platinum sheet was cleaned by holding it at white heat for several minutes in an oxygen flame, and it was then bombarded with deuterons. It showed an activity of 5 div./sec., decaying with a half-life of 126 ± 5 sec. Curve 1 of Fig. 3 is a logarithmic plot of the decay of this effect showing by its linearity that there was only one decay period present and that there was no appreciable carbon contamination. Clean copper and oxidized copper gave identical effects. This made it seem probable that the observed activity came from the gas surrounding the target, and therefore the effects produced on a platinum target when bombarded in various gases were examined. Displacing the air with O_2, H_2 and A reduced the effect to nearly zero; N_2 gave the same effect as air, and CO_2 gave an effect of the same magnitude (5 div./sec.) but decaying with the characteristic carbon period of 10.4 min. Curve 4, Fig. 3, shows the decay of the activity found on platinum bombarded in CO_2.

INTERPRETATION OF THE EFFECT OBSERVED ON PLATINUM

The foregoing results make it obvious that the activity found on platinum when bombarded in air arises from nitrogen and is deposited on the target surface in some way. The existence of convection currents due to the heating of the target and window makes it unlikely that activated atoms in the gas would remain near the target long enough to diffuse to its surface and be adsorbed. It was also found that the active substance was firmly attached to the platinum, being unaffected by hot HNO_3 and only half removed by heating the target to white heat for 10 seconds.

These observations suggested that the activated nuclei were driven into the target surface from the gas by the recoil momentum imparted by the incident deuterons. The following experiment established this mechanism with certainty. A platinum target bombarded in vacuum showed an activity of 2.5 div./sec. decaying with the 156 second period of activated aluminum (curve 3, Fig. 3). This could come only from the aluminum window, and could be transferred onto the target only by recoil.

THE RADIATIONS FROM ACTIVATED NITROGEN

The beta-particles from a platinum target containing activated nitrogen were found by magnetic deflection to have a positive sign. Their absorption in aluminum is shown in Fig. 4, together with that of the beta-particles from activated carbon. From these curves one cannot make a precise estimate of the maximum ranges, but by extrapolating according to the known

[4] H. R. Crane and C. C. Lauritsen, Phys. Rev. **45**, 430 (1934); J. D. Cockcroft, C. W. Gilbert and E. T. S. Walton, Nature **133**, 328 (1934); M. C. Henderson, M. S. Livingston and E. O. Lawrence, Phys. Rev. **45**, 428 (1934).

[5] All rates of leak given in this paper are corrected in the same way.

[6] Further information about the aluminum activity is given by E. McMillan and E. O. Lawrence, Phys. Rev. **47**, 343 (1935).

shape of beta-absorption curves (and taking account of the gamma-ray background) one sees that they cannot be far different from 0.5 g/cm² for activated nitrogen and 0.4 g/cm² for activated carbon. The upper energy limits computed from these values by Feather's[7] formula are 1.2 and 1.0 mv, respectively. The value 1.0 mv for activated carbon is not in perfect agreement with Anderson and Neddermeyer's[8] value 1.2 mv obtained by measuring the curvature of cloud chamber tracks in a magnetic field; whether this discrepancy arises from an underestimate of the maximum range given by our absorption curve or from scattering of the beta-particles producing Anderson and Neddermeyer's tracks must await further experiment for a decision.

Our upper limit of 1.2 mv for activated nitrogen, together with the half-life of 126 sec., places the active substance very slightly above Sargent's[9] upper curve.

The gamma-rays from activated nitrogen produce the same ionization relative to that of the beta-particles as is observed in the case of carbon, which indicates that no intense gamma-ray is present other than the annihilation radiation associated with the emitted positrons (2 quanta of ½mv radiation per beta-particle).

Activation of Gas Targets

Samples of gases activated, transferred to a bulb, and examined by means of their gamma-radiation, gave the following activities: Air, period 126 sec. and activity 0.5 div./sec. (decay shown by curve 2, Fig. 3); nitrogen, the same; CO_2, period 10.4 min. and activity 0.25 div./sec.[10] If one compares the value for CO_2 with the activity produced in a solid carbon target, using the conversion factor between beta- and gamma-ray measurements mentioned above, and remembering that the stopping power per carbon atom is 3.5 times as great in CO_2 as in C, it appears that only one-seventh of the activity produced in the gas passes into the bulb. This is undoubtedly explained by the fact that the active product (N^{13}) is left in the monatomic state after its formation; in this state it is chemically reactive and has a large chance of combining with the brass wall of the activating chamber before forming a stable gaseous compound. Because of this fact no good estimates of activation probabilities can be made from the gas-target experiments.

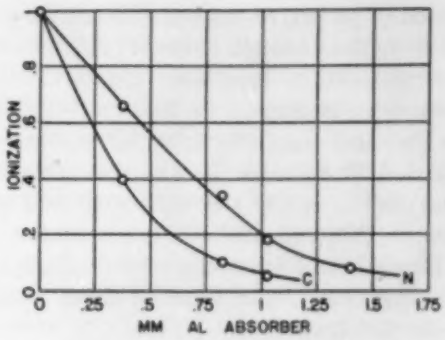

FIG. 4. Absorption in aluminum of the beta-particles from activated nitrogen and carbon.

Chemical Identification of the Active Product from Nitrogen

The active substance produced from nitrogen must be an isotope of C, N or O if it is formed in any expected type of nuclear reaction. A very simple gas analysis was able to show that it is definitely oxygen. A sample of air was activated and allowed to flow into the bulb B_1 (Fig. 2). Then the activating chamber was filled to one atmosphere with hydrogen, which was also let into B_1. The resulting mixture was then passed by way of a platinized asbestos tube P and a $CaCl_2$ drying tube D into the previously evacuated bulb B_2 and flushed through with nitrogen admitted at S. The drying tube and the bulb B_2 were then removed and examined separately for activity. The result was that with the platinized asbestos tube heated to 500°C (being then a very efficient catalyst for the combination of oxygen and hydrogen to form water) the activity went quantitatively into the drying tube; with the platinized asbestos tube cold, it went equally quantitatively into B_2. This is what would be

[7] N. Feather, Phys. Rev. **35**, 1559 (1930).
[8] C. D. Anderson and S. H. Neddermeyer, Phys. Rev. **45**, 653 (1934).
[9] B. W. Sargent, Proc. Roy. Soc. **A139**, 659 (1933).
[10] A search was made also for possible activity produced in deuterium by deuteron bombardment. The activating chamber was filled with ½ atmosphere of deuterium, and no activity was found other than a small effect of 0.01 div./sec. with the carbon period, probably coming from a trace of wax on the surface of the window.

expected of an active oxygen. The added hydrogen is more than enough to convert all the oxygen in the air sample into water; and the active oxygen, even if present as N_2O or NO_2 because of its chemical reactivity after formation, would be carried along with it. On the other hand, carbon (as CO or CO_2) would be reduced to free carbon or CO, and nitrogen or its oxides to N_2 (the formation of ammonia is very slight under these conditions), and none of these would go into the $CaCl_2$ tube.

Nuclear Reaction for the Formation of Radio-Oxygen

The reactions involved in the formation and disintegration of this active oxygen are presumably:

$$N^{14}+H^2 \rightarrow O^{15}+n, \quad (1)$$

$$O^{15} \rightarrow N^{15}+e^+. \quad (2)$$

Since nothing is known about the energy of the emitted neutrons, a mass for O^{15} cannot be calculated. But the energy available in the total process (1)+(2) can be computed, taking $N^{14}=14.0074$, $H^2=2.0136$, $n=1.008$ and $N^{15}=15.0041$.[11] It is found in this way to be 7.3 mv.

Yield of Radio-Oxygen

As explained above, the magnitude of the gas-target effect does not give a trustworthy measure of the activation yield, but it suggests that this yield is of the same order as that for carbon. A better estimate can be made from the activity deposited by recoil. The mean forward momentum of the O^{15} nuclei immediately after formation is 15/16 that of the incident deuterons, the momentum imparted by the expelled neutrons being random in direction and therefore canceling out. The mean forward range of the recoil O^{15} nuclei activated by 2 mv deuterons is accordingly, to a first approximation at least, one mm of air. Nearly the same value is obtained for the N^{13} nuclei produced by the activation of carbon. This means that the activity deposited on platinum in N_2 or CO_2 comes effectively from a layer of the gas of thickness one mm air equivalent.

Since the equilibrium activity of a one mm layer of air when bombarded by $\frac{1}{2}\mu$A of 2 mv deuterons is thus found to be 5 div./sec. (10^5 disintegrations/sec.), the cross section for the activation of nitrogen at this deuteron energy is 6×10^{-27} cm^2. The corresponding cross section for carbon is three times as great, since the same recoil activity is found on platinum bombarded in CO_2, and the number of carbon atoms per unit stopping power in this substance is only one-third as great as the corresponding number of nitrogen atoms in air.

The total activity produced in nitrogen over the whole deuteron range cannot be calculated from the available data, but it can be estimated by assuming that the form of the activation function for nitrogen is about the same as that for carbon. On this assumption the total yields for nitrogen and carbon would be in the same ratio as their cross sections at the maximum energy; the total yield found in this way for 2 mv deuterons in N_2 is one activation per million deuterons. The actual value is certainly somewhat smaller, since the nitrogen activation function is expected to fall off more rapidly at low voltages than that for carbon.

These values of the cross sections and yields cannot be considered as precise, and may easily be wrong by a factor of two. Some justification of the calculations involving the recoil ranges is given by the fact that in the case of Al^6 it was possible to check the computed recoil range experimentally.

Attempt to Activate a Solid Target Containing Nitrogen

The yield values given above suggested that a target of a solid nitrogen compound could be activated to considerable intensity. Trying this with NH_4NO_3 and KNO_3 we found an activity of 8 divisions per second, scarcely larger than that deposited by recoil on platinum. This curious result may mean that oxygen can diffuse readily through a salt of this sort, so that the active substance "evaporates" rapidly from the target.

[11] From the disintegration data of E. O. Lawrence, E. McMillan and M. C. Henderson, Phys. Rev. **47**, 273 (1935).

The Neutrons from Nitrogen

Some evidence for the existence of the neutrons indicated by Eq. (1) has been given by earlier work in this laboratory.[12] A further investigation was made in connection with the present report. The neutron emission was observed by a Wynn-Williams ionization chamber (with a paraffin sheet in front) and linear amplifier, connected to a thyratron scale-of-eight counter. At first an attempt was made to measure the neutrons from gases contained in the activating chamber, placing the counter as close to it as possible (about 15 cm). The numbers of counts obtained with the chamber full of air, CO_2, H_2[13] ($\frac{1}{2}$ atmos.),[13] and evacuated were the same within the constancy of the measurements and were one-sixth as large as the number of counts obtained with a beryllium target in the path of the beam in vacuum just inside the window. This was interpreted as showing that the neutron background (arising partly from contamination throughout the apparatus and partly from the wax and aluminum of the window) was larger than the effects from the gas targets at that distance. It was therefore necessary to place the counter closer to the bombarded gas to obtain significant results. This was done by sliding the counter into the brass tube containing the window, to within 3 cm of the deuteron beam.

With this arrangement counts were made with the bombarding space full of air, nitrogen and oxygen, and also with a clean sheet of copper stopping the beam next to the window. With a deuteron beam of 0.1μ A, the following counting rates were obtained: Copper sheet in place, 500 counts per minute; oxygen target, 500 counts per minute; nitrogen and air targets 700 counts per minute. The difference of 200 counts per minute is attributed to the neutrons from nitrogen; its reality was checked by taking many alternate counts with the copper sheet in and out.

A value for the total neutron yield from nitrogen bombarded by 2 mv deuterons can be obtained from this result if one assumes that one neutron is counted per thousand traversing the counter and notes that the fraction of the total solid angle subtended by the counter at the target is 1/50. The resulting value for the yield is 0.3 per million deuterons; the difference between this and the yield of radioactivity is certainly within the accuracy of these estimates.

[12] E. O. Lawrence and M. S. Livingston, Phys. Rev. **45**, 220 (1934).

[13] This observation of the neutrons from deuterium was made to see whether the enormously large yields reported by other investigators for lower energy deuterons are also produced at 2 mv; it shows that the yield in this case is at most one-sixth of that from beryllium, and is probably less. It must be noted that with the activating chamber filled with deuterium to $\frac{1}{2}$ atmosphere the deuterons use only one-tenth of their range in traversing the gas, since they are just able to cross the chamber when it is filled with air at atmospheric pressure.

Acknowledgments

The authors wish to express their sincere appreciation to Professor E. O. Lawrence for the opportunity of doing this work and to the Research Corporation and the Chemical Foundation for their helpful financial support.

Note on the Spectrum of Boron Fluoride

RAYMOND B. DULL, *Ryerson Physical Laboratory, University of Chicago*

(Received January 23, 1935)

The spectrum of boron fluoride was photographed in the first order of a 21-foot concave grating. Three new bands were found in the ultraviolet, the structure of which appears to be similar to that of the third positive bands of CO. The visible bands, most of which were known previously, are unlike those in the ultraviolet, having a very diffuse appearance.

VERY little is known of the spectrum of boron fluoride. Johnson and Jenkins[1] attempted to photograph it, but failed because of the presence of numerous SiF bands. Since then these experimenters have photographed and classified the bands of SiF, thus simplifying the difficulties involved in examining the bands of boron fluoride.

Since the boron fluoride molecule has the same number of electrons as N_2 and CO, its electronic structure should be similar to that of those molecules. Johnson and Tawde,[2] although they succeeded in photographing the boron fluoride spectrum with a Hilger E1 spectrograph, failed to find any resemblance between its bands and those of CO and N_2.

In the present investigation boron trifluoride was generated by treating a finely powdered mixture of calcium fluoride and boric anhydride with concentrated sulfuric acid. The gas was passed through a drying tube of phosphorus pentoxide, and through traps of fused sodium fluoride to remove hydrogen fluoride. A capillary discharge tube with nickel electrodes was used as a light source. Best results were obtained at a pressure of about 5 mm and with a current of 10 milliamperes. The photographs were taken with a 21-foot concave, Paschen mounted grating, having 14,000 lines per inch. Good first order plates were obtained, the dispersion being about 2.4–2.5A per millimeter, but the source was too weak to produce good second and third order plates. The exposure time ranged from twelve to sixty hours.

BANDS IN THE VISIBLE REGION

As Johnson and Tawde[2] pointed out, the bands in the visible region are unlike any in the spectra of N_2 and CO. The bands seem to be too diffuse to show much rotational structure.

In the writer's photographs, as in those of Johnson and Tawde, there is a background of many unresolved lines, extending from λ3500 into the red. These may be due to BO, but perhaps also to CO_2, since this has been observed to accompany the third positive CO bands,[3] which are very prominent in the present photographs. Table I contains measurements on the band heads by Johnson and Tawde, and by the present writer.

TABLE I. *Wavelengths of band heads observed by Johnson, Tawde and the present writer.*

Bands degrading to the violet				Bands degrading to the red			
Johnson and Tawde		Present work		Johnson and Tawde		Present work	
λ(A)	Int.	λ(A)	Int.	λ(A)	Int.	λ(A)	Int.
6399.7 ?	3	—	—	5476.3	2	—	—
6395.5 ?	1	—	—	5471.8	6	5470.8	6vd
6327.1 ?	3	—	—	5460.8	10	5460.1	4vd
6323.5 ?	2	—	—	5457.7	8	5456.8	8vd
6176.1	4	—	—	5451.1	4	4550.2	4vd
6112.2	4	—	—	5447.9	4	5447.0	4vd
				5441.5	1	—	—
5993.7	8	5993.8	8vd	5437.2	3	5436.7	3vd
5983.9	6	5984.4	6vd	5435.5	2	—	—
5975.6	4	5974.3	4vd	5421.6	2	5420.6	2vd
				4465.0	8d	4464.9	8vd
—	–	5825.7	7vd	4461.7 ?	8d	4461.4 ?	6vd
5822.1	10	5822.1	10vd	4460.4 ?	6d	—	—
5814.3	8	5815.1	8vd	4443.5	8d	4443.5	6vd
5806.9	6	5807.3	6vd	4440.2 ?	6d	—	—
5803.5	6	5803.8	6vd	4438.8 ?	6d	—	—
5663.8	6	5664.0	6vd				
5655.9	3	—	—				
5649.8	1	—	—				
5646.3	1	—	—				

d = diffuse, vd = very diffuse.

[1] R. C. Johnson and H. G. Jenkins, Proc. Roy. Soc. **A116**, 327 (1927).

[2] R. C. Johnson and N. R. Tawde, Phil. Mag. **13**, 501 (1932).

[3] G. H. Dieke and J. W. Mauchly, Phys. Rev. **43**, 12 (1933).

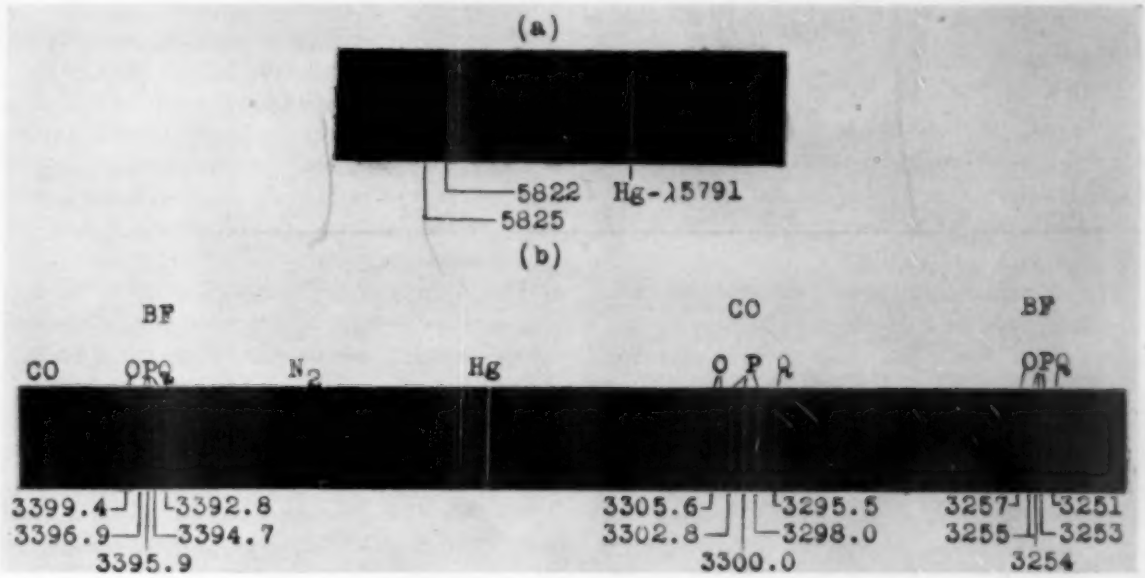

FIG. 1. (a) Part of visible spectrum, showing diffuse looking BF (?) bands. (b) Ultraviolet bands showing structure similar to the CO third positive band λ3305.

NEW BANDS

In addition to the bands listed above, the present investigation revealed three new bands, all in the ultraviolet region, and degrading to the ultraviolet. These bands differ greatly in appearance from those in the visible region. They appear to be similar in structure to those of the third positive group of CO (Fig. 1b, where one of the third positive CO bands appears strongly in the same region as the BF bands shown). Dieke and Mauchly[3] have made an analysis of these CO bands, and have shown them to belong to a $^3\Sigma \rightarrow {}^3\Pi$ transition. A comparison of the BF and CO bands seems to indicate that the former are either $^3\Sigma \rightarrow {}^3\Pi$ or $^3\Pi \rightarrow {}^3\Sigma$ transitions. The heads of the BF bands are lettered in Fig. 1b to correspond with similar heads of the CO bands. Proof that the *O*, *P* and *Q* branches have been identified correctly cannot be definitely established until an analysis of the bands has been made. The triplet separation shown by the new BF bands is much smaller than that in the $^3\Pi$ state of the third positive bands of the CO molecule, indicating that the BF bands are nearer case *b* type than the CO bands. The *O* branches of the BF bands are much fainter than the corresponding branches of the CO bands; in fact only one of the *O* branches is intense enough to be observed. This fact is further evidence that the $^3\Pi$ state of BF, presumably involved here, is nearer case *b* type than that of the third positive CO bands.

There are a number of faint lines on the long wavelength side of the observed *O* branches. These lines are hidden, in the case of the BF band λ3399.40, by the 5*B* band of CO at λ3419. Dieke and Mauchly[3] found similar lines on the long wavelength side of the *O* branches of the CO bands. They assigned these lines to an *N* branch (Table II).

TABLE II. *New bands.*

λ	Int.	λ	Int.	λ	Int.
3552.2	1	3399.40	3	3256.61	5
3549.9	2	3396.94	5	3254.76	7
3548.6	4	3395.96	6	3253.77	8
3547.3	4	3394.71	7	3252.73	9
3545.4 ?	4	3392.85	8	3250.94	10

There is evidence of another band in the region λ3720–λ3670, but the background is so strong that no definite proof of its existence can be offered.

Suggestions for Further Work

There are indications of the presence of faint bands in part of the region obscured by the background. It would be interesting to examine this region for such bands, and to determine whether they are to be classed with those observed in the ultraviolet, or with those in the visible region.

The rotational analysis of the ultraviolet bands should be feasible if undertaken with a stronger source and somewhat greater resolution than here. Such an analysis may be facilitated by the work of Dieke and Mauchly[3] on the probably similar third positive group of CO.

No explanation can be offered for the diffuse appearance of the bands in the visible region. It may be caused by predissociation in the upper state, or perhaps these bands are due to BF_2 or BF_3, and not to the diatomic molecule BF.

The writer wishes to acknowledge the suggestions and helpful advice which Professor R. S. Mulliken has given in the course of this work.

MARCH 15, 1935 PHYSICAL REVIEW VOLUME 47

Spectral and Impact Phenomena in the Faraday Dark Space

K. G. Emeleus and O. S. Duffendack, *Department of Physics, University of Michigan*

(Received December 17, 1934)

Observations on the spectra of the negative glow and Faraday dark space in pure helium and in helium containing a trace of nitrogen lead to the conclusion that in the negative glow the phenomena are due mainly to collisions of fast (primary) electrons with normal atoms while in the Faraday dark space impacts of the second kind between normal and metastable atoms are of primary importance. The metastable atoms present in the latter region are probably produced by the absorption of resonance radiation from the negative glow and are thus in the 2^1S state. The negative glow proper emits the He I and He II lines strongly and a band spectrum of He_2. The band spectrum is, relatively, much stronger in the region of transition between the negative glow and the Faraday dark space and this last region emits only the He I line $\lambda 5016$ (2^1S-3^1P) in sufficient intensity to be observed. When a trace of nitrogen is added to the helium, the N I spectrum replaces the He_2 bands in the transition region. A consideration of the phenomena observed leads to the conclusion that $He_2 2^{1,3}\Sigma$ molecules are formed by the union of a 1^1S atom and a $2^{1,3}S$ atom in a three body collision and that the possibility of observing the visible He_2 bands at all depends on the metastable nature of the $2^3\Sigma$ level of the He_2 molecule. These metastable molecules are excited to higher levels by slow electron impacts in pure helium, whereas when nitrogen is present, they are destroyed by impacts of the second kind with nitrogen molecules before they can be excited. N_2 molecules may be dissociated in these collisions, the dissociation occurring as a secondary consequence of the molecule's being raised to a higher electronic level from which dissociation occurs through predissociation or because the upper level is repulsive or simply because the molecule is excited to a degree above its dissociation asymptote. The effects from admixtures of oxygen and of carbon monoxide to helium and similar experiments on neon and argon support the conclusions drawn from the phenomena observed with helium and helium-nitrogen mixtures.

Introduction

THE Faraday dark space is the name given to the feebly luminous space between the two regions of strong luminosity in the fully developed glow discharge. It is bounded fairly sharply at its anode end by the positive column and passes without sharp demarcation into the negative glow at its negative end. Early measurements on the electric field in this region indicated that the field is very small, or even reversed[1] for electrons, and more recent measurements[2] confirm this observation, the current being due to a concentration gradient[3] of ions and electrons. The properties of the negative glow and the Faraday dark space together approximate those

[1] J. J. Thomson, Phil. Mag. **18**, 441 (1909).
[2] McCurdy, Phil. Mag. **46**, 524 (1924); Compton, Turner and McCurdy, Phys. Rev. **24**, 597 (1924).
[3] Emeleus and Harris, Phil. Mag. **4**, 49 (1927).

of a plasma,[4] but an attempt to formulate an exact quantitative theory of these regions on this basis proved unsatisfactory,[5] the fundamental difficulty being that the rate of ion formation at different distances from the cathode was unknown. The nature of the ionizing agent was uncertain, it being improbable that fast electrons from the cathode dark space could penetrate far into the negative glow in any considerable numbers, although probe analyses[6] indicate that such are present. It now appears that a too simple model had been adopted.

From the spectra emitted by different regions the negative glow and Faraday dark space may be divided into four merging regions, *viz.*, I the negative glow proper, II the region of transition from negative glow to Faraday dark space, III the main Faraday dark space and IV the region of transition from the Faraday dark space to the positive column. In IV there is a considerable accelerating field for electrons toward the anode, a case that has been treated theoretically by Sir J. J. Thomson and G. P. Thomson.[7] The existence of a difference in the spectra of II and III (usually treated together) and I has been recognized for some time, a part of II and III often being called the "aureole." From a spectroscopic study of this in neon and argon, Druyvesteyn[8] concluded that its special properties were due to the presence of metastable atoms formed as a secondary result of the absorption of ultraviolet resonance radiation from I.

In the present work we have studied the regions I, II and III mainly by spectroscopic methods and used the three lightest inert gases, both pure and with controlled contaminations. We believe that, in I, collisions of fast electrons with normal atoms are of primary importance,[9] in III, impacts of the second kind with metastable atoms, and in II, the combined effects of electrons and metastable atoms. The investigation has proved of interest in other connections: (1) Since diffusing resonance radiation occurs in III, spectroscopic studies on this region give rather direct information about secondary effects of this diffusion in inert gases obtained otherwise only by indirect electrical methods.[10] (2) Some information has been obtained which bears on two molecular problems, namely, the formation of helium molecules and the dissociation of nitrogen. (3) The results lead to a clearer understanding of the mechanism of chemical reactions in this part of the discharge. This will be dealt with elsewhere.

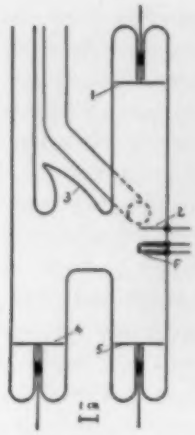

FIG. 1. Glow discharge tube. 1, 4, 5, circular disk electrodes; 2, semicircular disk electrode; 3, light trap; *F*, filament.

EXPERIMENTAL ARRANGEMENTS

The tubes used were (i) a cylinder 3.5 cm in diameter with two disk electrodes of nickel and one copper wire electrode between the two disks; (ii) the tube shown in Fig. 1 with a variety of tungsten electrodes, which, used in turn, enabled us to avoid sputtered regions and thus prolong the life of the tube; (iii) a bulb 8 cm in diameter, stemmed with a vertical tube 3 cm in diameter and containing a small anode at the center of the bulb and a nickel disk cathode movable vertically in the stem. Tube (ii) proved very useful and most data were taken with it. Direct-current discharges of from 0.1 to 10 milliamperes per cm^2 at 150 to 1000 volts were run in helium, neon and argon, respectively, at pressures from 0.5 to 7 mm. The helium and the neon were purified

[4] Langmuir and Tonks, Phys. Rev. **34**, 896 (1929).
[5] Cowan, Thesis, Belfast (1931).
[6] Emeleus and Brown, Phil. Mag. **7**, 17 (1929); Emeleus, Brown and Cowan, Phil. Mag. **17**, 146 (1934).
[7] Thomson and Thomson, *Conduction of Electricity through Gases* Vol. II, p. 361.
[8] Druyvesteyn, Zeits. f. Physik **57**, 292 (1929).
[9] Emeleus, Brown and Cowan, Nature **127**, 593 (1931).
[10] Kenty, Phys. Rev. **44**, 891 (1933); Duffendack and Smith, Phys. Rev. **43**, 586 (1933).

by prolonged standing over charcoal cooled by liquid air and the argon was purified by the use of mischmetal arcs. During use with tubes (ii) and (iii), the gas was circulated, and the final purification of the gas was effected by passing it, immediately before admitting it into the discharge tube, through a strong glow discharge between tungsten plate electrodes. The criterion aimed at was freedom from spectroscopic impurities in the visible and near ultraviolet. The only contaminant found was neon in the helium used with (ii) and (iii) and this was probably present to less than 0.05 percent. When required, nitrogen from sodium azide, or oxygen from potassium permanganate was added. In this case, the auxiliary discharge in the circulating system was discontinued. In the observation of the spectra final recourse was always had to photography.

Spectroscopic Data

1. *Pure helium.* Our results are essentially similar to those of Seeliger and Mierdel,[11] who first investigated this case, and of Keyston.[12] Region I (green) is a strong source of the singlet He I and He II lines by virtue of the excitation by high speed electrons. Bands are present also and these include some from high electronic levels so that it is possible that a recombination spectrum of He_2 is present. This can, however, account for only a part of the band spectrum. Region II (peach) is a strong source of He_2 bands which are relatively far less intense in I in comparison with the He I lines than they are in II. The light from III is very feeble and we are certain only that it emits the He I line 5016 (2^1S-3^1P).

Formation and excitation of He_2 molecules

A consideration of our results in comparison with those of other observers and in the light of present knowledge of kinetic and spectral theories, leads us to the conclusion that He_2 molecules are formed in three body collisions involving two normal 1^1S atoms and one metastable $2^{1,3}S$ atom. The resulting molecule will be in the $2^1\Sigma$ or $2^3\Sigma$ state, depending upon whether the metastable atom is 2^1S or 2^3S. $2^3\Sigma$ molecules are metastable and are therefore subject to higher excitation by electron impact. It is this metastable character of the $2^1\Sigma$ molecules that enables us to observe the visible helium bands at all.

To discuss these results we need certain numerical data, *viz.*, (1) the mean life of an excited He atom or He_2 molecule, about 10^{-7} sec. if in an unstable, excited state, and infinitely large, for present purposes, if metastable; (2) the mean time between kinetic theory collisions of the He atoms, about $10^{-7}p^{-1}$ sec. under discharge condition ($\sim 350°K$) at a pressure of p mm; (3) the fundamental vibration time[13] of the lowest $^3\Sigma$ state of He_2, approximately 2×10^{-14} sec. We cannot carry out better than order of magnitude calculations, and to that approximation (2) will also give the time between the collision of normal He atoms and excited atoms or molecules, and (3) the effective time of contact of 2^3S and 1^1S He atoms on impact when they separate again without permanent molecule formation.

Seeliger and Mierdel supposed the relative weakness of bands in I was due (a) to the He_2 molecule's being formed from one metastable and one normal atom, and (b) to the loss of metastable atoms by their reverting to the normal state by impacts of the second kind with slow electrons. These processes are compatible with data now available. The chance of two atoms uniting to form a molecule in a two-body collision in the gas phase is known to be very small, and hence the approximate equality of the times (1) and (2) under typical discharge conditions shows that most unstable excited atoms will revert to the normal or to a lower excited state by radiation in preference to disappearing by molecule formation. Assuming that (b) is correct, in the form that metastable atoms are removed by either first or second type collisions with slow electrons, probe analyses of discharges enables an estimate to be made of the chance of molecule formation on collision between a metastable atom and a normal atom. From simple kinetic theory considerations, the relative chances that an electron will collide with the metastable atom and that a normal atom will collide with

[11] Seeliger and Mierdel, Zeits. f. Physik **19**, 230 (1923).
[12] Keyston, Phil. Mag. **15**, 1162 (1933).
[13] Jevons, *Report on Band Spectra.*

it are about in the ratio $0.2n_e/n_{He}(m_{He}/m_e)^{\frac{1}{2}} \times (T_e/T_{He})^{\frac{1}{2}}$, where n denotes concentration, m mass, T temperature of the electrons and atoms, respectively, and the numerical factor allows roughly for the difference in mean free path for an electron and an atom neglecting Ramsauer effects. Under typical negative glow conditions,[6] ($n_e = 10^{10}$ per cc, $T_e = 7000°K$) this is of the order 10^{-5} at 1 mm pressure. Hence, if metastable atoms are preferentially destroyed by electron collisions, the chance of molecule formation on atom collisions must be of this order or less. This, again, is compatible with a three-body process for the formation of He_2 (the third atom taking off excess kinetic energy), the chance of a third 1^1S atom colliding with a potentially combining $1^1S + 2^{1,3}S$ pair during the time (3) being, from (2), about $10^{-7}p$. This chance being proportional to p is in accord with the well-known high pressure character of the He_2 bands and their absence from stellar spectra,[14] which are produced under essentially low-pressure conditions.

Seeliger and Mierdel's process (a) is not in itself sufficient to account for the production of the visible band spectrum, since it gives rise to He_2 molecules only in the $2^{1,3}\Sigma$ states, whereas the bands arise in transitions from higher levels. A second process must be involved in reaching the higher levels. This process is, fairly certainly, electron collision with $2^{1,3}\Sigma$ He_2 molecules. From the numerical considerations already advanced it is clear electron collision can only be of importance if these molecules are metastable. Since the ground state of He_2 is $1^1\Sigma$ (a repulsive level) and radiative intercombinations do not occur in this light molecule, the $2^3\Sigma$ state is metastable, the $2^1\Sigma$ not. The possibility of observing the visible He_2 bands at all appears to depend, then, on the metastable nature of the $2^3\Sigma$ level, a result which has a bearing on the spectroscopic properties of Ne_2.[14a]

The part played by this level also enables us to understand the preponderance of triplet bands in the visible spectrum, particularly in the "uncondensed" positive column.[12] The reason is that changes in multiplicity produced as a result of electron impact occur most readily when the electron energy available is not much in excess of the minimum required to effect the transition, whereas inelastic impacts which do not involve a change in multiplicity take place most efficiently when there is considerable excess energy. The excitation energy of higher states[13] from $2^3\Sigma$, the effective ground state in this case, is of the order of 3 volts, whereas to produce the metastable 2^3S parent atom from the normal 1^1S atom requires 19.7 volts. In a simple system such as the uncondensed positive column, where most of the free electrons are included in a single group of rather high mean energy, comparable with that of the least excitation potential of the gas, or rather less, the conditions for the formation of 2^3S atoms in quantity is thus incompatible with that for producing excited singlet molecular states. It is only when the distribution of energy amongst the free electrons is more complex, with one group of high energy and one of low energy present simultaneously, as in the negative glow at medium pressures, that conditions are right for producing, first 2^3S atoms, and second both excited singlet and triplet molecular states from the $2^3\Sigma$ molecules. Conditions in a condensed positive column appear to approximate to those in the negative glow.[15] The importance of having very pure helium to obtain the bands can now be understood, since it is necessary not only that the metastable 2^3S atoms be not quenched by collisions with impurities, but also that the metastable $2^3\Sigma$ molecules are not lost likewise.

The spectrum of the Faraday dark space

The spectrum of III in impure helium indicates that it contains metastable atoms. So far as they are produced by absorption of resonance radiation, they must be in the 2^1S state, since there is no intercombination resonance line in He I. The observed emission of 5015 ($2^1S - 3^1P$) can be ascribed to fluorescence of these metastable atoms in the green light from the negative glow with probably also a stronger infrared fluorescence of $2^1S - 2^1P$. Absence of He_2 bands would go with the absence of 2^3S atoms, or, if these were present (produced by electron impact with 1^1S or 2^1S atoms), with the known small concentration of electrons to excite them to higher

[14] Struve and Christy, Astrophys. J. **71**, 277 (1930).

[14a] Emeleus and Duffendack, Phys. Rev. **44**, 945 (1933); Druyvesteyn, Nature **128**, 1026 (1932), has obtained bands which he attributed to a HeNe molecule.

[15] K. G. Emeleus and F. M. Emeleus, Phil. Mag. **8**, 383 (1929).

molecular states. The bands are strong in II because there is a large concentration of both fast electrons to produce 2^3S atoms, and slow electrons to excite the $2^3\Sigma$ molecules. We were unable to excite bands in III by injecting electrons from the filament F of tube (ii). Positive space charge sheaths in II were observed to be green, emitting the 5016 line but not the bands. The origin of this singlet line in these sheaths may be the same as in III, but perhaps also partly due to direct excitation of 3^1P by electrons emitted by secondary processes at the walls and accelerated in the sheath. In any event, the absence of bands follows from the small concentration of electrons in the sheaths.

The excitation of gas admixtures

2. *Helium, neon and argon+nitrogen.* When nitrogen is added to pure helium, the N I spectrum replaces the band spectrum of He_2. Lines of N I are visible with 0.05 percent nitrogen, N I lines and He_2 bands are about equally intense with one percent nitrogen, and the He_2 bands disappear when the percentage of nitrogen is increased to three percent. Concentrations of nitrogen greater than five percent were not studied but cannot result in much further increase in the strength of N I. This spectrum is not observed in I, II or III with pure nitrogen.[16] The negative bands of N_2^+ appeared in the same parts of the tube as the N I lines, and, in addition, were the only spectrum observed from III and the space charge sheaths. These latter turned blue on account of these bands. The intensity of the bands in III was a maximum for some two percent nitrogen, and they were not visible with five percent nitrogen. Neither N I lines nor N_2^+ bands were observed with neon-nitrogen and argon-nitrogen mixtures.

The initial levels of the N_2^+ bands are probably excited by second type collisions between metastable He atoms and normal $^1\Sigma N_2$ molecules, as follows:

$$He(MS)+N_2 \rightarrow He(1^1S)+N_2^+\delta(B\Sigma^2)+e.$$

The energy discrepancy is much less than one volt, the energy of ionization and excitation of N_2 being 19.6 volts,[17] and the process thus likely. It is not known if one or both of the metastable states of He are involved, although it is probably mainly the singlet state in III. The weakness of the negative bands in II for higher concentrations of N_2 may be ascribed to the absorption of He resonance radiation by nitrogen between I and III, or to the quenching of metastable He atoms by collision with N_2 molecules in the same region. The energy of metastable Ne and A is too small for the excitation of the N_2 bands.

The production of N I is more complicated. Duffendack and Wolfe[18] have already shown it to be a two stage process, the first being supposed to be the dissociation of N_2 into two normal (^4S) atoms. Dissociation by electron impact, although possible,[19] can be ruled out as an important factor in the present case from the absence of N I lines in a similar discharge in pure N_2[16] and, furthermore, that metastable He is involved one may deduce from the observed steady replacement of He_2 bands by N I lines on adding N_2 to He. It cannot, however, be decided from this observation whether the metastable systems are $2^{1,3}S$ He atoms or $2^3\Sigma He_2$ molecules. In any case, if the resulting atoms of nitrogen are in the normal state, the difficulty arises that there is a large energy discrepancy, as the heat of dissociation of N_2 is less than 8 volts and the energy of the metastable He atoms about 20 volts and that of the metastable He_2 molecules about 17.5 volts.[20] The evidence that the N atoms are in the normal state is itself not conclusive, as the dissociation $N_2 \rightarrow N(^4S)+N(^4P)$ is possible, it being only that the intensity distribution in the N I spectrum is much the same when it is produced in a heavy current arc at high pressure,[21] on the cathode of the glow discharge in the pure gas,[16] and in the present case and in the presence of argon.[22] This similarity is understandable if in each case the excitation, after the atoms have once been formed, is by electron collisions with them in the ground state.

We attempted to decide this by examining the line width of the stronger visible N I lines with a Fabry-Perot interferometer. They might be

[16] Emeleus and Hall, Proc. Roy. Irish Acad. **A40**, 1 (1931).
[17] Smyth, Rev. Mod. Phys. **3**, 347 (1931).
[18] Duffendack and Wolfe, Phys. Rev. **34**, 409 (1929).
[19] Kondratew, Zeits. f. Physik **38**, 346 (1926); Turner and Samson, Phys. Rev. **34**, 743 (1929).
[20] Mullikan, Rev. Mod. Phys. **4**, 61 (1932).
[21] Ryde, Proc. Roy. Soc. **A117**, 164 (1927).
[22] Anderson and More, Phys. Rev. **38**, 1995 (1931).

expected to be broadened if there were the large energy discrepancy mentioned going into kinetic energy of the N and He atoms. No broadening was found with a 17.5 mm etalon, nor was any found with a slightly different form of $He-N_2$ discharge by Bacher.[23] However, calculations like those made for pure helium show that even if the N atoms were formed in the ground state with high kinetic energy, they would make some million collisions with other atoms or molecules before excitation by electron impact and would by that time be in thermal equilibrium with the gas.

Cameron[24] obtained N I lines in $Ne-N_2$ discharges. His observations are, however, unreliable, since his neon probably contained helium.[25] Anderson and More[22] produced the N I lines in a low voltage arc in $A-N_2$ mixtures, contrary to a negative result under similar conditions by Duffendack.[26] The only obvious difference in the experiments is that Anderson and More used an oxide coated filament and Duffendack bare tungsten. In view of the rapid interaction between hot tungsten and N atoms, it is possible that in Duffendack's tube the tungsten filament kept the N atom concentration low. Whatever the reason, it is clearly much easier to produce the N I spectrum in helium than it is in argon or in neon.

An ultimate explanation may be looked for on the following lines. The dissociation of N_2 to 2N on impact with a metastable atom of sufficient energy may occur either by increase in vibrational energy in the $1^1\Sigma$ ground state of N_2 or as a secondary consequence of the molecule's being raised to a higher electronic level from which dissociation occurs either through predissociation or because the upper level is repulsive, or simply because it is excited above its dissociation asymptote. So far as energy considerations go, any upper level can be reached in the latter manner if some one of its sublevels has less energy than is possessed by the metastable particles. Since, however, the changes involved are electronic, we might expect the internuclear distance to be fairly closely conserved as in Franck-Condon transitions. Thus the transition becomes comparable to an atomic energy interchange in requiring fairly close energy resonance for the transition to be a probable one. Compared with an electronic change at close resonance, the direct vibrational dissociation is unlikely.[27] The experimental evidence points, then, to the dissociation of N_2 in He being due to an electronic transition in N_2 with close resonance, followed by a separation of the atoms, and in Ne and in A to any dissociation either through an electronic transition with less close resonance or by vibrational dissociation. Knowledge of the electronic levels of N_2 is too fragmentary to make further discussion worth while, but it may be noted that when once a case of dissociation through an electronic change has been established, it provides a way for obtaining a point on a $V-r$ curve for a molecule which it may not be possible to obtain otherwise.

3. *Helium and oxygen.* With about one percent O_2 in He, III turns a brilliant apple-green and shows the first negative bands of O_2^++. No such effect was observed with Ne or A. The initial state of the O_2^+ bands ($b\,^4\Sigma?$) requires about 19.5 volts[28] for excitation from the normal $(^3\Sigma)O_2$, so that the interaction

$$He(MS)+O_2=He(1^1S)+O_2^+(b\,^4\Sigma?)+\text{electron}$$

is likely. Metastable Ne and A have again too little energy to effect the transition.

4. *Helium and carbon monoxide.* This mixture was studied by Seeliger and Mierdel[11] who found that the Baldet-Johnson bands of CO^+ replaced those of He_2 in the aureole. The upper state of these is $B\Sigma^2$, with its state of least vibrational energy about 19.6 volts above the normal state of CO,[17] and hence the resonance:

$$He(MS)+CO=He(1^1S)+CO^+(B\Sigma^2)+\text{electron}$$

is again likely. Seeliger and Mierdel did not observe the ultraviolet $B\,^2\Sigma-X\,^2\Sigma$ negative bands of CO^+, but they must certainly have been present as they are enhanced in other discharges in He–CO mixtures.[29] It is noticeable that with both CO and N_2, the foot of the $V-r$ curve for the ionized state excited by metastable helium is almost directly above the foot of the curve for

[23] Bacher, Phys. Rev. **43**, 1001 (1933).
[24] Cameron, Phil. Mag. **1**, 405 (1926).
[25] According to later work by one of us (K.G.E.) with the same specimen of neon.
[26] Unpublished observation.
[27] Dr. H. S. W. Massey informs us this is the case.
[28] Roy. Phil. Mag. **15**, 421 (1933).
[29] Weizel, *Bandenspektren*, p. 393.

the normal molecule. The same may also be true of O_2 and O_2^+.

5. *Helium and mercury and molybdenum.* These provide apparent exceptions to the principle of resonance. With a trace of the vapor of either metal in helium, a strong development of its arc spectrum was observed in the aureole. The energy discrepancy, if the initial states are produced by impacts with metastable helium atoms in a single act, would be in each case greater than 10 volts. Insufficient data are available to make an attempt at an explanation of these cases profitable.

Mechanism of the discharge

The results of the last section, taken with those obtained by Druyvesteyn,[8] show the importance of resonance radiation and metastable systems in II and III. In several cases (e.g., O_2 admixture in He), new ions result through their action, and it was, in fact, observed in these cases that there was a great increase in conductivity relative to the conductivity of the pure gas. With O_2 in He at 2 mm this was some fivefold for a one percent admixture; with N_2 rather less. However, beyond the recognition of the importance of such processes, the general theory of the Faraday dark space is not advanced quantitatively since we do not know either the concentration of metastable systems or the efficiency of their second type interactions in any individual case. The discharge properties of gases of extreme purity[10] become an interesting problem, and also the question of whether such purity can be attained in a glow discharge. More generally, the difficulty in the way of formulating an exact theory in this and many other cases comes from our very incomplete knowledge of the extent to which the system as a whole departs from a state of thermal equilibrium. We merely know that this is approached in certain unit processes occurring (such as those effecting energy interchanges amongst the free electrons of low energy which have almost a Maxwellian energy distribution),[6] and must, therefore, pick out the individual atomic and molecular acts which seem likely to be of most significance under the circumstances and examine their consequences as far as we are able. The model of the discharge then errs on the side of simplicity, and it is to the neglect of important factors (perhaps the formation of negative ions) that we may attribute the failure of the present theory to explain, in the present case, such phenomena as the occasional appearance of striations in the Faraday dark space.[30]

A consideration of all the data at present available seems to point to the following conclusions. The negative glow proper, region I, is produced by the excitation of the gas molecules by high speed primary electrons. Simultaneous ionization and the excitation of the resultant ion is responsible for the spark spectra and negative bands observed in the negative glow. In the transition region II the effects of electron impacts are of less importance and the effects of the absorption of resonance radiation and of impacts of the second kind with metastable atoms and molecules become important. In region III, the phenomena are due almost wholly to these latter effects. The current through the Faraday dark space is a diffusion current of electrons and positive ions giving a resultant electron current toward the anode.

The results have an application in spectroscopy. A common method for exciting spectra of an element is to volatilize it in a hollow cathode tube in an inert gas, when excitation of the added material occurs through second type collisions between the metastable atoms and ions of the inert gas and the added atoms.[31] The somewhat different properties of I, II and III suggest that differential excitation might be observed if the three regions, or some of them, were observed separately instead of, as in the usual form of hollow cathode tube, effectively together.

The greater part of the experimental work was done at the University of Michigan during 1932–33. One of us (K.G.E.) gratefully acknowledges the facilities put at his disposal by Professor H. M. Randall during this time while he was a guest of the University. Mr. A. Helz gave much help with the experiments.

[30] Holm, Phil. Mag. **11**, 194 (1931); Zeleny, Nature **125**, 562 (1930).

[31] Duffendack, Henshaw and Goyer, Phys. Rev. **34**, 1132 (1929).

The Probability of Collision for Slow H^+, $(H^1H^1)^+$, $(H^1H^2)^+$, $(H^2H^2)^+$, $(H^2)^+$ and He^+ Ions in Argon

EDWARD B. JORDAN,* *University of California, Berkeley*

(Received December 24, 1934)

The probability of collision P_c for slow H^+, $(H^1H^1)^+$, $(H^1H^2)^+$, $(H^2H^2)^+$, $(H^2)^+$ and He^+ ions in argon has been measured. The energy range studied was 225 to 4200 volts for the H^+ and $(H^1H^1)^+$ ions, 225 to 1300 volts for the $(H^1H^2)^+$, $(H^2H^2)^+$ and He^+ ions and 300 to 1225 volts for the deuteron hydrogen molecular ion $(H^1H^1)^+$ beam. The probability of collision for the $(H^1H^1)^+$ ion decreased from a value of $P_c=56$ at 225 volts to a minimum value of 48 at 784 volts with a subsequent increase to $P_c=57$ at 3840 volts. The proton curve increases from $P_c=38$ at 225 volts to $P_c=46$ at 4220 volts. It gradually flattens out at the higher voltages. The $(H^1H^2)^+$ and $(H^2H^2)^+$ curves remain nearly constant at $P_c \leqq 41$ and 39, respectively, while the He^+ curve decreases from $P_c=28$ at 225 volts to 24 at 1225 volts. The curve obtained by using a deuteron hydrogen molecular ion beam shows two distinct minima at 380 volts and 806 volts. The percentage of $(H^1H^1)^+$ ions in the beam was estimated to be 15 percent. The $(H^1H^1)^+$ and H^+ curves, and the $(H^1H^1)^+$, $(H^1H^2)^+$, $(H^2H^2)^+$ and He^+ curves are grouped separately for comparison, and the probable processes in each case are discussed. It is significant to note that the heavier isotopic molecular ions have a longer mean free path in argon than the lighter $(H^1H^1)^+$ ion. A possible source of the discrepancies between the results of different authors in this field is discussed.

INTRODUCTION

IF a positive ion is sent into a gas, there is a certain chance that it will reach a point, a given distance in the direction of its initial velocity, in its original condition. The chance is known to be an exponential function of the pressure, distance and a term called the probability of collision,[1] P_c which depends on the process involved and is a function only of the nature of the ion, its velocity and the nature of the gas. The unit of P_c is cm^2/cm^3 or $1/cm$. It may be interpreted either as an area per cubic centimeter per unit pressure at 0°C or as a number of collisions per unit ion current per unit path length per unit pressure at 0°C. The latter interpretation is used throughout this paper. The effective area q for a single atomic collision is found by dividing P_c by the number of atoms per unit volume per unit pressure. If the unit of pressure is one mm Hg at 0°C and the unit of volume one cubic centimeter then $q=0.281 \times 10^{-16} P_c$ cm^2. The mean free path is given by $1/P_c p$ where p is the pressure in mm Hg at 0°C. A determination of P_c and a knowledge of the process involved is very important in the study of gaseous discharge phenomena.

The first quantitative measurements of P_c were made for slow protons in hydrogen. Aich[2] in 1922 found that the collision radius of an H_2 molecule and a 25-volt proton was approximately the same as the kinetic theory value of the radius of the H_2 molecule.

In 1925, Dempster[3] studied the nature of the collisions between H^+, H_2^+, He^+ ions and helium atoms. He concluded that no ionization was produced by 900-volt protons and that the decrease in intensity of a proton beam in helium was due chiefly to small angle scattering, and not to neutralization. Neutralization of the He^+ ions usually occurred upon the first collision while the H_2^+ ions were for the most part dissociated. The direction of the dissociated H^+ ion was at a small angle to that of the parent H_2^+ ion. G. P. Thomson[4] likewise found appreciable small angle scattering for protons of 5000 to 25,000 volts energy in hydrogen, helium and argon.

The next important measurements were made in 1930 by Holzer.[5] He found a variation of P_c with ion velocity when H^+, H_2^+ and H_3^+ ions were sent into hydrogen gas. The velocity range corresponded to a change in energy of 60 to 850 volts. The probability of collision for the H_3^+ ion was found to be smaller than the corresponding value for the H_2^+ ion. He concluded that the absorption of H_2^+ by hydrogen was due to

* National Research Fellow, Harvard University.

[1] R. B. Brode, Rev. Mod. Phys. **5**, 258 (1933).

[2] W. Aich, Zeits. f. Physik **9**, 372 (1922).

[3] A. J. Dempster, Proc. Nat. Acad. Sci. **11**, 552 (1925).

[4] G. P. Thomson, Phil. Mag. **1**, 961 (1926).

[5] R. E. Holzer, Phys. Rev. **36**, 1204 (1930).

neutralization while the important factor in the absorption of H^+ and H_3^+ was scattering. Holzer[6] later reported some measurements for H^+, H_2^+ and H_3^+ ions in argon and helium but did not give the magnitudes of his values.

In 1931, Ramsauer, Kollath and Lilienthal[7] measured the probability of collision for protons in H_2, He, A, N_2 and Ne for ion energies of 30 to 2500 volts. When P_c was plotted against the velocity of the protons in root volts, a minimum between $(V)^{\frac{1}{2}}=40$ and $(V)^{\frac{1}{2}}=50$ was observed for most of the gases studied. Their curve for hydrogen is in complete disagreement with Holzer's curve. Ramsauer, Kollath and Lilienthal also found a large variation in the magnitude and slope of their curves as the slit dimensions in the scattering cylinder were decreased. These variations were more marked at the lower velocities.

The present experiment was undertaken in an attempt to explain some of the discrepencies in this field and to investigate the variation in the mean free path of ions having the same number of external electrons but different masses.

Apparatus and Experimental Procedure

Diagrams of the experimental apparatus and circuit are shown in Figs. 1 and 2. They are for the most part self-explanatory, thus only a few details will be given.

A hot cathode a.c. arc was used to produce the ions. It was housed in a water-cooled brass cylinder insulated from the rest of the apparatus by means of a hardened lavite ring. A 20-mil spiral tungsten filament was used for a cathode. The pressure control of the gas in the arc was effected by steady flow through capillary leaks from reservoirs. A pressure of approximately 5×10^{-3} mm Hg was used. The ions were drawn from the arc by means of a water-cooled copper electrode placed at a negative potential (V_1) of 400 to 700 volts with respect to the filament. There was a 2-mm hole in this electrode which allowed some of the ions to pass through it into a region maintained at a low pressure by means of a 40-liter per sec. Apiezon oil pump. The ions

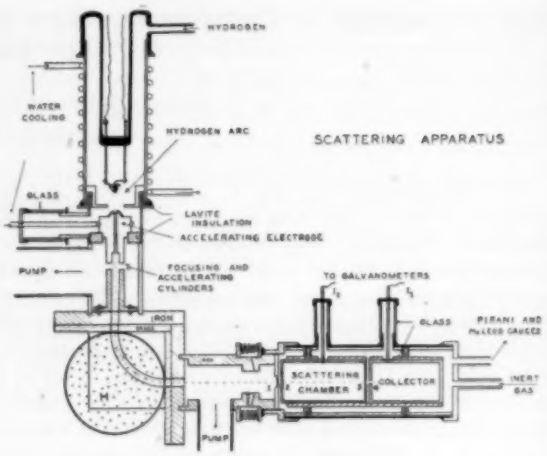

FIG. 1. Scattering apparatus.

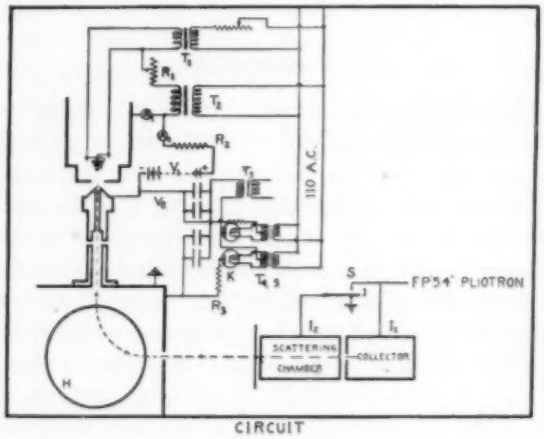

FIG. 2. Circuit.

were next accelerated or retarded to the desired velocity by means of an applied potential difference between the first electrode and a grounded iron cylinder shown in Figs. 1 and 2. The potential V_2 was supplied by a voltage doubling circuit shown in Fig. 2. The path of the beam was shielded from stray magnetic fields by means of the iron cylinder through which the ions passed and additional external iron shielding.

The magnetic field, calibrated by means of a test coil and Grassot fluxmeter, was found to be roughly proportional to the current flowing in the coils of the magnet when care was taken to reverse the magnetic field before measurement. When the ion beam emerged into this magnetic field, its constituent ions described different cir-

[6] R. E. Holzer. Pasadena meeting of the Am. Phys. Soc., June 15, 1931. Phys. Rev. **38**, 585A (1931).
[7] C. Ramsauer, R. Kollath and Lilienthal, Ann. d. Physik **8**, 709 (1931).

cular paths, the radius of any one of which was determined by the mass, charge and velocity of the ions in that path and by the magnetic field strength. If the field strength was so adjusted that the radius of curvature of a particular ion path was 5.21 cm, then these ions passed through the quarter circle into a field free region just preceding the scattering chamber and collector.

The scattering chamber was 4.3 cm in diameter and 8.41 cm long, and the collector was 7.0 cm deep. They were both held in position and insulated by means of short lengths of glass tubing, care being taken that there was no resistance to flow of gas in the region immediately surrounding the cylinders. The areas of the openings were:

Area of aperture No.				1 = 0.33	sq	mm
"	"	"	"	2 = 0.50	"	"
"	"	"	"	3 = 2.0	"	"
"	"	"	"	4 = 7.1	"	"

The first aperture was made small so that differential pumping could be used and in order that a beam of small cross section would enter the chamber. The area of the third aperture must be quite small or the measurement of P_c for ions will have no significance, especially in the case where the process involved is one of small angle scattering.

Fig. 3 is a graph of the current received by the collector as the magnetic field was varied when ordinary hydrogen and also deuterium were used in the arc.

The equation which expresses the fraction of the initial number of ions that still remain in a beam after it has traversed a distance x through a gas is:

$$I_x/I_0 = e^{-P_c p x}.$$

p represents the pressure in mm Hg at 0°C and P_c the probability of collision. For use in the experimental determination of P_c the equation may be written in the following form:

$$I_1 = [I_1 + I_2] a_s e^{-P_c p x}.$$

I_1 represents the current which reaches the collector when the scattering chamber is grounded, I_2 the current to the scattering cylinder, x the effective length of the cylinder and a_s the fraction of current which reaches the collector when no gas is flowing through the scattering chamber. The magnitude of a_s may be as small as 0.5 for

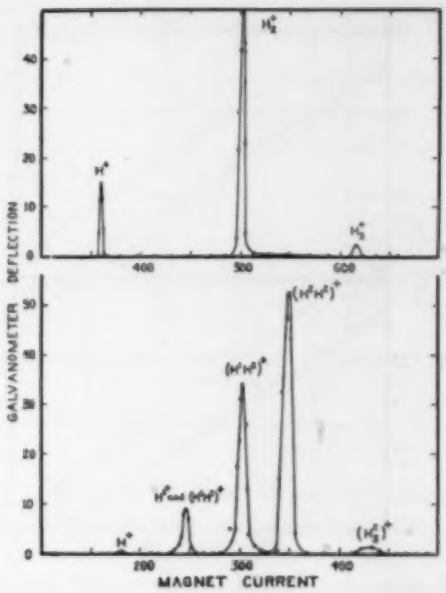

FIG. 3. Collector current as a function of the magnetic field for ordinary hydrogen and deuterium in the arc.

the lower energies on account of the electrostatic spreading of the beam. This is especially true in accurate measurements where the third aperture is relatively small. The loss of ions from the beam because of the presence of a vapor will also contribute to the magnitude of a_s. The derivative of the above equation when expressed in logarithmic form

$$d[\log_e (I_1/(I_1+I_2))]/dp = -P_c x$$

does not contain a_s, and thus P_c may be calculated from the slope of an experimentally determined pressure *vs.* $\log_e I_1(I_1+I_2)$ straight line. Fig. 4 shows five of these experimental curves, each one of which corresponds to a different initial ion velocity. The pressures as marked on the plot have not been corrected for temperature, however this correction was made before computing P_c.

The procedure in determining a value of P_c for a given ion at a particular velocity was briefly as follows. After the tube had reached a steady state, the magnetic field was so adjusted that the maximum of one of the peaks was observed. The deflections of the pliotron galvanometer for I_1 and I_1+I_2 were recorded while the gas in the scattering chamber was maintained

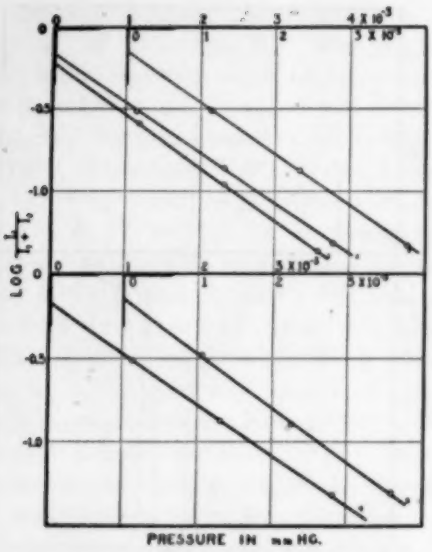

FIG. 4. Pressure *vs.* $\log_e I_1/(I_1+I_2)$ straight lines for the deuteron hydrogen molecular beam in argon.

constant at p_1 (measured by a McLeod gauge). In practice the value of I_1 was taken as the average of several trials. The pressure was raised by compressing the gas in the reservoir behind the leak to the scattering chamber. A Pirani gauge was used to indicate when equilibrium was again reached at the new pressure P_2, which was 1 or 2×10^{-3} mm higher than P_1, and again I_1 and I_1+I_2 were both recorded. The pressure was then raised to P_3 and the process was repeated. The data thus obtained were sufficient to determine a pressure *vs.* $\log_e I_1/(I_1+I_2)$ straight line from which P_c could be calculated. In those cases where a straight line could not be made to touch the three determined points and the pliotron showed signs of fluctuation the measurements were discarded. P_c was found to be independent of the pressure within the range studied.

It is clear from the above discussion of the differential method by which P_c is calculated that no error will be introduced by the presence of an unknown vapor in the scattering chamber, providing its vapor pressure remains constant. However, any impurity in the gas in which the measurements are made will obviously introduce an error. 99 percent pure argon was purchased and tested for impurities before being employed. The same gas supply was used for all measurements presented in this paper.

The Pirani and McLeod gauges were attached directly to the scattering chamber unit. No correction for flow resistance was necessary because of the construction of this unit and the position of attachment of these gauges.

RESULTS AND DISCUSSION

The results of the measurements are shown in Figs. 5, 6 and 7. Fig. 5 shows the number of collisions per cm path length per mm pressure at 0°C as a function of the velocity in root volts for $(H^1H^1)^+$ and H^+ ions in argon. The range in velocity studied corresponds to an energy range of 225 to 4200 volts. To change over to velocity in cm per second one can use the approximate equation $v=1.39\times10^6(V/M)^{\frac{1}{2}}$ cm/sec., where V is in equivalent electron volts and M in atomic mass units.

Upon a single encounter with an atom of the gas, a monatomic ion may be deviated from its original direction by scattering, or it may become neutralized, either continuing in the same or in a different direction. A diatomic ion may, in addition to the above, be dissociated. The products of dissociation may or not continue in the same direction.

Since the ionization potential of the (H^1H^1) molecule (15.9 volts),[8] is nearly equal to the ionization potential of argon (15.7 volts)[8] it appears that the neutralization of the $(H^1H^1)^+$ ion is very probably the process taking place and should account for at least the initial portion of the $(H^1H^1)^+$ curve.[9] The final rise is, however, difficult to interpret, as some other process such as dissociation may be taking place at these higher voltages. Further experiments in which the shape of the beam is studied at various pressures will have to be carried out before the nature of the collision can be definitely established.

The proton curve increases from $P_c=38$ at 225 volts to $P_c=46$ at 4220 volts. It gradually flattens out at the higher voltages. Previous experiments indicate that scattering is taking place in this case. Ramsauer, Kollath and

[8] H. D. Smyth, Rev. Mod. Phys. **3**, 389 (1931).

[9] Holzer[5] has shown that a similarly shaped curve is obtained in this velocity region when $(H^1H^1)^+$ ions were sent into hydrogen gas and that the process involved was neutralization.

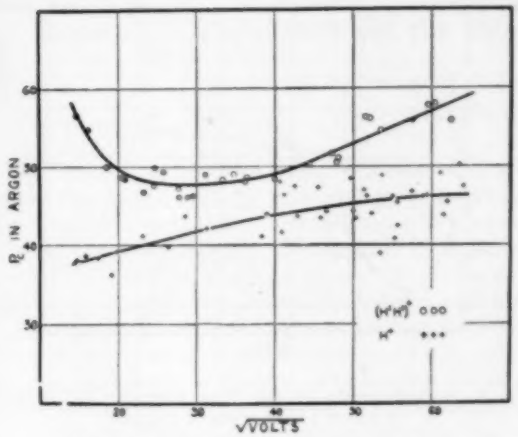

FIG. 5. Probability of collision, P_c.

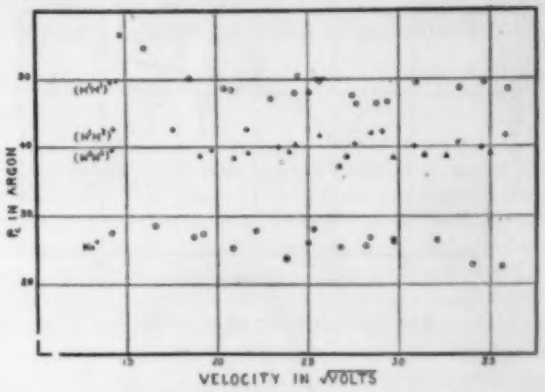

FIG. 6. Probability of collision, P_c.

Lilienthal[7] have definitely shown that there is no ionization by 2000-volt protons in argon and that scattering is important at the lower velocities. Ramsauer and Kollath[10] have since shown that for very low velocities practically all of the scattered protons continue in a direction at a small angle to their original direction. The work of G. P. Thomson[4] likewise indicates that there is appreciable small angle scattering for protons of 5000 to 25,000 volts energy in argon. An explanation of the positive slope found will undoubtedly involve a solution of the wave equation. It is not at all improbable that this curve may rise at still lower velocities and that there exists an effect for protons in argon similar to the Ramsauer effect for electrons.

The curves shown in Fig. 6 are for the $(H^1H^2)^+$, $(H^2H^2)^+$ hydrogen molecular ions and He^+ ions in argon. A portion of the $(H^1H^1)^+$ curve is replotted here for purposes of comparison. The value of P_c for the $(H^1H^2)^+$ ion is considerably smaller than for the $(H^1H^1)^+$ ion, while the value for $(H^2H^2)^+$ is only slightly less than that for the $(H^1H^2)^+$ ion. The heavier hydrogen molecular ions thus have a longer mean free path than the lighter $(H^1H^1)^+$ ion, and the variation for different ions is no simple function of the mass. It is also remarkable that P_c does not vary markedly with ion velocity over the range studied. Undoubtedly the same process is taking place in all three cases and is probably one of neutralization.

The magnitude of P_c for the helium ion curve shows a slight uniform decrease over the range studied. Since the ionization potential of helium is so much greater than for the argon atom, it may be concluded that the process here is not one of neutralization but is probably one of scattering. Its mean free path in argon is much greater than that of the hydrogen molecular ions in the same velocity range.

Fig. 7 shows the curve obtained when the composite $(H^2)^+$, $(H^1H^1)^+$ beam was used. The percentage of $(H^1H^1)^+$ ions present was unknown although a study of the magnitudes of the different peaks when ordinary and heavy hydrogen were used in the arc indicates a value of 15 percent. This can only be considered as an exceedingly rough estimate. This peak was considerably broader and flatter on top than any of the others, thus slight fluctuations in the applied potentials or magnetic field did not affect the readings so markedly. The experimental points were not taken in any regular manner and each set of readings obtained was found to lie accurately on a pressure *vs.* $\log_e I_1/(I_1+I_2)$ straight line, consequently no points were discarded. Some of these curves are shown in Fig. 4. The end values of P_c are approximately the same as those for protons at the corresponding energy values and the average trend of the curve is likewise upward; however, two unexpected minima were observed. The minimum which occurs at 806 volts is much sharper and slightly deeper than that observed at 380 volts. The de Broglie wavelengths corresponding to these minimum values are $\lambda = 0.010$A and $\lambda = 0.0071$A.

[10] C. Ramsauer and R. Kollath, Ann. d. Physik (5) **16**, 570 (1933).

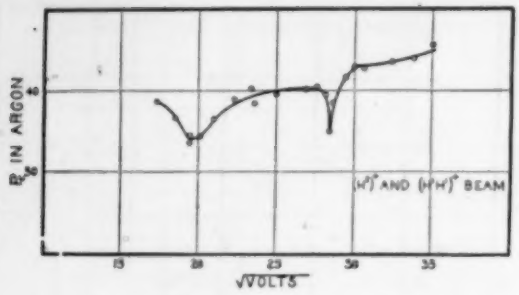

FIG. 7. Probability of collision, P_c.

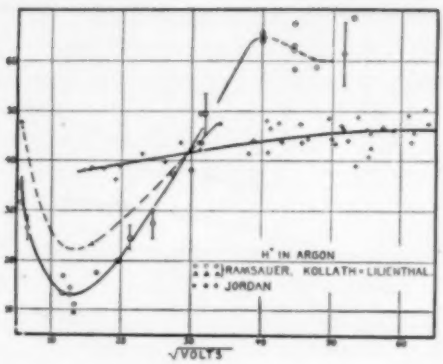

FIG. 8. A comparison of the data obtained by different authors for protons in argon.

The non-existence of such minima in the proton or the $(H^1H^1)^+$ curves shown in Fig. 5 is by no means established, for the fluctuations in P_c were sufficiently large to render a study of their fine structure impossible. A similar study using a pure deuteron beam is planned for the near future.

The only data available for comparison are those obtained by Ramsauer, Kollath and Lilienthal[7] for protons in argon. Fig. 8 shows the corresponding curves. A clue to the cause of the discrepancies which have occurred in this field is found in Ramsauer, Kollath and Lilienthal's own data. Using a slit aperture of 150 square millimeters area (which corresponds to the third aperture of 2 square millimeters area used in this experiment), they obtained the curve represented by the solid line. A circle with a stroke through it represents a possible variation in P_c due to an uncertainty in the pressure *vs.* log straight line. Using a smaller aperture area of 40 square millimeters they next obtained four points, three of which are well outside the limit of error of their previous measurements. These points are indicated by triangles. A curve (dashed line) which is similar in shape to their other one is drawn through them by the author. It will be noticed that this second curve approaches more closely to the one reported in this paper using a circular aperture of two square millimeters area. It is difficult to understand how data, obtained using slit apertures of such large area, can have any meaning, especially when the process involved is one of small angle scattering. Even for small aperture areas a slit introduces distortion since ions which are scattered at a small angle in the lengthwise direction of the slit can get through into the collector while those scattered in the opposite direction cannot. The amount of distortion would depend on the relative width and length of the slit. A well-defined circular beam of small cross-sectional area is also necessary if accurate measurements are to be obtained. If the process involved had been one of neutralization, an agreement would probably have been found regardless of the shapes or sizes of the apertures.

In conclusion, the author wishes to thank Professor R. B. Brode for many valuable discussions and comments and to acknowledge gratefully an appointment by the National Research Council which made the completion of this work possible.

The Conductivity Produced in Neon and Helium by Irradiation with Their Own Resonance Radiations and the Effect of Foreign Gases on This Conductivity

R. W. SMITH AND O. S. DUFFENDACK, *University of Michigan*

(Received February 1, 1935)

The conductivity observed ten tube diameters or more beyond the end of a discharge in Ne or in He is investigated at pressures of from 0.25 mm to 14 mm. Great care is taken to insure rigorously pure gas. The conductivity is deduced from the characteristic of a rotatable pair of parallel plane collectors and guard rings completely shielded with glass. At pressures above about 0.25 mm no current is observed when the collectors are perpendicular to the tube axis so that the space between them is shielded from the direct radiation. The total current (to collectors and guard rings) is considerable. When the collectors are turned so that the primary radiation illuminates the space between them, considerable currents are obtained and the much larger total current is of the same order of magnitude as in the perpendicular position. These results show that the ions which give rise to the conductivity must be formed in the space between the collectors and also that any metastable atoms which may produce these ions must also be formed in this space. It is difficult to reconcile these results with the propagation of resonance radiation through the gas by diffusion for they indicate an abnormally long free path for the resonance radiation of He and Ne. The large conductivity observed in the pure gas under conditions such that the photoelectric action of the primary beam is very small suggests that electron emission by impacts of metastable atoms is of major importance. Argon and krypton in small admixtures increase the conductivity of neon or of helium due to the action of the metastable atoms of the main gas in ionizing the argon or krypton. Neon greatly decreases the conductivity of helium while helium has no measurable effect in neon. In these cases ionizing collisions are not possible but the metastable atoms of helium readily transfer their energy to the nearby excited levels of neon.

INTRODUCTION AND PURPOSE

INVESTIGATIONS of the nature and properties of resonance radiations were for many years limited to those which could be pursued by the usual photographic methods. This restriction was severe in that it eliminated from consideration all of the interesting rare gases whose resonance radiations are much too short in wavelength to be transmitted by any known window material. These gases, particularly He, possess metastable states whose population under ordinary discharge conditions may be very large and whose lifetime is very long compared with that of the unstable states. It would be very significant to study quantitatively the part played by metastable atoms in the propagation of resonance radiation through a gas.

A few years ago a possible line of attack was suggested by Langmuir and Found[1] who discovered that the conductivity existing in a discharge tube at a considerable distance beyond the end of a discharge in Ne was much too large to be accounted for by any agent moving away from the discharge by diffusion. They ascribed this conductivity to electrons emitted from the glass walls and metal surfaces, and caused by metastable atoms. These metastable atoms, they suggested, were produced by resonance light of slightly different frequency from that of the core of the resonance line. As the primary light source produced a rather broad resonance line, such light would be present in considerable intensity. Kenty[2] repeated and extended these experiments and confirmed that many metastable atoms are produced at large distances (10 tube diameters or more) from the discharge, probably by the method suggested by Langmuir and Found. However, Kenty concluded that while these metastable atoms are of relatively great importance in causing conductivity in cases where there is present a small amount of impurity ionizable by metastable atoms, their effects in pure gases are very small compared with the photoelectric effect of the extreme ultraviolet radiations. Penning[3] made some important studies of this conductivity and the effect of small amounts of added impurities and agreed that the large increases in conductivity which result when argon is added to neon are caused by the ionization of A atoms by metastable Ne atoms in impacts of the second kind.

[1] Langmuir and Found, Phys. Rev. **36**, 604 (1930).

[2] Kenty, Phys. Rev. **38**, 377, 2079 (1931); **40**, 633 (1932); **43**, 181 (1933).

[3] Penning, Zeits. f. Physik **78**, 454 (1932).

Evidently the observed conductivity may be explained on at least three quite different bases: (1) The extraction of electrons from the discharge tube walls and electrode surfaces by metastable atoms; (2) photoelectric emission from the tube walls and electrode surfaces; (3) the ionization of traces of impurities present in the gas. However, all of these explanations are compatible with the conclusion that considerable concentrations of metastable atoms may be built up in a neutral rare gas which is irradiated by its own resonance radiation; and, further, that these metastable atoms may give evidence of their presence by their effectiveness in ionizing small traces of impurities. The investigations mentioned thus far do not permit a definite distinction to be made between the effects of the direct primary resonance radiation from the source, those of secondary resonance radiation produced by the absorption and reemission of resonance radiation in the gas and the effects of primary ultraviolet radiation multiply reflected from the tube walls. Collectors whose orientation with respect to the primary beam can be varied allow measurements to be made with the radiation directly incident on the collecting surface, just grazing it or not striking it at all. Plane parallel plates give more easily interpretable characteristics but only if they are fitted with guard rings of ample width. The use of unguarded collectors makes it difficult to interpret data taken in the presence of volume ionization. Especially would this be true in gas which was not rigorously purified as the conductivity is extremely sensitive to traces of impurities.

The present experiments, already briefly reported,[4] were begun with a threefold purpose: (1) To obtain gas as rigorously pure as possible; (2) to investigate quantitatively the effect of small admixtures of foreign gases on the conductivity produced in Ne and in He by irradiation with their own resonance radiations; (3) to study the various agencies contributing to the conductivity and the mechanism of the propagation of resonance radiation away from a source. Ordinary experience has shown that only the most elaborate precautions for long continued purification and complete degassing of the intimate apparatus will suffice to maintain rigorously pure gas. It was therefore felt that considerable effort could profitably be expended in an attempt to ascertain first what effects would be most important in a pure gas.

Apparatus

The vacuum system was rather elaborate and combined an efficient and flexible circulating and purifying system capable of purifying relatively large quantities of Ne and He together with a rapid and reliable means of adding very small amounts of foreign gases. The gases could be circulated through the purifying agents alone or also through the discharge tube during runs. In this way the gas could be purified continually while the tube was being baked and pumped dry. It was then very pure when admitted to the tube and could be maintained so by regulated circulation during the experimental runs.

The discharge tube used is shown in Fig. 1. It was 80 cm long and arranged so that a hot cathode arc could be maintained at the opposite ends. This made possible a fairly uniform illumination near the center of the tube. Midway between the two anodes, which were about 16 tube diameters apart, were supported two parallel plane nickel electrodes 1 cm in diameter fitted with guard rings 1 cm wide. These were completely shielded with glass except on their adjacent faces, the lead wires were also shielded, and the whole assembly was rotatable about a vertical axis perpendicular to the tube axis.

Great care was taken in procuring and maintaining pure gas. The rare gases used, Ne, He, A and Kr were obtained commercially spectroscopically pure. The Ne and A were further purified by prolonged circulation over charcoal in liquid air, chabazite in liquid air and over hot copper oxide. As a further precaution for the removal of H_2 the method of Paschen[5] was used. No waxed joints were used in the vacuum system and the few stopcocks were lubricated with a special low vapor pressure grease. Two liquid-air traps containing glass beads in series on each side of the discharge tube and wads of gold foil in the pumping leads served to exclude Hg vapor from the tube.

[4] Duffendack and Smith, Phys. Rev. **43**, 586 (1933).

[5] Paschen, Ann. d. Physik **45**, 625 (1914).

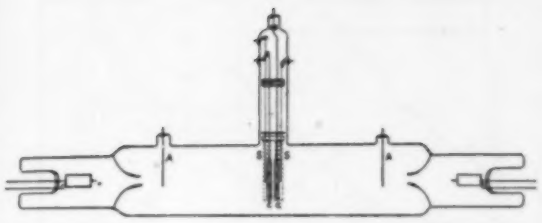

FIG. 1. Diagram of experimental tube.

Since the A and Kr were obtained already spectroscopically pure and in any case were to be used only as small admixtures it did not seem necessary to subject them to such exhaustive purification. As a precautionary measure, however, a low voltage arc was maintained in the A reservoir between Ca electrodes for about a month after which time the A was found to be very pure. The Kr was used directly from the original container.

Spectroscopic analysis of the various gases as received from the vendor revealed no trace of any impurities, except a trace of Ne in the He. Yet the experimental results revealed that impurities were certainly present and that these results were themselves probably the most sensitive test for such subspectroscopic traces of foreign gases. Throughout the investigation the actual behavior of the conductivity itself was taken as an indication of the gas purity.

PROCEDURE

The primary gas was circulated for two or three days through the purifying system until greatly overexposed spectrograms showed no trace of impurity. The gas was then pumped into a reservoir containing well-degassed charcoal immersed in liquid air where it was allowed to stand for 12 to 24 hours while the experimental tube was being baked at 400°C. After this the gas was slowly admitted to the tubes. Then the arcs were struck and maintained at a high current density while the gas was circulated through the tube and entire purifying system for 4 to 6 hours. This flushed out the tube and cleaned up residual impurities. The rate of circulation was then slowed down, the arcs adjusted to the proper current density and the run made.

When foreign gases were used, the charcoal and chabazite were shunted out of the circulating system as they readily absorb A and Kr. By means of a calibrated bulb and suitable cut-offs small amounts of the gas to be admixed could be accurately and rapidly added to the main gas and mixed by circulation. At low primary gas pressures equilibrium could be established in a minute or two while at pressures above about 6 mm it was necessary to wait about 15 minutes. This proved to be a convenient and accurate way of adding small amounts of foreign gases where large numbers of such additions were to be made. In the case of the addition of A or of Kr to He or to Ne, after the completion of a run, the gas was circulated for several hours through the charcoal and chabazite traps to remove the added gas. After it had been absorbed out the conductivity was compared with that observed before the addition of the foreign gas in order to ascertain that no unexpected contamination had occurred during the run.

The conductivity or ion concentration was determined from the volt-ampere characteristics of the collectors. The potential difference across the collectors was varied in small steps by means of a potentiometer arrangement and the corresponding current between them read on a current galvanometer having an overall sensitivity of 1.5×10^{-10} amp./mm. When plotted, these readings constitute the collector characteristic.

RESULTS

When the collecting disks are placed at right angles to the tube axis so that the space between them was shielded from the direct radiation, then, except at the lowest pressures (<0.25 mm Hg), no measurable current ($<10^{-10}$ ampere) flowed between the guarded collectors. The total current (to collectors and guard rings), however, was the same as that previously observed between unguarded collectors.[4] Fig. 2 shows that when the collectors were turned so that the primary radiation illuminated the space between them, appreciable currents were obtained and the much larger total current was of the same order of magnitude as before. All of the data were taken therefore with the space between the

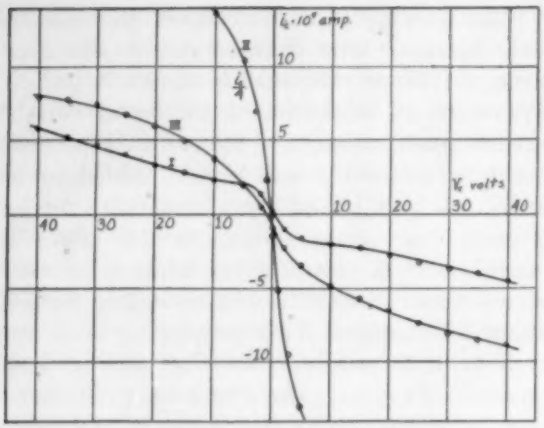

FIG. 2. Current to collectors as a function of potential difference between them. Collectors floating with respect to the discharge. I, current to guarded collector, parallel position; II, current to collector and guard rings, parallel position; III, current to collector and guard rings, perpendicular position.

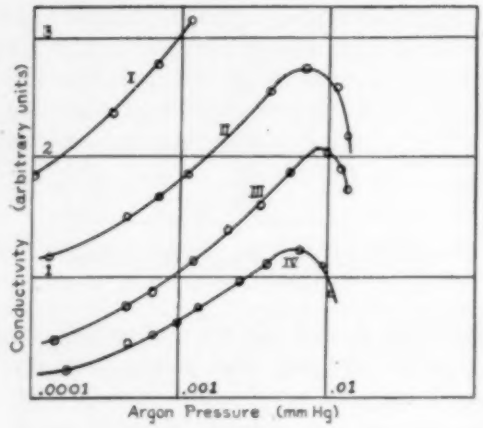

FIG. 3. Variation of the slope of the current voltage characteristic curve in neon with various argon admixtures. I, 2.6 mm Ne; II, 4.3 mm Ne; III, 7.0 mm Ne; IV, 11.5 mm Ne.

collectors irradiated by the primary beam. In no case were the collector surfaces exposed to the primary beams. All the characteristics of the guarded collectors are strictly linear through the voltage axis, and the slope at the voltage axis is taken as a measure of the conductivity of the gas. Figs. 3 to 5 inclusive show how this slope (in arbitrary units) varies with the pressure of the admixed gas. The variations are similar to those obtained with the unguarded collectors. For A added to Ne or to He the curve attains a maximum and then slowly decreases to a very low value. In agreement with Penning,[3] it has been found that if the percentage of A is greater than about one percent the curve again rises slowly, indicating the entrance of primary effects due to the A in addition to its secondary destroying effects. Kr is similar to A in its effects but is less efficient than A in increasing the conductivity of He or Ne. It is also seen that while A and Kr both increase the conductivity of Ne and of He, Ne effectively decreases the conductivity of He. He added to Ne causes no measurable effect even with large admixtures. In the case of pure He and pure Ne the residual conductivity decreases rapidly with increasing pressure and apparently reaches a constant limiting value at about 8 mm Hg. No further decrease was observed up to 14 mm pressure.

DISCUSSION

These results lead to two conclusions: First, that the ions which give rise to the observed conductivity must be formed in the space between the collectors; and second, that any metastable atoms which may produce these ions must also be formed in this space. In these experiments the photoelectric effect of the direct radiation from the source must be very small as the glass shields protect the collector surfaces in any position. The inference is that the agency giving rise to the conductivity is produced in or near the primary beam and cannot diffuse far from it at the pressures used (2–12 mm). Only at pressures below about 0.1 mm was any appreciable current collected when the collectors were perpendicular to the direct radiation. An accidental confirmation of these conclusions was obtained when one of the glass shields cracked in such a way as to leave a small opening behind the collecting electrode oriented so that no direct radiation could enter. Appreciable currents were then collected through the crack in the shield with the electrodes in the perpendicular position but were not collected after the shield had been replaced. Thus the surrounding gas must have been ionized.

The curves of Fig. 2 exhibit the same general form although the total current is very much larger than could be accounted for by any

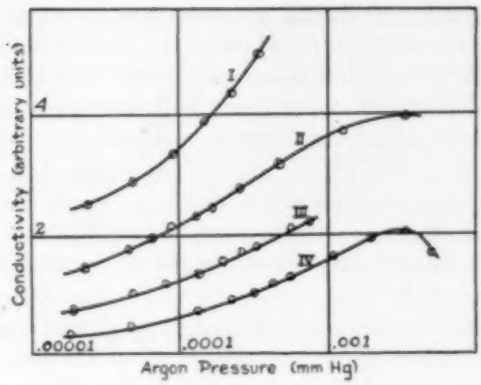

Fig. 4

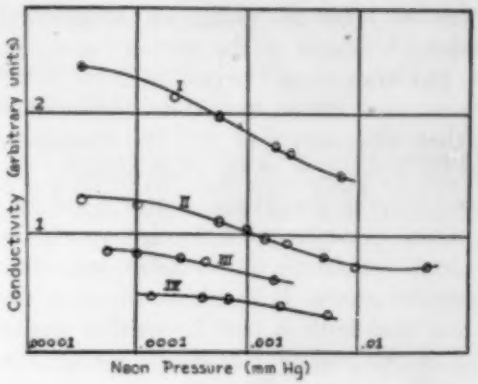

Fig. 5

FIG. 4. Variation of the slope of the current voltage characteristic curve in helium with various argon admixtures. I, 1.4 mm He; II, 3.2 mm He; III, 5.7 mm He; IV, 8.5 mm He.

FIG. 5. Variation of the slope of the current voltage characteristic curve in helium with various neon admixtures. I, 1.6 mm He; II, 2.2 mm He; III, 2.7 mm He; IV, 4.6 mm He.

difference in area between the collecting surfaces in the two cases. This discrepancy must be due to edge effects and indicates that when an unguarded collector is placed in an ionized gas a considerable portion of the ion current observed is due to edge effects so that such a collector, even if shielded on one side, would exhibit little difference in current collected regardless of its orientation.[2] Hence scattered short mean free path resonance radiation probably plays no important role in such experiments.

Further evidence for the existence of volume ionization arises from the fact that while at high pressures no current is collected by the guarded collectors in the perpendicular position, appreciable currents may be measured below about 0.25 mm. Moreover, the collector characteristics in He exhibit decided peaks at about 6 volts on either side of the voltage axis which become relatively more prominent as ionizable foreign gases are added. Penning[3] first observed these and showed that they were probably due to ions diffusing in from the surrounding volume when the field between the collectors was so small that the ions were not trapped by the guard rings.

It seems probable that the collector characteristics and the directional effect of the collectors as shown in Fig. 2 are mainly characteristic of the pure gas, as an apparent limiting value of conductivity was reached which could not be diminished by further purification or increase of gas pressure. Furthermore, this residual conductivity was remarkably reproducible. If this is true, the residual conductivity is surprisingly large in view of the amount of ionization that has been ascribed to the several processes suggested by previous investigators to account for this conductivity. However, abnormally large wall reflections and photoelectric efficiencies have been reported by Kenty[4] which might account for the ion concentrations ($\sim 10^8$ cm^{-3}) observed at these large distances from the source.

These experiments show definitely that, in gas which may be reasonably termed pure, short mean free path scattered resonance radiation contributes negligibly to the observed conductivity. Moreover, since while there is considerable volume ionization no ions are collected by a guarded collector except when it is adjacent to the primary beam from the source, the agencies giving rise to the observed conductivity must act in the path of the primary beam or, at most, only a few mean free paths from it.

FOREIGN GASES

The experimental results exhibit one outstanding regularity in that all of the foreign gases which effectively increase the conductivity of the gas to which they are added have ioniza-

[4] Kenty, Phys. Rev. **44**, 891 (1933).

tion potentials below the energy of excitation of the metastable states of the primary gas. Ne, the only gas to decrease the conductivity of He, is the only one whose ionization potential is higher than the energy of the He metastable states. This is also true of He when added to Ne. This confirms the conclusion that the conductivity in the presence of a foreign gas arises largely from ionization of ionizable impurities by metastable atoms. It should be noted in this connection that both A and Kr exhibit similar behavior in Ne and in He. While He appears more sensitive to impurities than Ne and while A is more effective than Kr in increasing the conductivity of the Ne or the He to which it is added, the differences are not in order of magnitude.

One interesting effect which was observed is the decided maximum which the conductivity attains as larger admixtures of ionizable impurity are introduced. The maxima occur at larger and larger percentages of foreign gas as the pressure of the main gas is decreased, due probably to the relative decrease in the number of collisions of metastable atoms with the admixture. These maxima may be accounted for briefly as follows.[3] If, as in ordinary quenching experiments, the resonance radiation is constant in intensity then the curves rise to a saturation value and remain constant; for this saturation occurs when all the metastable atoms are being destroyed as fast as formed and further addition of the destroying agency has no effect. However, in these experiments two factors may operate to decrease the intensity of the radiation: (1) Direct excitation of the radiation by electron impact in the arcs may be influenced by the foreign gas; and (2) if the resonance radiation which finally reaches the vicinity of the collectors is absorbed and reemitted at least once on the way, the intensity of this scattered radiation would be affected by the presence of any agency which could destroy the excited atoms giving rise to it. The maximum is thus a point of balance where the forces acting to destroy the metastable atoms are equal to those forming them.

Some interesting results have been obtained with Ne-He and He-Ne mixtures in which cases ionizing collisions are not possible between the metastable atoms of the main gas and the foreign gas atoms. Addition of an extremely small amount of Ne to He causes a marked decrease in conductivity which is difficult to explain if one attributes the action of the Ne to the weakening of the resonance lines of He which are excited entirely by direct electron impact. However, if one allows metastable He atoms largely to account for the conductivity in pure He[7] then the results are easier to interpret as there is very close resonance between the metastable levels of He and a large number of excited states of Ne. This reaction therefore should have quite a high probability of occurrence in He containing a small amount of Ne.

In the He-Ne mixtures the observed decrease is exceedingly small, being just detectable at about 30 percent He in the Ne. This should perhaps be expected in view of the fact that no collisions of the second kind can take place between excited Ne and neutral He because the excited states of He are all above the metastable levels of Ne. The slight decrease at the high percentages of He is probably due to considerable excitation by electron impact of the large number of He atoms present.

Because of the difficulties inherent in the inclusion, as here, of the source and of the measuring device all in the same vessel and the same gas, these experiments are probably not sufficiently accurate for any significant evaluation of action cross sections. The various effects mentioned limit any valid analysis of the variation of the conductivity with the foreign gas pressure to the range of very small admixtures. However, if one assumes the statistical processes occurring to be those discussed above, one can obtain a relation between conductivity and the pressure of the added foreign gas which fits the experimental results exceedingly well. The uncertainties in the interpretation of the collector characteristics and in the conceptions of the processes contributing to the conductivity do not justify a more detailed quantitative analysis of the experimental data.

[7] Reichrudel and Spiwak, Phys. Rev. **42**, 580 (1932); Ann. d. Physik **17**, 65 (1933).

Theory of Electrical Double Layers in Adsorbed Films

R. W. GURNEY, *University of Bristol, England*

(Received December 10, 1934)

The nature of an absorbed layer is discussed in terms of quantum mechanics, and the factors governing the sign and magnitude of the electrical double-layer are determined. Although the ionization potentials of Ca, Sr and Ba are greater than the electronic work function of tungsten, a sparse distribution of these atoms on a tungsten surface behaves in a way quite similar to atoms of alkali metals whose ionization potentials are much smaller. This behavior can be understood only in terms of quantum mechanics.

§1.

IT is well recognized that quite a sparse distribution of foreign atoms adsorbed onto a metal surface suffices to give rise to a strong electrical double-layer, which may be positive outwards or negative outwards according to the nature of the adsorbed atoms. That atoms of the alkali metals K, Rb and Cs, should reduce the effective work function of tungsten in this way has always been regarded as in agreement with expectation. Their ionization potentials (4.3, 4.1 and 3.85 e.v.) are smaller than the work function of tungsten (about 4.5 e.v.), and consequently, it is said, they will give up their valence electron to the metal, and the positive cores lying on the surface will give rise to an electrical double layer positive outwards.

To invoke the fact that the ionization potential is less than the work function of the underlying crystal is, however, to set up an unsatisfactory criterion. For it is found that a sparse distribution of barium atoms behaves very like caesium. The work on calcium and strontium has not been published; but Dr. Becker has kindly written to me that the curves for these metals are similar to those of barium, i.e., they reduce the work function of tungsten, though to a smaller extent. Yet the first ionization potentials of these elements—6.09, 5.67 and 5.2 e.v.—are all greater than the work function of tungsten. According to the simple picture they should not give up their electrons to the metal.

§2.

In order to see whether the work function is raised or lowered, we wish to know the electron density at the surface of a metal A near a point where an atom of a foreign metal B is adsorbed. This information will be most easily obtained by first considering in detail the state of affairs when the atom B, or its core, is held at a distance of a few atomic diameters from the surface; later we shall consider what happens when this distance d from the surface is diminished. We need to know the potential energy of an electron along a line perpendicular to the surface of A and passing through the core of B. Curve a of Fig. 1 shows this potential energy, using the Bloch model for the metal, and curve b using the simpler Sommerfeld model. In curve c the "potential box" provided by the core has been replaced by a rectangular potential box, which is useful for a preliminary treatment. For the sake of brevity, we shall proceed immediately to discuss this energy diagram by the methods which have recently been described in extenso by the author.[1] In the first place, if the box RS is deeper than PQ, and possesses an allowed level lying below the bottom of the box PQ, this level will remain discrete when the distance QR is diminished. Atoms with low-lying levels of this type will be discussed later. But each of the elements mentioned above has a valence level which will lie near the critical level of the metal: let the energy of this valence level be W_0. If we insert the potential energy of Fig. 1 into the Schrödinger equation, and solve, we obtain a set of allowed levels which belong jointly to the metal and to the atom. Strictly speaking, the atom has as many allowed levels as the metal, namely, millions. Yet when an atom is not too near to the surface we usually regard it as having a valence level, which may be somewhat broadened by the presence of the neighboring solid;

[1] Gurney, *Elementary Quantum Mechanics*, Cambridge University Press, 1934.

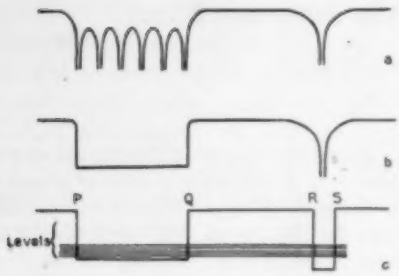

FIG. 1. Potential energy curves for an electron at the surface of a metal along a line passing through the core of an atom; curve *a*, for a Bloch model, curve *b*, for a Sommerfeld model, curve *c*, for a simplified rectangular potential box picture.

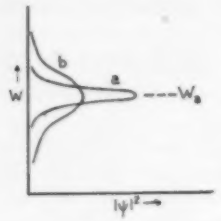

FIG. 2.

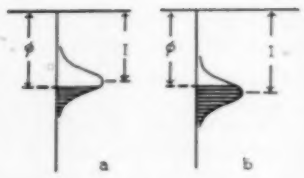

FIG. 3.

FIG. 2. Broadening of an energy level as the adsorbed atom approaches the metal surface.

FIG. 3. Representation of the filling of an atomic band up to the Fermi level; *a*, for an element of low ionization potential, *b*, for an element of rather higher ionization potential.

and we are certainly right in doing so. It will be convenient to state here exactly what we mean by this conception. We mean that the solutions of the Schrödinger equation are such that for certain values of W on either side of W_a the amplitude which the wave function has around the atomic core is large compared with the amplitude which it has inside the metal, while for all allowed energies more distant from W_a their amplitude around the atomic core is smaller than in the metal by a factor e^{-kd}, where d is the distance from the metal surface, and k depends on the height of the potential barrier. When d is large, the factor e^{-kd} is so small that we may regard the atom as having an almost sharp level of value W_a. The blurred level has no sharp edges, and if the atomic core is brought nearer to the metal, the level becomes broadened, owing to the increase in the value of e^{-kd}. In Fig. 2 let ordinates be W, and let abcissae be the mean value of $|\psi|^2$ around the atomic core when the latter is at a particular distance from the metal. Curve *a* shows the level when still fairly narrow, and curve *b* a broader band when the atomic core is nearer to the surface. When finally the atom is deposited on the surface, and the value of d is only one or two Angstroms, it is easily calculated[2] that the value of e^{-kd} is as large as 10^{-1} or more. Hence there are no longer near W_a any values of W for which the amplitude of ψ around the atomic core is much smaller or much larger than in the interior of the metal.

Returning to curve *a* of Fig. 1, we recall that the free electrons in a metal move about freely because the potential barriers between adjacent cores are transparent to the electrons. And we see now that, when the metallic atom B is adsorbed, the potential barrier between its core and the adjacent cores of the lattice is likewise transparent to the free electrons of the underlying metal. In its interior this underlying metal is neutral in every part, not because a valence electron is resident in every atom, but because the moving electrons spend on the average as much time in each atom as is required to produce uniform neutrality. In the same way, when the atom B is adsorbed, there will not be an electron resident in the atom, nor will there be a vacant level. But in every second 10^{14} or 10^{15} free electrons will approach this point of the boundary from within, and these will neutralize the positive core of B to a certain extent which we must now discuss.

The whole argument so far has dealt with the normalized wave functions appropriate to the potential energy of Fig. 1, without regard to the question as to whether they were occupied by electrons or not. When an atom of an element A is deposited on a crystal of A at ordinary low temperature, it is of course the critical Fermi level of the metal which determines which levels will be occupied, and which vacant. And we come now to the most important factor in the problem, namely, that when an atom of B is adsorbed onto a metal A, it is still the Fermi level of A which determines the extent to which the positive core of B is neutralized by valence electrons. The state of affairs may be visualized as in Figs. 3a and b. These represent the atomic

[2] Reference 1, Chapter 3.

band filled with electrons up to a certain level (the Fermi level) (a) for an element B of low ionization potential, and (b) for an element of rather higher ionization potential.

§3.

We have been dealing hitherto with the adsorption of atoms of any element B which has an ionization potential comparable with the work function of the metal A. There are, however, elements whose characteristic valence levels lie much lower, for example, oxygen with ionization potential 13.6 e.v., much greater than the work function of any metal. The adsorption of such an atom is somewhat different, because any level which falls below the valence band of the underlying metal will remain a single discrete level. It will be a localized level, with the amplitude of ψ falling off exponentially within the metal. It behaves like one of the x-ray levels which we have been able to disregard.

It is a property of elements like oxygen, that an atom in vacuum is able to accommodate a supernumerary electron and to become a negative ion. The potential energy which an additional electron has in the field of the neutral atom is such as to give a stable quantized state with the electron bound. When the atom is isolated, this vacant level is sharply defined; if the atom is brought towards a metal surface the level will become broadened out into a band, exactly as in the case of a valence level. It will again be the critical level of the underlying metal which determines to what extent this band is invaded by electrons from the metal. This will give rise to a double layer negative outwards, since we have an already neutral atom playing the part which was formerly played by a positive core. It is found that the adsorption of oxygen raises the work function of tungsten from 4.5 to more than 8 e.v.

Only positive double layers have been studied in detail experimentally; we will accordingly develop the discussion of Fig. 2. If the band of the adsorbed atom lies mainly above the Fermi level of the metal, as in Fig. 3a, the positive core will be only slightly neutralized by the electron cloud. If the center of the band lies near the Fermi level, the band will be about half full. One must not, however, conclude that the positive core is necessarily neutralized to a greater extent in the second case. For the valency of the adsorbed atom is also a determining factor. To neutralize the positive core of a monovalent atom it is only necessary that half the band be filled.[3] For a divalent atom, on the other hand, the whole band must be filled. If therefore the band of Fig. 3a is that of an adsorbed alkali atom, and that of Fig. 3b of a divalent atom, the contribution to the electrical double layer would be about the same, in spite of the fact that $I < \phi$ for the former, and $I > \phi$ for the latter. The remarkable similarity in the behavior of the alkalis and the alkaline earth metals on tungsten is thus to be expected.

§4.

In discussing the relation of the atomic band of B to the critical level of A, we have hitherto spoken as if for any two elements A and B there is a unique relation. There exists a unique relation so long as the number of adsorbed atoms is small. But it is found, for example, that when a tungsten surface is only one-tenth covered with caesium atoms, the electronic work function is already reduced by 0.8 e.v. This drop of potential takes place at the metal surface, as may easily be established by drawing the equipotential lines which run parallel to the surface between the adsorbed charges and their electrical images in the metal. The potential energy curve of Fig. 1 is of course modified, and the wave function for any energy W is no longer the same as before. In a positive layer the atomic band is shifted downward relative to the critical level of the metal, and consequently is invaded to a greater extent by electrons from the metal. When many atoms are present each atom makes a smaller contribution to the double layer than when few are present. When fresh atoms are deposited, each atom makes a positive contribution to the layer, but the growth of the potential drop diminishes the contribution being made by every atom already present. The strength of the double layer therefore does not grow linearly with the number of atoms deposited.[4] Clearly we may

[3] Gurney, reference 1, Chapter 8.

[4] Becker, Trans. Faraday Soc. **28**, 151 (1932); Taylor and Langmuir, Phys. Rev. **44**, 437 (1933).

even come to a stage in which the positive contribution by the added atom is almost wholly counterbalanced by the small diminution which it automatically causes in the contributions of the very large number of atoms already present in the film. It is, in fact, found that in the case of both caesium and barium the strength of the double layer passes through a maximum value.

An isolated atomic particle in vacuum must be exactly electrically neutral, or else must bear a charge $\pm ne$ where n is an integer. This is not true of an atom forming part of a polar molecule. And the essential basis of the above discussion is that there is no reason why this should be true of atoms adsorbed onto a metal surface. Recent experimental work has, however, been interpreted in terms of the separate existence of ions and neutral atoms on the surface. When the author criticized this interpretation at a meeting of the Faraday Society, Dr. Becker in his published reply wrote,

> The chief reason for believing that some adsorbed particles are completely ionized is the experimental fact that when caesium is evaporated from a hot tungsten surface sparsely covered with caesium, practically every particle comes off as an ion. Now, if the forces on the caesium adsorbed on the tungsten surface are not sufficient to completely ionize some of the caesium, one would not expect these forces to be sufficient to ionize the caesium when it is further from the surface and escaping from it. Consequently no caesium should evaporate as ions unless it is adsorbed on the surface as an ion.

More recent work has been interpreted in the same way.[5]

To clear up this question one must consider what happens when any metal atom tries to escape from the surface. The process pictured in Fig. 2 takes place in the reverse direction; the broad band of levels closes up into a narrow band, and tends to the discrete characteristic valency level of the atom in vacuum. This level may be above or below the Fermi critical level of the metal, depending on the ionization potential of the element considered and the effective work function of the metal modified by any double layer there may be present. Whether the particle escapes as an ion or a neutral atom depends entirely on what level in the metal happens at the moment to be opposite to the characteristic level of the atom. The motion of electrons being some thousand times more rapid than the thermal velocity of an ion, there is plenty of time for an electron to pass through the potential barrier of Fig. 1a while the atomic core is in the act of leaving the surface. In the case of caesium (ionization potential 3.85 e.v.) on sparsely covered tungsten (effective work function more than 4 e.v.) the characteristic level finds itself opposite an almost unoccupied level in the metal. The electron is accordingly almost always left behind in the metal. For progressively thicker films of caesium, the valency level of the escaping caesium becomes progressively lowered towards and beyond the Fermi critical level of the metal. We should therefore expect the proportion of caesium escaping as ions to be diminished, the fraction following exactly the Fermi population of the metallic levels at the temperature of the experiment. A double-layer of strength 0.7 volt should suffice to make the number of atoms and ions escaping of the same order of magnitude, since the work function of pure tungsten is about 4.5 volts; this is found to be the case.

[5] Evans, Proc. Roy. Soc. **A145**, 135 (1934); Proc. Camb. Phil. Soc. **29**, 161 (1933).

Ionization of Inert Gases by Positive Alkali Ions

ROBERT N. VARNEY, *University of California, Berkeley*

(Received February 4, 1935)

The ionization potentials of the noble gases under impact of various positive alkali ions have been determined in a new and independent manner which employs the neutralization of an electron space-charge by the newly formed positive ions to show the ionization. The method is extremely sensitive to the positive ions but is not affected by the secondary electrons which are liberated from the walls. The potentials found are different for each combination of gas and alkali ion and range in value from 5 to 20 times the electron ionization potentials. They are lower, by amounts running as high as 45 volts in some cases, than those found by Beeck and Mouzon. No ionization was observed by Li^+ ions, none by Na^+ ions except in Ne gas, or in Ne gas by any ions but Na^+. When the actual energies available for ionization, after conservation of energy and momentum have been taken into account, are calculated, the results are strikingly self-consistent, whereas the unreduced results are not at all so. Certain results published by Beeck and Mouzon, but which could not be checked by the author, fail to show this self-consistency.

THE ionization which results when positive ions strike atoms of various gases has occasioned surprise, on the one hand because the ionizing potentials were so low when compared with those for H^+ and He^{++} collisions, and on the other hand because the same potentials were so high when compared with electron ionization potentials. The argument on the question of whether ions need energies of 10,000 volts or more to ionize by collision or whether they needed only a few times the electron ionization potential of the target atom was settled by Loeb[1] in 1927 when he pointed out the existence of a distinct and different mechanism for ionization by fast ions and by slow ions. It was pointed out that the relatively slow ions might depend on some quantum-mechanical process of interaction to ionize by collision in which the ion and the atom formed a molecule for an instant which had an unstable electron when the ion had sufficient energy. This process has been discussed by Weizel and Beeck[2] in the light of subsequent experiments.

To investigate these low ionization potentials, Sutton,[3] Beeck,[4] Mouzon[5] and others undertook careful investigations of the ionization which occurred when noble gases were bombarded by low energy alkali ions. They found that the efficiency of ionization varied considerably with various combinations of gases and ions and that the greatest efficiency resulted in general when the ion and gas had the most nearly equal atomic weights. Careful investigation of the actual ionization potentials, or minimum speeds necessary for ionization, was completed in 1932 by Beeck and Mouzon,[6] and showed that the potentials ranged in fact from 6 to 20 times the electron ionizing potentials.

The method used to determine the minimum ionizing speeds depended on observing the electrons which were detached from the neutral gas atoms. This method has two serious disadvantages. The first is that the ionization process is inefficient enough to require measuring instruments of the highest possible sensitivity to detect the few ionization electrons. The second disadvantage is that having the instruments of necessary sensitivity, it becomes increasingly difficult to avoid measuring the spurious secondary electrons which are liberated from the walls of the apparatus by radiation, positive ion impact and metastable atom impact.

To eliminate both these difficulties at once, to provide independent checks of the previous results and to investigate whether ionization could be found at energies more nearly equal to the electron ionization potentials, the method of Lawrence and Edlefsen[7] for detecting photo-ionization in vapors was adapted to the problem of positive ion ionization. This method is highly

[1] Loeb, Science **66**, 627 (1927).
[2] Weizel and Beeck, Zeits. f. Physik **76**, 250 (1932).
[3] Sutton, Phys. Rev. **32**, 364 (1929).
[4] Beeck, Ann. d. Physik (5) **6**, 1001 (1930).
[5] Mouzon, Phys. Rev. **35**, 695 (1930).
[6] Beeck and Mouzon, Ann. d. Physik (5) **11**, 737, 858 (1931).
[7] Lawrence and Edlefsen, Phys. Rev. **34**, 233 (1929).

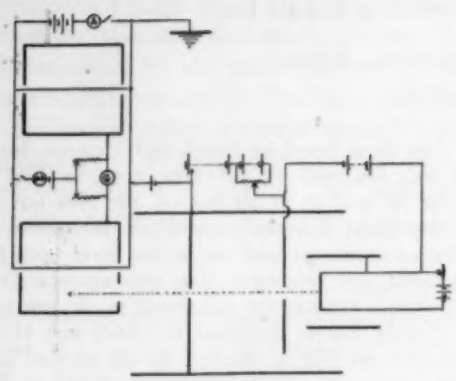

FIG. 1. Diagram of the apparatus showing connections.

sensitive to positive ions and is quite insensitive to electrons, primary or secondary.

Two hollow, monel metal cylinders, 19 by 20 mm, are mounted with a filament of 5 mil tungsten wire running axially down the center of each. (See Fig. 1.) The ends of the cylinders are closed except for small holes through which the filament connections project and except for a hole through which positive ions may enter one cylinder. A small potential of one or two volts is applied between the cylinders and filaments. When the filaments are heated, a space-charge limited current of electrons flows between the filaments and the cylinders. This electronic current is extremely sensitive to positive ions in the space-charge region. Since the positive ions remain in the region 30,000 to 40,000 times as long as the electrons, each ion is effective in neutralizing the space-charge of 30,000 to 40,000 electrons.

Since a space-charge limited electron current is already flowing in the cylinder, further electrons liberated by positive ions in any manner can have no effect on the electron current. In addition, if they could have an effect, it would only be about 10^{-4} times that of the positive ions. The measuring of the electron current thus provides an excellent means of observing any ionization that may be produced.

Two filament-cylinder units are used instead of one in order to provide means of eliminating small fluctuations in the electron current which would interfere with the measurements. Instead of connecting the two filaments in series as Lawrence and Edlefsen did, they were connected in parallel. This is more satisfactory for the following reason: Aside from geometrical factors, the space-charge limited current depends only on the voltage, $I=kV^{\frac{3}{2}}$. A fluctuation in voltage dV would cause a corresponding change in current $dI=3/2kV^{\frac{1}{2}}dV$. If the geometrical factor k is the same for both cylinders, dI will only be the same in both if V is the same in both (dV will be the same for either series or parallel connection). Because of the voltage drop down the filament, V will not be the same in both cylinders if the filaments are in series, but will be if they are in parallel.

Similarly to Lawrence and Edlefsen's method, the two space-charge units are connected as two arms of a Wheatstone bridge circuit; two variable resistances, about 10,000 ohms each, are used for the other two arms, and a galvanometer of sensitivity 9×10^{-11} amp./mm is used for the bridge.

The positive alkali ions are projected directly into one of the cylinders. The other cylinder is shielded from the ion beam, and so all fluctuations in electron current except those due to the positive ions and the ions they form are balanced out. The ions are obtained directly from a heated platinum filament coated with a Kunsman catalyst[8] containing the salt of the alkali ion desired. The ions are accelerated in two stages through a slit system and then enter the detector. The whole tube is filled with the gas to be ionized at a suitable pressure to insure that ionizing collisions will occur in the cylinder. This pressure ranges from 4×10^{-3} mm to 1.5×10^{-2} mm Hg. The average distance traveled by the alkali ions is about 5 cm. The ions of the beam affect the detector, as is to be expected, but above 10 volts energy, this effect becomes quite independent of speed. It can thus be eliminated by changing the resistances to bring the bridge back to balance.

As the accelerating voltage applied to the beam is raised, the galvanometer deflection is observed to remain constant or nearly so until a critical value of the voltage is reached. Above this voltage the galvanometer deflection increases linearly with the voltage (see Fig. 2). This critical voltage where ionization begins was determined for each of the 5 alkali ions in each of the 5 noble

[8] Kunsman, Science **62**, 269 (1925).

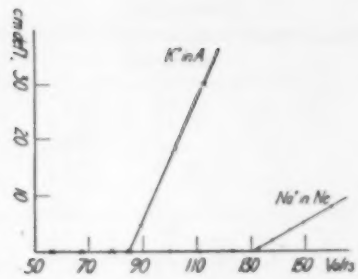

FIG. 2. Plot of galvanometer deflection in cm against alkali ion speed in volts.

gases (He, Ne, A, Kr, Xe). The potentials in volts at which ionization begins in each case are given in Table I.

These results have all been carefully checked. The unknown errors in speed of the ions do not exceed ±3 volts. Further errors which may exist must tend to give lower rather than higher values, for while it is possible that the ions do not gain the full energy of the applied field, it is quite impossible for them to be moving with greater energies than are actually applied to the tube.

The neon, krypton and xenon gases were purchased from the producers as 100 percent pure, and no further attempts at purification were made. The argon and helium were drawn from commercial tanks, and though they showed no spectroscopic traces of impurities, they were passed over hot copper to remove oxygen and over tubes of calcium chloride, phosphorus pentoxide, and potassium hydroxide to remove water and carbon dioxide. Further, the argon was treated in a calcium arc and the helium was run through a double, liquid-air cooled charcoal trap.

TABLE I.

	Ne	A	Kr	Xe
Li^+	*307*	*100*	*420?*	*250*
	—	—	—	—
Na^+	*175*	*105*	*400?*	*360?*
	130	—	—	—
K^+	*320*	*95*	*80*	*120*
	—	82	69	114
Rb^+	*423*	*180*	*100*	*145*
	—	135	97½	150
Cs^+	*437*	*365*	*243*	*105*
	—	338	200	77

Italics, Beeck and Mouzon results.
Ordinary figures, Varney results.

Before taking readings the tube was thoroughly baked out at about 400°C, the test of the thoroughness being that when the tube was cut off from the pumps with less than 10^{-6} mm Hg pressure, the pressure would not show any signs of starting up when all the filaments were heated to their maximum temperatures for half an hour. The time necessary for a complete set of readings with one ion source in one gas did not exceed this period. The pressure was measured on a large McLeod gauge. A liquid-air trap was connected to the tube at all times when readings were taken to remove Hg vapor and any last traces of water or grease vapors which might be present.

All the catalysts emitted only the ion desired with the exception of the Rb^+ source and the spodumene Li^+ source. The Rb^+ showed all the other alkali ions, and all the curves using the Rb^+ source had two or three break points corresponding to ionization by the "impurity" ions as well as the Rb^+ ions (see Fig. 3). Because of the great efficiency of K^+ in A and Kr, and of Cs^+ in Xe, the effect of one or another of these impurities was almost as great as the effect of the Rb^+. The voltage obtained as the ionization potential for any ion in a gas was of course the same whether the ion came directly from a pure source or as an impurity in some other source. The only possible doubt of the possibility of interference of an impurity with the results on the ion desired is that the values for Rb^+ in Kr and in Xe seem a little high. The spodumene used as a Li^+ source showed considerable quantities of K^+ which interfered with the use of the source in anything but He and Ne. No ionization was observed with the Li^+ nor with Na^+ in any gas except Ne. Likewise, no ionization was observed in He or in Ne (except for Na^+ in Ne). H_2, N_2 and CH_4 were also tried with several ion sources (Na, K, Rb, Cs) and although ionization by Na^+ and K^+ was originally reported in N_2,[9] the results could not be repeated, even under conditions of greater sensitivity, so it was necessary to conclude that it did not occur at all. It is possible that since the degassing of the tube was not so carefully done at first, traces of argon from previous readings gave wrong results. No ionization was observed at all in the other two gases.

It is believed that the sensitivity of the

[9] Varney, Phys. Rev. **46**, 235 (1934).

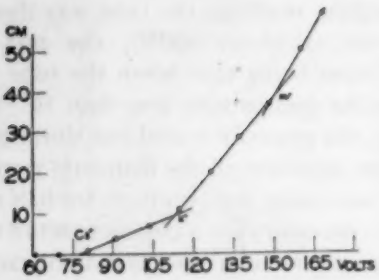

FIG. 3. Plot of galvanometer deflection in cm against alkali ion speed in volts when the Rb^+ ion catalyst containing impurities was used in Xe gas.

apparatus was sufficient to enable less ionization to be observed than Beeck and Mouzon reported, but this point is hard to establish because it is only possible to make qualitative comparisons of relative ionizing efficiencies.

When energy and momentum are conserved in an inelastic collision of the type above, it can easily be shown that only a fraction of the energy of the incident ion is available for changing the internal energies. This fraction has a maximum value for direct impact and is equal to $m_aE/(m_i+m_a)$, where m_a is the mass of the gas atom, m_i is the mass of the alkali ion and E is the incident energy of the alkali ion. When this factor is applied to the results, they assume a much more significant form. (Table II.)

Attention is called to the following features of Table II. First, in certain cases, the same electronic configuration is involved in two different collisions. For example, K^+ and A are identical in structure except for a difference of one proton in the nucleus, and the same is true for Rb^+ and Kr. Consequently, collisions of Rb^+ and A involve the same electron structures as K^+ in Kr, the only difference lying in which is the colliding ion and which is the atom ionized. Similarly, Cs^+ ions in A and K^+ in Xe involve collisions of identical groups of electrons, and likewise Cs^+ ions in Kr, and Rb^+ in Xe. Now the table of reduced results shows corresponding

TABLE II.

	Ne	A	Kr	Xe
Na^+	61			
K^+		41	47	83
Rb^+		43	48	90½
Cs^+		78	77	38

TABLE III.

	Reduced	Unreduced
Rb^+ in A	43	135
K^+ in Kr	47	69
Difference	− 4	66
Cs^+ in A	78	338
K^+ in Xe	83	114
Difference	− 5	224
Cs^+ in Kr	77	200
Rb^+ in Xe	90½	150
Difference	−13½	50

similarities in ionization potentials which do not appear in the unreduced results. (Table III.) This improvement in correlation of results in corresponding cases is decidedly striking.

The second feature of the reduced table is that with the exception of Rb^+ in Kr the voltages along the main diagonal of the table are less than any other values in the same row and column. (The deviation in the case of Rb^+ in Kr is, however, within the probable error claimed for the results.) This fits in with the expectation that the lowest potentials should be obtained for the ions most nearly alike in electronic configuration. Previous attempts to correlate results showed K^+ in Kr much lower than either K^+ in A or Rb^+ in Kr and by amounts well beyond the experimental error.

The results obtained in this experiment are with a single exception (Rb^+ in Xe) lower than those obtained by Beeck and Mouzon. The maximum difference amounts to 45 volts in a few cases. The results are, however, substantially in agreement with those obtained by Beeck and Mouzon. Nordmeyer[10] has obtained 75 volts for K^+ in A by using a method similar in principle but not in detail to that of Beeck and Mouzon. (Beeck had 95 volts, the author had 82 volts for K^+ in A.)

The greatest disagreement is in the results with Li^+ and Na^+ ions and in Ne gas. With the exception of Na^+ in Ne, no ionization has been observed by the space-charge method in these cases. The application of the reduction factor given above to the results in these cases obtained by Beeck and Mouzon are given in Table IV.

[10] Nordmeyer, Ann. d. Physik (5) **16**, 706 (1933).

TABLE IV.

	Ne	A	Kr	Xe
Li^+	228	85	385	237
Na^+	82	67	314	306
K^+	109			
Rb^+	81			
Cs^+	58			

Correlation similar to that found in other cases does not appear here.

K^+ in Ne	109	Rb^+ in Ne	81	Cs^+ in Ne	58
Na^+ in A	67	Na^+ in Kr	314	Na^+ in Xe	306
Difference	42		−233		−248

The potentials do not even drop off uniformly in one direction as might be anticipated. The difficulties of avoiding secondary electrons becomes increasingly great with ions of higher speeds, and this interference of secondaries may possibly explain the results of Beeck and Mouzon. It is to be noted that the ionization potentials they observed are in most cases up in the range of 300 to 400 volts. Oliphant[11] and others have shown that the emission of secondary electrons when positive ions strike metal surfaces increases strongly with increasing energy. Nordmeyer[10] has also discussed in detail the strong likelihood of certain disagreements between his results and Beeck's being due to secondary electrons.

Finally, it may be pointed out that the investigation was carried out on the ionization at energies from 5 volts up. Although the behavior of the ion detector is difficult to analyze when such slow ions are used in the beam, it was concluded that no ionization occurred at energies below those given in the table of results.

The writer is particularly indebted to Professor L. B. Loeb and Professor E. O. Lawrence who suggested the application of the space-charge method to this problem, and to the helpful direction of Professor Loeb. Doctor C. H. Kunsman, Chief of the Fertilizer Investigations of the U. S. Bureau of Chemistry and Soils, very kindly furnished the catalysts used as ion sources. The writer is also indebted to Doctor O. Beeck for numerous discussions of the problem.

[11] Oliphant, Proc. Roy. Soc. **A127**, 373 (1930).

MARCH 15, 1935 PHYSICAL REVIEW VOLUME 47

The Rotational Energy of Polyatomic Molecules

J. H. VAN VLECK, *Harvard University*

(Received February 5, 1935)

It is shown that the quantized energy of a polyatomic molecule is approximately separable into the internal electronic and vibrational energy plus the rotational energy with the latter determined by solving the conventional problem of the rigid asymmetrical top. Because of the large oscillating terms in the Hamiltonian function due to interaction between vibration and rotation, this conclusion is not as obvious as it sounds, and seemed, if anything, to be contradicted by Eckart's recent investigation on the choice of a reference frame. The discrepancy, however, disappears when a second order perturbation calculation is made with Eckart's coordinates.

IT has commonly been supposed in the literature that the rotational energy of a polyatomic molecule is very approximately the same as that of a rigid body with three unequal moments of inertia I_1, I_2, I_3. In other words, it is assumed that the total energy can be obtained by computing first the internal electronic and the vibrational energy, and then adding an eigenvalue of the "asymmetrical top" problem, whose Hamiltonian function is

$$H_{rot} = \sum_{i=1,\ 2,\ 3} (P_i - \zeta_i)^2 / 2I_i, \qquad (1)$$

where P_1, P_2, P_3 are the components of total angular momentum relative to the three principal

axes. In order to cover the most general case, we have here assumed that the mean angular momentum connected with the nuclear vibrations does not necessarily vanish, but instead may have components ζ_1, ζ_2, ζ_3 relative to the principal axes. In this event one must subtract the vibrational from the total angular momentum to obtain the purely rotational angular momentum, whose squares enter in (1). The ζ_i terms arise only if there is degeneracy, i.e., if several normal vibrations coincide in frequency. The possibility of such terms was first suggested by Kramers and Pauli,[1] and they have recently been employed by Teller and Tisza[2] and by Dennison and Johnston[3] in analyzing the spectra of symmetrical molecules. The case $\zeta_i \neq 0$ corresponds not to the ordinary or true asymmetrical top, but rather to a gyroscopic one with flywheels mounted thereon. We wish to stress that our primary interest is in the coefficients of P_1^2, P_2^2, P_3^2 in (1), not in the ζ terms, and we hope that the reader will not be unduly distracted by their inclusion.

The legitimacy of using (1) has recently been questioned by Eckart.[4] Although the first reaction of one's physical intuition is in favor of (1), closer examination (see below) shows that the interaction of rotation and vibration yields oscillatory terms in the Hamiltonian function which are of a larger order of magnitude than those due to rotation alone, so that conceivably the rotation-vibration coupling might make the energy structure different from that given by (1). In fact by devising a very ingeneous coordinate scheme, Eckart derives a Hamiltonian function which suggests that the coefficient of P_i^2 is more nearly equal to $I_i/2(I_{i+1}-I_{i+2})^2$ than to the conventional value $1/2I_i$. The same anomalous coefficients of P_1^2, P_2^2, P_3^2 also appear in a rotational wave equation given by Hirschfelder and Wigner.[5] As the main result of the present paper, we shall prove that the anomalies are illusory,[6] and disappear when the perturbation calculations with either the Eckart or H–W Hamiltonian function are pushed through to the proper approximation. Thus the final outcome is to restore the conventional form (1).

A simple two-dimensional example. Before we proceed to the general proof for the actual, three-dimensional case, the nature and solution of the paradox will be clearer if we first treat by way of illustration a hypothetical two-dimensional system, consisting of a set of n particles subject to forces exerted by each other and by a fixed attracting center. These forces are to be of such character that all particles can have equilibrium positions.[7] The general motion can be approximately described as harmonic vibrations about equilibrium superposed on a rigid rotation of the equilibrium configuration about the center of attraction. If r_k, φ_k be the polar coordinates of a typical particle, the Lagrangian function is

$$L=\tfrac{1}{2}\sum_{k=1}^{n} m_k(\dot{r}_k^2+r_k^2\dot{\varphi}_k^2)-V(r_1,\cdots r_n,\ \varphi_2-\varphi_1,\cdots\varphi_n-\varphi_1),$$

[1] Kramers and Pauli, Zeits. f. Physik **13**, 343 (1923).

[2] Teller and Tisza, Zeits. f. Physik **73**, 791 (1932); also especially the article by Teller in *Hand- und Jahrbuch der Chemischen Physik*, band 9, p. 151 ff.

[3] D. M. Dennison and M. Johnston, Phys. Rev. **47**, 93 (1935).

[4] C. Eckart, Phys. Rev. **46**, 383 (1934).

[5] J. O. Hirschfelder and E. Wigner, Proc. Nat. Acad. Sci., Feb. 1935. I am indebted to these writers for sending me the manuscript in advance of publication.

[6] I must by all means mention that in his dissertation, Groningen 1931, p. 103 ff., H. B. G. Casimir derives Eq. (1) for a model consisting of a single heavy particle oscillating about an equilibrium position on a rotating rigid frame whose mass is not negligible. This model is doubtless a sufficiently close approximation to the behavior of a real molecule to make it reasonably clear that (1) is the correct result. Further, in a letter to Professor Eckart, of which the writer learned after the present calculation was made, Casimir sketches a method whereby (1) can be derived with Eckart's coordinates and without the restriction to the "special model." Casimir's procedure differs from mine in using a contact transformation rather than second order perturbation theory. For instance, an alteration in the definition of the canonical momenta corresponding to the transformation

$$\psi\rightarrow\psi\exp\left[(-2\pi i/h)\Sigma_i\chi_i P_i E_i/2D_i\right]$$

in the wave function eliminates the troublesome linear terms from Eckart's Hamiltonian function in the case $\zeta_i=0$. The meaning of the notation is explained after our Eq. (17).

The difference between Casimir's method and mine is mainly superficial. The utilization of the contact transformation is the more elegant procedure, while perturbation theory is more explicit in showing how orders of magnitude enter in removal of the Eckart paradox, and seems to be easier to apply to unsymmetrical coordinate systems, as in our two-dimensional example.

[7] In the interest of simplicity we assume that the mean electronic angular momentum is zero, or, more generally, we do not include the interaction between rotation and the instantaneous electronic motion. Standard methods are available for handling this interaction (cf., for instance, Kronig, *Band Spectra and Molecular Structure*, Chaps. I, II) and so it need not be considered here.

with the understanding that the potential energy V has a sharp minimum at the equilibrium configuration

$$r_k = r_k^0, \quad \varphi_k - \varphi_1 = \varphi_k^0 - \varphi_1^0. \tag{2}$$

At the same time that we pass to the Hamiltonian form, it will be convenient to introduce in place of $\varphi_2, \cdots, \varphi_n$ a set of relative angular coordinates $\gamma_k = \varphi_k - \varphi_1$ $(k=2, \cdots f)$ whose apse line is the radius vector to the first particle. One readily finds that

$$H = \frac{1}{2m_1} p_{r_1}^2 + \sum \frac{1}{2m_k}\left(p_{r_k}^2 + \frac{p_k^2}{r_k^2}\right) + \frac{1}{2m_1 r_1^2}(P - \sum p_k)^2 + V, \tag{3}$$

where

$$p_{r_1} = m_1 \dot{r}_1, \quad p_{r_k} = m_k \dot{r}_k, \quad p_k = m_k r_k^2 (\dot{\gamma}_k + \dot{\varphi}_1), \tag{4}$$

$$P = m_1 r_1^2 \dot{\varphi}_1 + \sum m_k r_k^2 (\dot{\gamma}_k + \dot{\varphi}_1). \tag{5}$$

Here and elsewhere, to simplify printing, we write p_k for p_{γ_k}, and it is to be understood that all sums over k whose limits are unspecified are to extend from $k=2$ to $k=n$, with exclusion of $k=1$. The total angular momentum of the system is P, and is a constant of the motion since P is canonically conjugate to a cyclic coordinate φ_1. Our calculation can be regarded equally well as a classical or quantum-mechanical one. In the quantum version, expressions such as p_k, γ_k, P, φ_1, etc., are, of course, to be regarded as matrices, and the average values denoted by bars are the diagonal matrix elements.

Let us imagine that we have found a solution of the dynamical problem (3) such that all the coordinates, including φ_1, are periodic functions of the time (i.e., in quantum mechanics are matrices of the simple Heisenberg type, with time factors $e^{2\pi i\nu(n;n')t}$). Such a solution represents a motion devoid of mass rotation, since by hypothesis φ_1 contains no linear term in t. Let ζ be the value of the expression (5) for this solution. The quantity ζ can be termed the vibrational angular momentum, since it exists because instantaneously $r_k \neq r_k^0$. If we could replace r_k^2 by $r_k^{0^2}$, the expression (5) would vanish for the type of solution under consideration, since it has $\bar{\dot{\gamma}}_k = \bar{\dot{\varphi}}_1 = 0$. Such a replacement is not in general allowable, because $m_k \overline{r_k^2 \dot{\gamma}_k}$ is not necessarily the same as $m_k \bar{r}_k^2 \bar{\dot{\gamma}}_k$.

We now use perturbation theory to treat the general rotational case where $\bar{\dot{\varphi}}_1 \neq 0$ and so $P \neq \zeta$. This is done by replacing P by $\zeta + \lambda$ and making the perturbation calculation as a series development in the parameter λ. Actually, P can only have the quantized values $mh/2\pi$ in wave mechanics, and so is not an arbitrary number, but this difficulty may be circumvented by solving a hypothetical perturbation problem in which λ is arbitrary, and then substituting the proper quantized value of λ at the end.[8] This procedure is allowable since it is only when the last degree of freedom is introduced that P has any physical significance, and P plays only a parametric role for the reduced problem of $n-1$ degrees of freedom obtained by ignoring φ_1.

The unperturbed Hamiltonian function is thus obtained by taking $P=\zeta$ in (3) and represents irrotational motion. The perturbing potential is

$$[\lambda(\zeta - \sum p_k) + \tfrac{1}{2}\lambda^2]/m_1 r_1^2, \tag{6}$$

as this is the difference between the values of (3) with $P=\zeta+\lambda$ and of (3) with $P=\zeta$. The effect of the first term of (6) vanishes in the lowest approximation, since by (4) and (5) with[9] $P=\zeta$

$$(\zeta - \sum p_k)/m_1 r_1^2 = \dot{\varphi}_1, \tag{7}$$

and since by hypothesis the mean value of $\dot{\varphi}_1$ taken over the unperturbed motion is zero. The coefficient of λ^2 in (6), or what is the same, of P^2 in (3), does not have the value $1/2I$ which is characteristic of the rigid rotator. This is the Eckart paradox when specialized to our two-dimensional system. There is, however, the difference that in our two-dimensional example, the anomalous coefficient $1/2m_1 r_1^2$ cannot possibly, on symmetry grounds, be the right coefficient of λ^2 in the final expression for the energy, since the first particle surely cannot be preferred above all others. On the other hand, the anomalous coefficient yielded by Eckart's three-dimensional coordinate system is symmetrical in

[8] In particular, the unperturbed motion $\lambda=0$ need not be a quantized one as far as P is concerned, since ζ need not be an eigenvalue of P, although of course it is in the commonest case $\zeta=0$.

[9] In using (5) one can take $P=\zeta$ since the unperturbed motion has $\lambda=0$.

all particles, and so presents a much more recondite problem.

The answer to the paradox is that even though the linear term of (6) in λ does vanish on the average, its root mean square is of a larger order of magnitude than the part of (6) which is quadratic in λ. Hence, as mentioned to the writer by Professor Eckart, it is necessary to make a perturbation calculation which includes the second rather than just the first order effect of the linear term. For brevity, call the two parts of (6) $\alpha\lambda$ and $\beta\lambda^2$, respectively. One way of seeing that the root mean square of $\alpha\lambda$ is larger than $\beta\lambda^2$ is by actual performance of the perturbation calculation, as it will turn out that the second order effect of $\alpha\lambda$ is comparable in magnitude with the first order effect of $\beta\lambda^2$. Another way is by explicit dimensional examination, which shows that the orders of the unperturbed vibrational energy, of the r.m.s. of $\alpha\lambda$ and of $\beta\lambda^2$ are, respectively, $h\nu$, $h\nu x$, and $h\nu x^2$, where ν is a typical vibrational frequency, and x is of the order of magnitude $[\overline{(\gamma_k-\gamma_k{}^0)^2}/4\pi^2]^{\frac{1}{2}}$. As long as we are dealing with small vibrations, x is clearly a small quantity. For an actual molecular system it can be shown of the order of the fourth root of the ratio of electronic to nuclear mass.[10]

One must be careful to distinguish between two things, *viz.*, the coefficient of $\lambda^2=(P-\zeta)^2$ in the original perturbing potential (6), and the coefficient of λ^2 in the finally computed energy constant W. The two are, of course, not necessarily the same, and their difference is the cause of the Eckart paradox.

We now proceed to the requisite perturbation calculation, which we shall make in quantum-mechanical form. By standard formulas, the perturbed energy is

$$W=W_0+(\lambda^2/m_1{}^2r_1{}^{0^4})F(\zeta-\sum p_k;\zeta-\sum p_k)+(\lambda^2/2m_1r_1{}^{0^2}). \quad (8)$$

Here, in accord with previous remarks, we have included the second and first order effects of $\alpha\lambda$ and $\beta\lambda^2$, respectively. We find it convenient to use in many places the abbreviation,

$$F(u;w)=\sum_{n'(n'\neq n)}\frac{u(n;n')w(n';n)}{h\nu(n;n')}, \quad (9)$$

wherein $u(n;n')$ designates a typical matrix element of a quantity u, with n and n' symbolizing the totality of vibrational quantum numbers for the initial and final states, respectively. In virtue of (7) and (5), with $P=\zeta$,[9] we have

$$\zeta-\sum p_k=m_1r_1{}^{0^2}(\zeta-\sum m_kr_k{}^{0^2}\dot\gamma_k)/I, \quad (10)$$

where

$$I=m_1r_1{}^{0^2}+\sum m_kr_k{}^{0^2}. \quad (11)$$

In writing (8), (10) and (11) we have replaced r_k by $r_k{}^0$, which, unlike r_k itself, is a c-number independent of vibrational structure. This approximation is a great simplification, and is allowable because we have already reached the second order stage, making the corresponding error third order. A corresponding approximation was not permissible in earlier stages of the calculation; in fact we saw that it was the difference between r_k and $r_k{}^0$ which made $\zeta\neq 0$. By using (10) we find

$$F(\zeta-\sum p_k;\zeta-\sum p_k)=m_1r_1{}^{0^2}I^{-1}F(-\sum p_k;-\sum m_kr_k{}^{0^2}\dot\gamma_k), \quad (12)$$

inasmuch as $r_k{}^0$ is a constant which can be taken outside the summation in (9). It has been allowable to omit ζ as an argument of F since ζ is also a constant or c-number, and so does not contribute to a sum such as (9) in which diagonal members $n'=n$ are excluded. The advantage of manipulating results into the form (12) is that now the sum in (9) can readily be evaluated with the aid of the quantum conditions

$$p_k\gamma_l-\gamma_lp_k=(h/2\pi i)\delta_k{}^l, \quad (13)$$

which are valid since $\gamma_2,\cdots\gamma_n$, $p_2,\cdots p_n$ can be regarded as a set of multiply periodic canonical coordinates for the unperturbed problem obtained by taking $P=\zeta$ in (3). Furthermore, because the matrix elements all relate to the Heisenberg system of representation, the time factor is $e^{2\pi i\nu(n;n')t}$ and consequently

$$\dot\gamma(n;n')=2\pi i\nu(n;n')\gamma(n;n'). \quad (14)$$

Eqs. (14) and (9) show that the diagonal elements of (13) can be written as

$$-F(p_k;\dot\gamma_l)-F(\dot\gamma_l;p_k)=\delta_k{}^l, \quad (15)$$

inasmuch as $\nu(n';n)=-\nu(n;n')$. (There is no

[10] Born and Oppenheimer, Ann. d. Physik **84**, 457 (1927).

trouble from the fact that the matrix multiplication involved in (13) has a sum inclusive of the term $n'=n$, whereas $n'=n$ is excluded in (9): Namely, the two left-hand members of (13) cancel insofar as this term is concerned, since obviously $p_k(n;\ n)\gamma_l(n;\ n)=\gamma_l(n;\ n)p_k(n;\ n)$ meaning that effectively $n'=n$ can be excluded from (13).) Since our problem involves no vector potentials or magnetic forces, we can without loss of generality suppose the coordinate matrices for the unperturbed problem all to be real, and the momentum matrices, which are linear functions of the first time derivatives of these coordinates (cf. Eqs. 4–5), to all be pure imaginaries. Then $F(p_k;\ \dot{\gamma}_l)=F(\dot{\gamma}_l;\ p_k)$, and combination of this relation with (15) yields

$$-2F(p_k;\ \dot{\gamma}_l)=\delta_k{}^l. \tag{16}$$

Eqs. (16) show that the expression (12) has the value $-\frac{1}{2}m_1r_1{}^{02}\sum m_kr_k{}^{02}/I$ and so after putting $\lambda=P-\zeta$ (8) reduces by (11) to $W=W_0+\frac{1}{2}(P-\zeta)^2/I$, the two-dimensional equivalent of (1).

In this demonstration we have used ostensibly a quantum-mechanical calculation, but classical theory could have been employed equally well instead. It is well known that there is a general agreement of classical and quantum results for harmonically oscillating systems. With the classical treatment, the quantum conditions (13) would be replaced by corresponding expressions involving Poisson brackets. One would then use Fourier series containing action and angle variables instead of Heisenberg matrices, and in place of (8) one would employ the classical second order perturbation formula,[11] which involves derivatives with respect to the action variables. The quantum proof is fully as easy as the classical, since the difference quotients in the former are quite as readily handled as the derivatives in the latter.

Calculation with Eckart's coordinates. The procedure for the three-dimensional case is very similar to that for the preceding example. In terms of Eckart's coordinates,[12] the formula for the second order perturbation energy analogous to (8) with $\lambda=P-\zeta$ is

$$H'=W_0+\sum_{i,\,j}E_iE_jF(N_i,\ N_j)(P_i-\zeta_i)(P_j-\zeta_j)+\sum_iD_i(P_i-\zeta_i)^2, \tag{17}$$

where F still has the significance (9), and where the D's and E's have the values

$$D_i=(R^2{}_{i+1}+R^2{}_{i+2})/2M(R^2{}_{i+1}-R^2{}_{i+2})^2,$$
$$E_i=2R_{i+1}R_{i+2}/M(R^2{}_{i+1}-R^2{}_{i+2})^2,\ (i=1,2,3) \tag{18}$$

in terms of the principal radii of gyration R_1, R_2, R_3 of the molecule. The corresponding principal moments of inertia are

$$I_i=M(R^2{}_{i+1}+R^2{}_{i+2}). \tag{19}$$

Here and elsewhere, the total mass of the system is denoted by M, and $i+3$ is the same as i. Since (17) is a second-order expression, no harm will be done if the R's are calculated for the equilibrium position, so that the C's, E's, I's and R's can all now be regarded as constants independent of the vibrational structure. To facilitate printing, we do not, however, any longer attach zero superscripts to show explicitly that they relate to the equilibrium position. As in the previous example, it is nevertheless the difference between R_i and $R_i{}^0$, important in the earlier stages of the calculation, which makes $\zeta_i\neq 0$. If we forgot the second order effect of the terms which were linear in $(P_i-\zeta_i)$ in the original Hamiltonian function (Eq. (26) of Eckart), the F terms in (17) would be wanting, and the coefficient of $(P_i-\zeta_i)^2$ would have the anomalous value D_i rather than $1/2I_i$ as demanded by (1). This discrepancy is what we have called the Eckart paradox.

The expressions N_i appearing in (17) are momenta conjugate to certain oscillatory coordinates χ_i,[13] and from the quantum and reality

[11] Cf., for instance, M. Born, *Vorlesungen über Atommechanik*, p. 291, Eq. (24).

[12] The complete Hamiltonian function corresponding to (3) is given in Eq. (26) of Eckart's paper, and so is not reproduced here. Our expressions P_i, N_i, $\dot{\chi}_i$, D_i, E_i are respectively the same as M_i, $N_{i+1\ i+2}$, $\omega_{i+1\ i+2}$, $1/2B_i$, $1/C_i$ in Eckart's notation, and we do not choose the scale constants so as to make the mass of each particle unity. The signs of the coefficients of N_{ij} are in error in his Eqs. (25) and (26) as is seen by reference to his Eqs. (21.2) and (22), which are the same as our (22) and (21), respectively.

[13] Eckart's Eq. (13) gives an explicit expression for $\dot{\chi}_i$ rather than χ_i. To find χ_i itself, one can integrate his Eq. (13) with his $\omega_{\beta\gamma,\ \alpha}$ regarded as constant coefficients, which is allowable for our second order perturbation calculation. As a matter of fact, one can see that the χ_i are purely oscillatory coordinates even without making this approximation, since the second of Eckart's relations (12) integrates rigorously into $\frac{1}{2}\Sigma c_{\beta\alpha}c_{\gamma\alpha}$.

conditions it follows in the same way as did (16), that

$$-2F(N_j, \dot{\chi}_i) = \delta_j^i. \tag{20}$$

We shall need the following relations given by Eckart which are the analogs for his problem of our previous formulas (4–5)

$$P_i = I_i\omega_i - 2MR_{i+1}R_{i+2}\dot{\chi}_i, \tag{21}$$

$$N_i = I_i\dot{\chi}_i - 2MR_{i+1}R_{i+2}\omega_i. \tag{22}$$

Here ω_1, ω_2, ω_3 are linear functions of the time derivatives of the Eulerian angles specifying rigid rotation of the molecule. The unperturbed problem is to be so chosen as to make the motion devoid of mass rotation, so that the mean values of ω_1, ω_2, ω_3 are all zero. Let ζ_1, ζ_2, ζ_3 be the corresponding mean values of P_1, P_2, P_3 which, as previously noted, need not be zero. Strictly speaking, there are vibrational oscillations in the expression (21), as (21) gives the components of angular momentum projected upon the instantaneous principal axes of inertia of the molecule,[14] instead of upon axes fixed in space, and the vibrations will cause small nutations in the positions of these instantaneous axes. The resulting oscillations in (21) are, however, unimportant, *viz.*, of the order $h(\gamma_k - \gamma_k^0)/2\pi \sim h(m/M)^{\frac{1}{4}}$ whereas the oscillations in (22) are of the order h itself. The mean value of (21) likewise is of the order h if it does not vanish, i.e., if there really is vibrational angular momentum. For our purposes it is thus legitimate to regard (21) as constant over the vibration, and equal to the angular momentum relative to the equilibrium position. We cannot emphasize too strongly that one cannot correspondingly neglect the vibrational oscillations in (22) which are much greater and which will prove responsible for the removal of the Eckart paradox. One finds that in the perturbation calculation, the first order effect of the linear terms in the $P_i - \zeta_i$ equals[15] $\sum \bar{\omega}_i(P_i - \zeta_i)$ and so vanishes, since by hypothesis, the unperturbed motion has $\bar{\omega}_i = 0$ (cf. Eq. (7) in two-dimensional example). In fact, the whole point of using $P_i - \zeta_i$ rather than P_i as an argument is to eliminate this first order effect. Hence in writing (17), we have included only the second order effect of the linear terms.

When we use (21) with $P_i = \zeta_i$ and (22), and remember that ζ_i is a constant which does not contribute to the sum in (9), we obtain

$$2D_iF(N_i, N_j) = F(N_i, \dot{\chi}_j), \tag{23}$$

with D_i as in (18). From (18) and (19) we have $D_i - (E_i^2/4D_i) = 1/2I_i$. Hence (23) and (20) reduce (17) to the desired form (1), and the proof is thereby completed.

In the two-dimensional illustrative example, the angular momentum P could be treated as a c-number. In the actual, three-dimensional case, P_1, P_2, P_3 must be regarded instead as matrices, since they obey the usual commutation (or rather, non-commutation) rules for angular momentum. We have seen, however, that the vibrational oscillations in (21) could be neglected, and so their non-diagonal elements are in the rotational rather than vibrational quantum number, and they commute with all of the N's to our degree of approximation. (The kinematical interpretation is that in the perturbed motion, P_1, P_2, P_3 vary slowly with time due to rigid rotation of the molecule.) Hence the matrices P_1, P_2, P_3 could be regarded as parameters as far as our preceding vibrational perturbation calculation embodied in Eqs. (17–23) was concerned. However, even when the result (1) is obtained, the secular problem connected with (1), namely that of the asymmetrical top, must be solved. Hence we have used the notation H' rather than W for the left side of (17). It is convenient to use a system of representation in which say P_3 is diagonal: the matrix elements of P_1, P_2, P_3 can then be deduced from the commutation rules, and the secular problem connected with (1) formulated, giving the Wang-Kramers-Ittmann[16, 17] determinant for the asymmetrical top. We omit

[14] This projection is the same as the angular momentum relative to fixed axes which instantaneously coincide with the principal axes of inertia, and the choice of which hence varies continuously with time (cf. Eckart's Eq. (24)). Do not confuse with the angular momentum in an *accelerated* coordinate system which travels with the principal axes; the latter angular momentum presumably involves oscillations of the same order of magnitude as those in (22).

[15] This result is derived from Eqs. (21.2), (22), (26) of Eckart's paper, with sign correction mentioned at end of our footnote 12.

[16] S. C. Wang, Phys. Rev. **34**, 243 (1929).

[17] H. A. Kramers and G. P. Ittmann, Zeits. f. Physik **53**, 533; **58**, 217; **60**, 663 (1929–30).

details, as they are found in Klein's[18] paper or Casimir's thesis. The only point we need emphasize is that the rotational secular problem is to be solved after the vibrational matrix structure has been diagonalized. This is allowable in virtue of the general result of perturbation theory[19] that when degeneracy difficulties do not appear in the first approximation (i.e., for us, retention of the first order effect of the linear terms in $P_i-\zeta_i$) due to the vanishing of average values, it is not necessary to lift the degeneracy until after one has pushed a perturbation calculation for the non-degenerate or high frequency part of the problem sufficiently far to introduce trouble from the degeneracy.

Calculation with Hirschfelder and Wigner's coordinates. Instead of using the Eckart scheme, one may alternatively start the perturbation calculation from the wave equation for polyatomic molecules given by Hirschfelder and Wigner. Their system of reference resembles Eckart's in that it presents the same anomalous initial coefficients D_i of $(P_i-\zeta_i)^2$ defined in (18), but differs in the choice of internal coordinates. Also it exhibits explicitly the matrix elements of P_1, P_2, P_3, giving us the Wang determinant as the immediate result of the perturbation calculation, whereas in Eckart's paper it was not necessary to choose a scheme of representation for P_1, P_2, P_3.

We shall here outline briefly how the Wang determinant is extracted from the H–W wave equation, and shall for simplicity consider only molecules in which the vibrations do not involve angular momentum, so that the irrotational case has $P_i=\zeta_i=0$, and corresponds to zero values for the H–W quantum numbers l and γ. The first step is to establish the relation

$$\begin{aligned}\dot{y}_{n_1} &= (p_{n_1}/m_n)+y_{n_3}Q_2-y_{n_2}Q_3\\ &\quad-(\Sigma p_{n_1}/M)-(MR_1^2-MR_2^2)^{-1}y_{n_3}M_3\\ &\quad-(MR_3^2-MR_1^2)^{-1}y_{n_2}M_2-2D_3y_{n_2}M_3+2D_2y_{n_3}M_2, \quad (24)\end{aligned}$$

which is the content of the Hamiltonian equation $\dot{y}_{n_1}=\partial H/\partial p_{n_1}$ for a molecule devoid of mass rotation. The expression D_i is defined as in (18), and

$$\begin{aligned}Q_3&=(MR_1^2-MR_2^2)^{-1}\Sigma_n(y_{n_1}p_{n_2}+y_{n_2}p_{n_1}),\\ M_3&=\Sigma(y_{n_1}p_{n_2}-p_{n_1}y_{n_2}),\end{aligned}$$

where y_{n_1}, y_{n_2}, y_{n_3} are the Cartesian coordinates of particle n relative to the principal axes of inertia with origin at the center of gravity. The H–W paper gives the explicit form of the wave equation rather than Hamiltonian function, but the latter is obtained in the usual way by replacing $h\partial\cdots/2\pi i\partial y_{n_1}$ by p_{n_1}. With the aid of the formulas

$$\Sigma_n m_n y_{n_i} y_{n_j} = MR_i^2\delta_j^i \quad (25)$$

one finds from (24), and equations symmetrical therewith, that

$$-I_3^{-1}\Sigma m_n(y_{n_1}\dot{y}_{n_2}-y_{n_2}\dot{y}_{n_1})=Q_3-2D_3M_3.$$

The sums encountered in the perturbation calculation are, except for a constant factor, all of the form $F(Q_i-2D_iM_i;\ Q_j-2D_jM_j)$. When one uses relations $-2F(p_{n_i};\ \dot{y}_{n_j})=\delta_j^i$ analogous to (16) or (20), and notices that the y's, R's, and D's may be considered as constant coefficients in the second order perturbation calculation, one deduces that

$$F(Q_i-2D_iM_i;\ Q_j-2D_jM_j)=[\tfrac{1}{4}I_i^{-1}-D_i]\delta_j^i. \quad (26)$$

The zero value when $i\neq j$ is a consequence of the vanishing of the products of inertia in (25). The role of the second term in the right side of (26) is clearly to cancel the anomalous coefficient D_i found if F terms are omitted, while the first term substitutes the normal value. As a typical case, we shall indicate how one derives the matrix element $H'(\gamma;\ \gamma+2)$ of the Wang determinant. This element must be the same as the matrix element of the transformed Hamiltonian for which the non-diagonal elements in the vibrational quantum number have been eliminated by making a second order perturbation calculation. Hence

$$\begin{aligned}H'(\gamma;\ \gamma+2)&=H^{(2)}(n\gamma;\ n\gamma+2)\\ &+\Sigma_{n'}H^{(1)}(n\gamma;\ n'\gamma+1)H^{(1)}(n'\gamma+1;\ n\gamma+2)/h\nu(n;\ n'), \quad (27)\end{aligned}$$

where $H^{(2)}(n\gamma;\ n\gamma+2)$, $H^{(1)}(n\gamma;\ n'\gamma+1)$ are, except for a constant factor $h^2/8\pi^2$, the same as $H_1^{(2)}$ and $H_1^{(1)}+H_2^{(1)}$ in the H–W notation, which is not well adapted to our perturbation calculation, since their subscripts have no meaning regarding orders of magnitude. When explicit values of the right-hand members of (27) are substituted from the H–W paper, and the sum evaluated by means of (26), it is found that (27) acquires the proper Wang value

$$\begin{aligned}(h^2/32\pi^2)&[l^2+l-\gamma^2-\gamma]^{\frac{1}{2}}[l^2+l-(\gamma+1)^2\\ &-(\gamma+1)]^{\frac{1}{2}}[I_2^{-1}-I_1^{-1}].\end{aligned}$$

Case of two or more equal moments of inertia. This case requires special consideration, for, although the conventional formula (1) involves no singularity, the anomalous coefficients D_i found by Eckart and by Hirschfelder and Wigner are seen by (18) to become infinite here. Hence a perturbation calculation cannot be made with their coordinate system as a starting point. One way of partially sidestepping the difficulty is to let the moments of inertia approach equality after rather than before the perturbation calculation is made. The formula (1) then holds as one approaches the limiting case of equal moments of inertia, and so presumably holds in the limit. Another, and more solid procedure is to choose the three Eulerian angles so as to specify not a rotating coordinate frame coincident with the principal axes of inertia, but rather a different rotating frame in which the first axis coincides with the radius vector of one particle, the second axis is in the plane determined by this vector and the radius vector of another particle, and the third axis is of course normal to this plane. Such a set of axes has been used by Wigner in

[18] O. Klein, Zeits. f. Physik **58**, 730 (1929). An anomaly in sign is found in the commutation relations, because the angular momentum is projected on moving rather than fixed axes.

[19] Born and Jordan, *Elementare Quantenmechanik*, pp. 209 ff; J. H. Van Vleck, Phys. Rev. **33**, 467 (1929).

connection with formal applications of group theory to atomic spectra.[20] With this new choice of Eulerian angles, there is no catastrophe when the moments of inertia become equal. The difficulty is rather that the anomalous coefficients, now different from (18), show an undue preference for one particle. In fact, the situation is analogous to that upon which we commented after Eq. (7) in the two-dimensional example, where we chose the coordinate φ_1 to specify the radius vector of one particle. The second order perturbation calculation, of course, removes the dissymmetry, and restores the conventional result (1). This calculation might not be easy to make explicitly, due to the clumsy, unsymmetrical nature of the coordinates, but can only lead to (1), at least when the moments of inertia are unequal, since we have proved by means of Eckart's coordinates that (1) then is inevitable. With the unsymmetrical coordinates, there is nothing to single out the case of equal moments of inertia, so that (1) must remain valid in the limit of equality. This argument furnishes the safest way to see that the terms of the third degree in P_1, P_2, P_3 neglected in our perturbation calculation extending to the second order, are not unduly important when the moments of inertia nearly coincide. This result is not obvious when the symmetrical coordinate system is used.

We may remark incidentally, that it is only when two or more moments of inertia coincide that the expressions ζ_i involved in (1) can have non-vanishing values, for otherwise the molecule will not have sufficient symmetry to permit the vibrational degeneracy requisite for $\zeta_i \neq 0$.

The writer wishes to thank Professor Carl Eckart for interesting discussion and correspondence.

[20] E. Wigner, Zeits. f. Physik **43**, 624 (1927).

MARCH 15, 1935 PHYSICAL REVIEW VOLUME 47

On the Plasticity of Crystals

POL DUWEZ,* *Norman Bridge Laboratory of Physics, California Institute of Technology, Pasadena*

(Received December 26, 1934)

In the following, a theory is given with the purpose of establishing a mathematical relation between the stress and the strain in a crystal when plastically deformed. The existence of a "secondary structure" in crystals is adopted as a basic hypothesis. This structure was pointed out by Professor F. Zwicky to be a consequence of what he calls "cooperative phenomena." The assumption that gliding in crystals takes place between the blocks of the secondary structure is the starting point of the following theory. The additional hypothesis of assuming a statistical distribution of the different forces which produce gliding between the blocks, gives us the means for going further in the calculations. The final result which is the stress strain curve of a crystal, is an exponential law containing three constants, i.e., the torsional modulus G, the elastic limit, (γ_e, τ_e) and the maximum applicable stress τ_m. The form of the hysteresis cycles is deduced from the same considerations and moreover a formula is obtained for the areas of the cycles. Experimental verifications were made on a single crystal of copper, and also on ordinary microcrystalline copper.

PART I

IT is well known that when the yield point is reached in a crystal, gliding takes place between some of the crystallographic planes. If we plastically deform a crystal through application of a sufficiently high stress in a given direction, and then reverse the stress, the gliding is reversed also, but we never obtain the initial state. Plastic deformation of a crystal at low temperatures in general leads to "cold hardening." The conception of the ideal crystal, defined by a geometrical arrangement of particles in a lattice, cannot explain the phenomenon of cold hardening. Zwicky[1–6] has studied other physical properties of crystals which are incompatible with the idea of an ideal lattice. He comes to the conclusion that these properties may be understood in terms of a "secondary structure" in crystals. In this discussion we admit the existence of this secondary structure, and, following Zwicky, we denote as π-planes the crystallographic planes characterizing the secondary lattice. Gliding

* Research Fellow of the Commission for Relief in Belgium, Educational Foundation.

[1] F. Zwicky, Proc. Nat. Acad. Sci. **15**, 253 (1929).
[2] F. Zwicky, Phys. Rev. **40**, 63 (1932).
[3] F. Zwicky, Phys. Rev. **43**, 270 (1933).
[4] F. Zwicky, Helv. Phys. Acta **16**, 210 (1933).
[5] F. Zwicky, Mech. Eng. **28**, 427 (1933).
[6] F. Zwicky, Rev. Mod. Phys. **6**, 193 (1934).

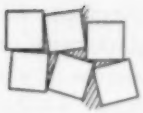

FIG. 1. Model of plastically deformed crystal after Zwicky.

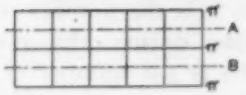

FIG. 2.

occurs in these planes for shearing stresses far smaller than these derived from the theory of ideal lattices.

The laws governing gliding between two planes are not known very accurately. Two different theories were proposed by Frenkel[7] and Becker[8] with the view of defining the conditions under which gliding takes place. Neither of them gives any physical explanation of cold hardening.

Experimentally we know that gliding increases with the shearing stress following a regular curve. In this connection aluminum crystals were studied with very great care by Taylor.[9]

Schematically the pseudostable configuration of a plastically deformed cubic crystal can be represented as shown in Fig. 1. (Rotation of the blocks is exaggerated.) Deformation has taken place along the planes and the blocks have different relative orientations. The shearing stress which is necessary to produce a new gliding is visibly increased (cold hardening). Let us consider a part of a crystal consisting of two slices of elementary secondary blocks (Fig. 2). Let us call A and B the two planes of symmetry of each one of the slices. These two planes are at a distance equal to the constant of the secondary lattice. If we apply a tangential force between A and B great enough to produce gliding along the π-plane, the blocks are disturbed and the configuration becomes that represented by Fig. 1. From the level A to the level B the force is transmitted in two different ways. From A to π, the transmission is purely elastic; along π we must consider a friction between the blocks; from π to B, we have again an elastic transmission. We may assume that the *translation* of each block is the same. On the contrary, the *rotation* is different, and the force required to produce a gliding between two corresponding blocks is consequently *different*.

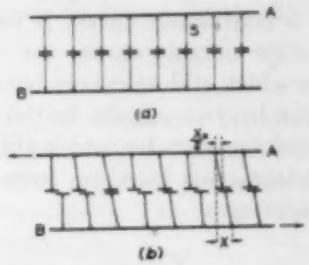

FIG. 3. Mechanical model showing the way the force is transmitted between the blocks of the "secondary structure."

To depict the phenomenon of plastic deformation we consider the mechanical *model* illustrated in Fig. 3. The two planes A and B previously mentioned are represented by two parallel plates to which are attached a series of springs S. These springs are connected by small plates. These can glide on each other. Let us assume that the elastic constants of the springs are all the same, but that the forces required to produce gliding of the surfaces are different. These hypotheses are suggested by the correspondence between the crystal and the model. If we displace the two plates A and B in such a way that they remain essentially parallel, the tangential force will be determined by the values of the elastic constants of the springs and the different forces of each gliding element. Let x be the displacement of the plane A with respect to the plane B. Consider n elements per unit length. To each element corresponds a parameter f_n, which is the minimum value of the force which must be applied to obtain a gliding. It is more convenient in computation to consider the elastic displacement x_n corresponding to this force f_n, as given by the relation $f_n = Kx_n$, K being the constant of the spring. The amplitude of the gliding is, for each element equal to the displacement $x - x_n$, x being the displacement which we impose on every element. Let us divide the interval x into small intervals Δx. In each of these intervals, we have a given number Δn of elements which begin to glide; we have a correspondance between the Δn and the Δx. If we divide the deformation into intervals small enough, we can assume that the correspondance between the ratio dn/dx and x

[7] J. Frenkel, Zeits. f. Physik **37**, 572 (1926).
[8] R. Becker, Physik. Zeits. **26**, 919 (1925).
[9] G. Taylor, Proc. Roy. Soc. **A102**, 650 (1923); **A111**, 533 (1926).

is given by a continuous curve. If $dn/dx=\varphi(x)$ is the equation of this curve, the number of elements for which gliding occurs between x and $x+dx$ is given by $dn=\varphi(x)dx$. In the same way, the number of elements for which gliding occurs when the deformation increases from x_1 to x_2 is given by the integral

$$n_{12}=\int_{x_1}^{x_2}\varphi(x)dx.$$

Knowing the analytical form of the function $\varphi(x)$, we are able to compute, as we shall see later, the total force transmitted by all the elements for a given value of the deformation.

The form of the function $\varphi(x)$ is to some extent arbitrary, and the choice of this function is the main hypothesis on which the following computations are based. We suppose that the number dn of elements which glide between x and $x+dx$, is given by an exponential law of the form

$$dn=Ae^{-ax}dx. \tag{1}$$

We can justify the exponential law by a very simple argument which is used in the kinetic theory of gases to introduce the notion of the mean free path of a particle. Let us consider a *total* displacement x and denote by $P(x)$ the probability of an element retaining an *elastic* displacement x. Suppose that the probability of obtaining gliding for an elementary total displacement dx is proportional to dx. If a is the constant of proportionality, the probability of having no gliding in the length dx is $1-adx$. If we apply the theorem of combined probabilities we have the relation

$$P(x+dx)=P(x)[1-adx].$$

The Taylor expansion theorem limited to the two first terms gives

$$dP(x)/dx=-aP(x).$$

If b denotes a constant, we have $P(x)=be^{-ax}$. The constant b is equal to 1 because the function $P(x)$ must be unity when $x=0$. Consequently $P(x)=e^{-ax}$. Let n be the total number of elements per unit length. The number dn of these having a gliding between x and $x+dx$ will be

$$dn=ne^{-ax}-ne^{-a(x+dx)},$$

since ne^{-ax} is the number of elements which do not glide during the displacement x, and $ne^{-a(x+dx)}$ is the number of elements which do not glide during the displacement $x+dx$. If we develop the exponential function, we obtain

$$dn=nae^{-ax}dx. \tag{2}$$

By definition, the factor a has the dimension of the inverse of a length. Let us put

$$L=1/a.$$

The formula (2) becomes

$$dn=(n/L)e^{-x/L}dx \tag{3}$$

in which L is a length.

It is now possible to calculate the force which we must apply between the two planes A and B (Fig. 3) in order to produce a given deformation x_1. The elements of the mechanical model (or the blocks of the secondary structure in the crystal) may be divided into two classes, depending upon the value of the deformation x_1. In the first class we put those elements for which the gliding occurs between the two surfaces during the increase of the deformation from 0 to x_1. In the second class are put the elements whose deformation is purely elastic. We shall calculate separately the force corresponding to those two classes and the sum will be the total force.

Each element of the first class takes a different part in the transmission of the force. The element for which gliding occurred when the deformation was x transmits a force equal to Kx. This force remains constant as the deformation increases up to the value x_1. If we multiply the number dn given by Eq. (3) by the force Kx, we obtain the elementary force corresponding to the elements dn, i.e.,

$$dF_1=Kx(n/L)e^{-x/L}dx.$$

The total force will be obtained by an integration from 0 to x_1.

$$F_1=(Kn/L)\int_0^{x_1}xe^{-x/L}dx. \tag{4}$$

In the second class we consider the elements for which the deformation is essentially elastic. All those elements, when the deformation is x_1, transmit the same force Kx_1. The same argument

as before gives us the elementary force

$$dF_2 = Kx_1(n/L)e^{-x/L}dx,$$

and the total force will be

$$F_2 = (Kn/L)x_1\int_{x_1}^{\infty} e^{-x/L}dx. \tag{5}$$

If we combine Eqs. (4) and (5), we obtain the total force per unit length transmitted by the elements of the two classes,

$$F = -KnL[1-e^{-x_1/L}].$$

The minus sign means that the force is in the direction opposite to that taken as positive for the deformation. In the following, we shall not take this sign into consideration.

We can replace our linear model by a two-dimensional one in which we consider n^2 elements per unit area. The argument is exactly the same, and we have the formula

$$F = Kn^2L[1-e^{-x_1/L}]. \tag{6}$$

Let us denote $\gamma = x/D, \quad l = L/D, \tag{6'}$

in which D is the constant of the secondary lattice. These ratios are without dimension and the first one corresponds to the definition of a shearing strain in a solid. With those notations, Eq. (6) becomes

$$F = Kn^2Dl[1-e^{-\gamma/l}].$$

By definition, F, being the force per unit area, is the stress. We call it τ. On the other hand, the factor Kn has the dimensions of a modulus of elasticity; let us call it G. The product Dn is obviously unity. Thus we have the final formula

$$\tau = Gl[1-e^{-\gamma/l}]. \tag{7}$$

The slope of the tangent at the origin of this exponential curve (Fig. 4) is G. The asymptote has an ordinate Gl. Let us denote this ordinate by

$$\tau_m = Gl. \tag{8}$$

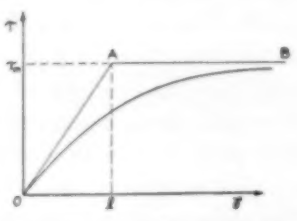

FIG. 4. Form of the plastic stress strain curve.

Hence τ_m is the maximum stress that can be applied without producing rupture of the crystal. We can calculate the mean value of the elastic displacement. This mean value is given by the formula

$$(1/n)\int_0^{\infty} xdn.$$

If we replace dn by its value (3), we find that this mean value is precisely L. We suggest to call "average element" the element having L as elastic displacement. Eqs. (6) and (8) show us that the two lines OA and AB (Fig. 4) are the stress strain diagram of this average element. Hence complete separation of the gliding parts is reached when gliding occurs in the average element.

The constant D of the secondary structure does not appear in Eq. (7) of the stress strain curve. The argument implies the existence of such a structure since we consider a certain number of blocks per unit area. The only hypothesis is that this number has to be of a different order of magnitude than that measuring the size of the specimen from which we derive the stress strain curve. As we are interested in the mean value of the stress over a macroscopic area, it is natural that the size of the blocks is not involved in the result of these calculations. To establish a relation between D and l, we have to introduce a new hypothesis and take into account a physical property of the average block. We can assume, for example, that the average block is such that its elastic deformation is of the order of magnitude of one atomic distance. In this case l would be equal to the ratio of the constants of the primary and the secondary lattice, i.e., d/D. Thence we may obtain an approximate value of D, as l is known experimentally. We shall see in the second part of this paper that the mean experimental value of l is 0.5×10^{-3}, for copper. The resulting approximate value for D is 0.8μ which is in good agreement with the value which Zwicky deduces from other considerations.

Stress strain curve of a crystal having an elastic limit

In the preceding sections we assumed that however small the tension is, a gliding occurs in a certain number of blocks. We can transform our results very easily if we admit the existence of an elastic limit, i.e., a range of deformation in which Hooke's law is applicable. The stress strain curve for which we found the equation represents the phenomenon of plastic deformation starting from the elastic limit, because at this point the first elements are ready to glide, and the conditions required by our hypotheses are present. Mathematically, if we call τ_e the elastic limit and γ_e the corresponding deformation, it is easy to see that we have to replace in Eq. (7), γ by $\gamma-\gamma_e$, τ_m by $\tau_m-\tau_e$, and add the value τ_e of the elastic limit to the result. So that the new formula is

$$\tau=\tau_e+(\tau_m-\tau_e)[1-e^{-G(\gamma-\gamma_e)/(\tau_m-\tau_e)}]. \quad (9)$$

This equation is applicable for $\tau>\tau_e$. When τ is less than τ_e, we make use of Hooke's law $\tau=G\gamma$. We must point out here that all these results are valid only for a tension inferior to the creep limit. The creep phenomenon occurs for rather small tensions in single crystals of pure metals, and in this case the stress strain curve has to be derived from a more general theory.

Possible explanation of plastic hysteresis and measure of the lost energy

The calculations made in the preceding chapter are independent of the direction of the deformation. The stress strain curve 1 (Fig. 5) may be completed by a curve 4, symmetrical with respect to the origin. This curve is obtained experimentally by taking the crystal free from tension, and applying the stress in the opposite direction.

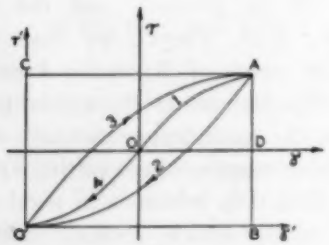

FIG. 5. Form of a hysteresis cycle.

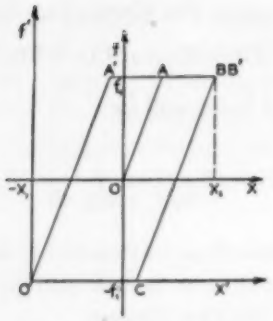

FIG. 6. Hysteresis cycle for a single element of the model Fig. 3.

If, after having deformed the crystal to the state corresponding to point A (Fig. 5), we decrease the stress and then increase it in the opposite direction until we reach the same absolute value, we obtain curve 2. The inverse process gives us curve 3 symmetrical to 2 with respect to O. We obtain a hysteresis cycle. The model which we used to explain the form of the stress strain curve gives a good explanation of the hysteresis phenomenon. The existence of a cycle can be derived (Fig. 6) by considering a *single* element of the model. The stress strain curve of this element is formed by two straight lines OA and AB if we stop the deformation x_1 at this point. If we impose on this element a deformation equal to $-x_1$, the force f will at first decrease linearly, following a straight line parallel to OA, until it reaches the symmetrical value $-f_1$. This is due to the fact that, so far, the spring alone is responsible for the deformation. As we continue to increase the deformation, gliding occurs between the two surfaces and the force remains constant until O'. The inverse process gives us the lines $O'A'$ and $A'B'$ closing up the parallelogram. If we take the axes $O'x'f'$ parallel to Oxf, we easily find that the curve $O'A'B'$ is, considered with respect to the axes $O'x'f'$, obtained by multiplying by two the coordinates of the points of the curve OAB. The two curves are similar. A very simple calculation shows that this property is also applicable in the case of n elements in the model. So if $\tau=f(\gamma)$ is the equation of the stress strain curve 1 (Fig. 5) the equation of curve 3 with respect to a system of axis $O'\gamma'\tau'$, will be $\tau'=f(\gamma')$. The correspondence between τ, τ', γ, γ' is given by $\gamma'=2\gamma$, $\tau'=2\tau$. Curves 1 and 3 are

exactly the same but the scale is changed. Therefore when in possession of the stress strain curve we may draw the hysteresis cycle corresponding to any one point A of this curve; the condition being that the deformation varies between two equal and opposite values.

Hence the calculation of the area of the cycles is very easy. The double of the area of the cycle represented in Fig. 5 is equal to the sum of the two areas $O'3AB$ and $O'2AC$, minus the area of the rectangle $ABO'C$. The area $O'3AB$ (identical to $O'2AC$) is equal to four times the area $O1AD$. Finally we have, if we denote by A the area of the cycle, and by γ and τ the coordinates of the summit of the cycle,

$$A = 8\int_0^{\gamma} \tau d\gamma - 4\gamma\tau.$$

In the general case, we have, between τ and γ, Eq. (9). If we replace τ by this value, the final formula will be

$$A = 4(\tau_m - \tau_s)[\gamma + 2(\tau_m - \tau_s)/G]e^{-G(\gamma-\gamma_s)/(\tau_m-\tau_s)} + 4\gamma\tau_m - (8/G)(\tau_m - \tau_s)^2 - 8\gamma_s\tau_m + 4\gamma_s\tau_s.$$

The mathematical form of this exponential is

$$A = a_1(\gamma + a_2)e^{-C(\gamma-\gamma_s)} + a_3\gamma + a_4$$

in which the a_i's, and C are obtainable from the three constants τ_s, G, τ_m. Beyond a certain deformation, we can see that the term $a_3\gamma$ becomes the most important and the variation of the area with respect to the deformation is almost linear. This amounts to neglecting the curvature of the cycles and considering them as parallelograms.

PART II

The second part of this paper contains some experimental verifications of the preceding considerations. The main results needing confirmations are:

(1) The formula of the stress strain curve.

(2) The similitude between the stress strain curve and a branch of a cycle and as a consequence, the exponential law giving the area of the cycles in terms of the deformation.

The following experimental results were obtained from torsion tests made on specimens of copper of different crystalline structure. The torsion machine was built for small cylindrical specimens of about 2 mm diameter. The torque was directly measured by weights and the angle of deformation by means of the ordinary optical method. The specimens which were used for the experiments are called A, B, C and D. They have the following characteristics: A, B and C were cylinders of polycrystalline copper; the deformation was measured on a length of 10 mm. The specimen A was simply annealed by heating in vacuum a few hours in order to have it free from tension. The structure was microcrystalline. Specimens B and C were recrystallized after cold hardening, by heating in vacuum for five days at a temperature of about 1000°C. The average size of the crystals was 0.2 mm for B and 2 mm for C. Specimen D was a single crystal of copper which had been obtained by recrystallization. The copper wire was first annealed by heating two hours in vacuum at 900°C. Then it was permanently deformed about 1 percent, and heated for eight days at 1000°C. By operating on several wires, we obtained a few single crystals greater than 10 mm in length. The three specimens A, B and C were used to obtain the cycles given in Figs. 7, 8, 9. To have a series of regular cycles, it is advisable to begin with the one corresponding to the greatest stress. Having fixed the absolute value of this stress, we measure the deformations corresponding to different intermediate stresses. A very important condition which must be satisfied is that we must never change the sense of the stress before having reached the summit of the cycle. The deformations which we measure are taken with respect to the summit of the cycle as origin. The axis of deformation is fixed later as an

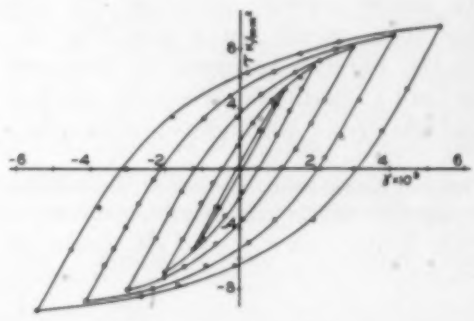

FIG. 7. Hysteresis cycles for polycrystalline copper (microcrystalline structure).

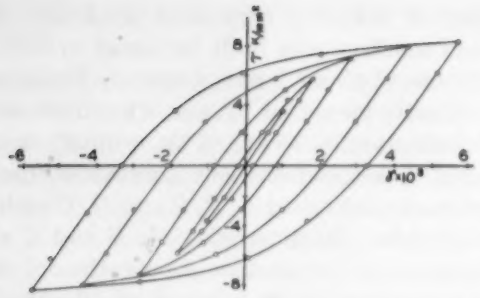

FIG. 8. Hysteresis cycles for polycrystalline copper (*B*). (Approximate size of the grain 0.2 mm.)

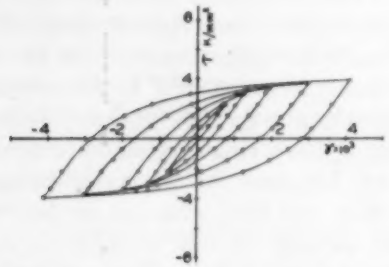

FIG. 9. Hysteresis cycles for polycrystalline copper (*C*). (Approximate size of the grain 2 mm.)

axis of symmetry of the cycle. The cycles of smaller amplitude are obtained by the same process. They are finally all drawn on the same diagram, taking into account the conditions of symmetry. The locus of the summits of the cycles of the resulting diagram gives us the stress strain curve. Having the experimental values of the constants τ_a, τ_m and G, we can calculate the stress strain curve by Eq. (9). The values of these constants and the theoretical and experimental values found for the stresses and the areas of the cycles are given in Tables I and II. The discrepancies are collected in two columns.

The single crystal (specimen *D*) gives a similar stress strain curve (see Fig. 10 and Table II). For this specimen we increased the stress until a measurable creep was reached. By measurable creep, we understand that the angular deformation γ, observed 24 hours after application of the load, increases more than 2.2×10^{-5}, which is the accuracy of the measurements. The hysteresis cycles represented in Fig. 10 are obtained as follows: We increase the stress from zero to 2.7 kg/mm² (point *A*) where we observe a creep. The speed of creep is such that the deformation reaches point *B* after 192 hours (the increase of deformation seems to follow an exponential law). Then, decreasing the stress, we reach point *C* where the creep phenomenon takes place again. After 94 hours, the deformation has increased to point *D*. We apply the inverse process, and the branch *DE* is obtained. We observe the creep between *D* and *F* for 330 hours. Finally we can obtain the hysteresis cycle *FG* without measurable creep if we do not wait more than one hour before reversing the stress at the end of the cycle.

The mechanical model considered in the former section does not take into account the phenomenon of creep. But we can easily understand that when the deformation has reached a certain value, gliding has already occurred in a great number of elements and since very few of them remain elastic, these few are alone responsible for the stability of the deformation. Practically this number is so small that creep occurs. After a certain amount of this creep, there is no

TABLE I. *Elastic limits, deformations and constants.*

SPECIMEN	τ_a (kg/mm²)	$\gamma_a\times10^5$	τ_m (kg/mm²)	G (kg/mm²)
A	3.0	66	9.5	4550
B	3.15	87	8.65	3620
C	0.6	18	4.0	3380
D	1.0	31	2.9	3180

TABLE II. *Theoretical and experimental values of the stresses of the hysteresis cycles.*

SPECIMEN	$\gamma\times10^5$	THEOR. STRESS (kg/mm²)	EXP. STRESS (kg/mm²)	DIFF.	THEOR. AREA (kg/mm²)	EXP. AREA (kg/mm²)	DIFF.
	66.0	—	—	—	—	—	—
	120.0	5.07	5.09	+0.02	0.0008	0.0008	0
A	197.2	6.90	6.87	−0.03	0.0089	0.0094	+0.0005
	299.5	8.22	8.06	−0.16	0.0267	0.0276	+0.0009
	410.0	8.90	8.82	−0.08	0.0595	0.0572	−0.0023
	540.0	9.25	9.48	+0.23	0.0964	0.0936	−0.0029
	101.7	3.67	3.62	−0.05	0.0002	0.0000	−0.0002
	176.2	5.60	5.84	+0.24	0.0040	0.0037	−0.0003
B	281.0	7.12	7.25	+0.13	0.0172	0.0174	+0.0002
	434.0	8.10	7.98	−0.12	0.0549	0.0538	−0.0011
	569.0	8.31	8.35	+0.04	0.0889	0.0906	+0.0017
	78.6	2.14	2.22	+0.08	0.0007	0.0005	−0.0002
	132.0	2.93	2.96	+0.03	0.0028	0.0032	+0.0004
C	195.0	3.40	3.34	−0.06	0.0080	0.0084	+0.0004
	298.2	3.79	3.71	−0.08	0.0191	0.0192	+0.0001
	410.0	3.93	3.90	−0.03	0.0347	0.0353	+0.0006
	37.8	1.19	1.20	+0.01			
	47.1	1.44	1.44	0.00			
	56.3	1.65	1.68	+0.03			
D	67.8	1.87	1.93	+0.06			
	82.7	2.09	2.16	+0.07			
	110.0	2.39	2.41	0.02			
	126.5	2.51	2.53	+0.02			
	162.0	2.68	2.65	−0.03			

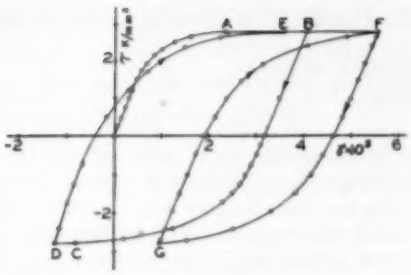

FIG. 10. Hysteresis cycles for a copper single crystal (D) in torsion.

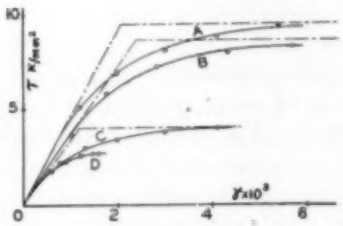

FIG. 11. Stress strain curves in torsion for polycrystalline copper (A, B and C) and a single crystal of copper (D).

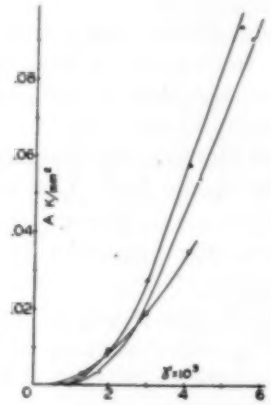

FIG. 12. Areas of the hysteresis cycles in function of the deformation (A, B and C).

reason at all why we could not reproduce a hysteresis cycle identical to the cycle before creep. This is proved experimentally by the fact that the branches of the different cycles drawn in Fig. 10 are identical.

Figs. 11 and 12 show graphically the experimental verifications.

CONCLUDING REMARKS

The experimental results shown in Table II confirm the theory. In addition to the two main results which confirm the theoretical conclusions (1) and (2) stated at the beginning of Part II, we can point out that the tangent at the end of each cycle has always a slope equal to the modulus of elasticity. More generally, each time we reverse the sense of the deformation, we obtained an inclined straight line, if the elastic limit was different from zero. This can be deduced from the theory.

This study does not constitute a direct proof of the existence of a secondary structure in crystals. However, the experimental verifications agree so well with the calculations based on the existence of a secondary structure that it gives a proof *a posteriori* of the reality of such a structure. Our mechanical model is only a model, and we do not maintain that gliding along a π-plane is identical to that of two material surfaces. But, however complicated the motion of the particles in the π-plane may be, the final situation of the two atomic rows is about the same as that which we would obtain by simple gliding.

We can also point out the great regularity which we found in the form of the hysteresis curves obtained with four different specimens. We think that this regularity could be extended to other crystals. And this seems to prove that there is something fundamental in the structure of any crystal which is responsible for the plastic deformation. The notion of a secondary structure has this character of something fundamental and provides a very good tool for systematic researches on the mechanical properties of crystals.

In our experiments we have used the method of torsion as it is the simplest way of obtaining states of pure shearing stress. However, this stress is not uniform over the cross section of the wires. We therefore intend to conduct further experiments on crystals which are subjected to uniform alternating shearing stresses in order to reduce the problem of mechanical hysteresis to the simplest possible case.

In conclusion I wish to express my gratitude to Professors Th. von Kármán and F. Zwicky, under whose direction this investigation was carried out. I am indebted to them for frequent and valuable advice.

The Photoelectric Properties of the (100) and (111) Faces of a Single Copper Crystal

NEWTON UNDERWOOD, *Hood College, Frederick, Maryland*

(Received February 1, 1935)

The two faces were cut from the same single crystal, and etched to remove the broken surface pieces and to expose only crystal facets which were parallel to the geometric boundaries in question. Care was taken to prevent any contacts between the prepared planes and foreign objects. The two specimens were heated simultaneously by electronic bombardment at various red-heat temperatures for over 1500 hours in a good vacuum. The photoelectric thresholds were measured by the use of filters as the outgassing proceeded. During readings, the pressure was less than 5×10^{-8} mm Hg. After 500 hours of outgassing the threshold wavelengths were approximately 2540A for the (111) face and 2200A for the (100) face. The results show that the etching produced by evaporation should be avoided in such an experiment.

INTRODUCTION

THIS experiment was undertaken as a part of a rather extended series of investigations concerning the properties of single metallic crystals instituted at Brown University several years ago. The main work has of course been Dr. Farnsworth's investigations on electron diffraction. M. L. Williams[1] has reported on soft x-rays from copper crystals, and B. A. Rose[2] has published an account of his work on the contact difference of potential. The purpose of this experiment is to investigate the photoelectric properties of the (100) and the (111) faces of a single copper crystal.

The experiments of Goetz,[3] Cardwell,[4] Linder,[5] Dillon,[6] Nitzsche[7] and others have indicated the influence of crystal structure on photoelectric phenomena. The work of Nitzsche is the first in which the photoelectric thresholds have been measured for more than one distinctly prepared crystal face of the same single crystal. However, no attempt was made to remove occluded gases by heating in a good vacuum, and contaminating vapors were present.

PREPARATION OF CRYSTALS

Two pieces were cut from a large single copper crystal in such a manner that a geometrical face of one was parallel to a (100) set of planes and that of the other parallel to a (111) set of planes. The method of accomplishing this is described in detail by Dr. Farnsworth.[8] The surfaces were smoothed on stones, and the final grinding was done on plate glass with a very fine grinding compound. The final grinding was considerably speeded up by using a dilute solution of nitric acid (about 5 percent) as a lubricant instead of water.

After the surfaces were made as scratch free as possible they were given a final etching. The (111) face was exposed by electrolysis in a copper sulphate solution (30 ma at 0.8 volt for 3 hours). It is important to have the electrode plane and parallel to the crystal face. This method gives an exceptionally good crystal face, very few reflections from other planes being visible. The preparation of the (100) face presented considerable difficulty. It was found best to use a preliminary etching bath consisting of a 55 percent (by volume) solution of nitric acid at 25°C until all of the broken crystals were removed and a smooth matte surface was secured. The face was then finally etched in a 64 percent solution of nitric acid at 27°C. The concentration required varies with the temperature. It is highly important to keep the face wet. If it becomes dry when it is taken out for inspection, it must not be put back into the strong solution until it is first wetted in the weaker one; otherwise, a streaked surface will result. If the acid is too strong a reddish brown surface is formed; if it is too weak the surface has a silky appearance. Once a good surface was obtained care was taken to prevent anything from touching it. As soon

[1] Williams, Phys. Rev. **44**, 610 (1933).
[2] Rose, Phys. Rev. **44**, 585 (1933).
[3] Goetz, Phys. Rev. **33**, 373 (1929).
[4] Cardwell, Proc. Nat. Acad. Sci. **14**, 439 (1928).
[5] Linder, Phys. Rev. **30**, 649 (1927).
[6] Dillon, Phys. Rev. **38**, 408 (1931).
[7] Nitzsche, Ann. d. Physik **5**, 14, 463 (1932).
[8] Farnsworth, Phys. Rev. **34**, 683 (1929).

as practical after giving the crystals a final cleaning in a cyanide solution and then distilled water, they were placed in the experimental tube which was quickly evacuated.

Experimental Tube

The mountings of the crystals were designed so as to minimize illumination by stray light, to prevent recrystallization at the crystal faces and to reduce to a minimum the amount of metal containing occluded gases. The first condition is primarily a matter of geometry. In order to realize the second requirement, the point of mechanical contact with the crystal was placed as far away from the front face as possible and the crystal was backed with molybdenum, since direct electronic bombardment causes recrystallization. The third condition was fulfilled by making the movable parts almost entirely out of glass. The mechanical arrangement was such that the two faces could be alternately moved in front of a quartz window, and could also be moved into position for heating by electronic bombardment. The motion was accomplished by external electromagnets acting on iron armatures inside the vacuum. These armatures were completely enclosed in snug fitting vacuum-tight glass tubes, thus eliminating a large source of gas. The whole assembly fitted into the containing tube, the walls of which were the bearing surfaces. A glass guide was introduced which accurately determined the position of the crystals when they were moved into their different locations. The only exposed metal parts, except the crystals, were the two supporting wires, two very thin shields (not shown) and the anode, all of which were made of molybdenum. The scale drawing in Fig. 1 shows the constructional details.

Procedure and Results

The experimental tube was attached to a two-stage diffusion pump vacuum system, and the trap between the last oil diffusion pump and the experimental tube was cooled by solid carbon dioxide in acetone. The vapor pumps were kept running continuously throughout the experiment. After baking the tube for about 36 hours at 400°C the filaments were given a short outgassing at red-heat temperatures, the exposed glass parts were torched, and the carbon dioxide refrigerant was then removed from the trap. After 10 minutes the lower end of the trap was surrounded by carbon dioxide snow for an additional 15 minutes. This allowed the inside walls to warm up so that the water vapor and other condensed gases were pumped out, and at the same time oil vapor was kept from contaminating the experimental tube. The Dewar flask containing the cooling agent was then immediately replaced. The exposed glass parts were again torched and the baking process continued for another 48 hours. Under the best conditions the pressure was about 1×10^{-8} mm Hg as read on an ionization gauge. After the filaments were sufficiently outgassed the crystals were heated by electronic bombardment. The ionization gauge was kept running continuously during the early stages of heating, and the power input was adjusted so that the pressure was kept below 10^{-6} mm Hg and usually nearer 10^{-6} mm Hg. It required several hours of cautious heating to bring the crystals up to a very dull red heat without any unduly high pressure surges. The heatings were continued at dull red heat for 550 hours before any noticeable evaporation appeared. The deposit from evaporation became appreciable after the 875th hour of heating. The two crystals were outgassed simultaneously for over 1500 hours.

A quartz mercury arc was used as a source of light in conjunction with a set of liquid light filters, which were checked at frequent intervals by photographing the mercury spectrum when the different ones were placed in front of the slit of a Hilger quartz spectrograph. The photo-currents were measured by means of a Soller[9] amplifier whose maximum sensitivity was 2×10^{-15} amp./mm.

The experimental data were obtained by measuring successively the photo-currents from the two crystal faces when the various filters were placed in front of the quartz window. Although this procedure does not permit an application of Fowler's[10] method for a precise determination of the long wavelength limits, it should reveal any differences in the photoelectric

[9] Soller, Rev. Sci. Inst. **3**, 416 (1932).
[10] Fowler, Phys. Rev. **38**, 45 (1931).

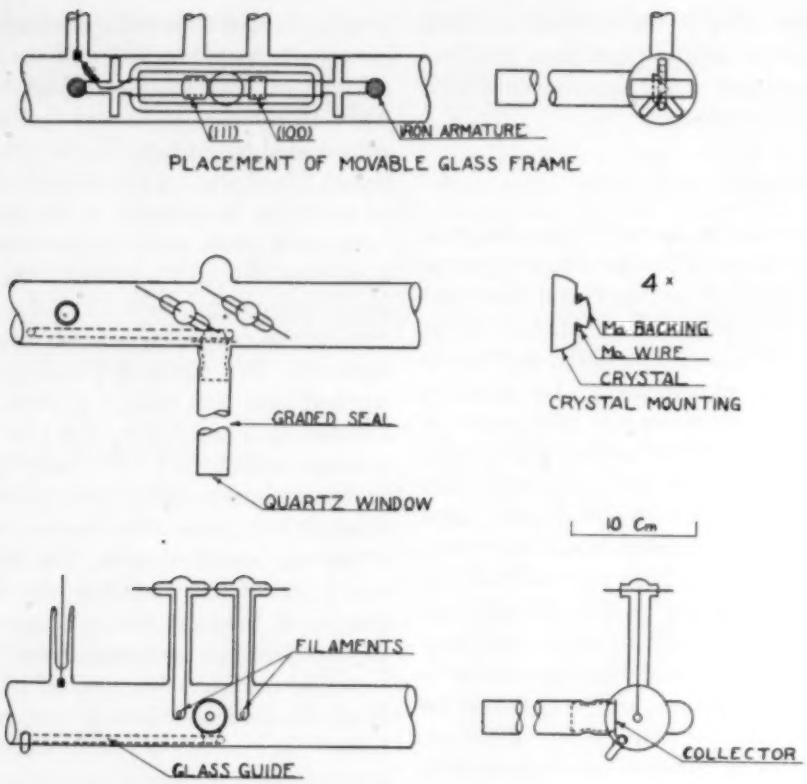

Fig. 1. Experimental tube.

characteristics of the two faces. These currents were plotted against the filter number. An inspection of all the curves shows that the greatest difference in the work function for the two faces appeared after about the 500th hour of accumulated heat treatment. This difference is shown by the graph in Fig. 2. The marked points are believed to indicate the true difference between the two faces which at this stage of the outgassing amounts to approximately 0.73 volt. The surface work function is readily obtained in volts from the relationship $\phi = 12{,}336/\lambda$ (λ expressed in A) and a knowledge of the short wave cut-offs of the filters. The lower horizontal portion at the bottom of the (100) graph has been ignored and ascribed to the presence of foreign crystal planes. The assumption that the small currents represented by this portion of the (100) curves are due to the presence of contaminating facets is supported by the appearance of the curves after evaporation had taken place. After evaporation became appreciable at about the 875th hour of heating, these currents were greatly increased in magnitude. One should expect that the face with the larger work function would be affected most by the contaminating facets, and that as the contamination increased the curves would come to represent the photoelectric characteristics of the plane of smallest work function rather than the characteristics of the prepared faces. This is what was observed. As the heatings were continued at temperatures high enough to produce evaporation, the curves for the two faces became more and more alike, so that finally they were barely distinguishable and the thresholds were extended to about 2536–2650A. An examination of a carefully prepared crystal plane before and after evaporation shows quite definitely that the evaporation process does expose other planes. In order to be sure that the difference observed between the two faces was not due to different outgassing rates, the

FIG. 2. Photo-current *vs.* filter number for the (111) and (100) faces.

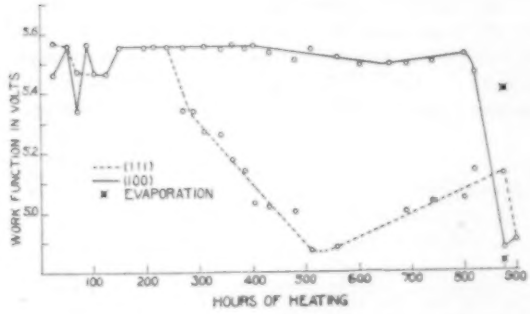

FIG. 3. Work function in volts *vs.* hours of heating for the (111) and (100) faces.

outgassing was occasionally carried out with one of the crystals at a higher temperature than the other. This deliberate heating of either crystal at a higher temperature did not cause the graphs to reverse their relative positions.

All of the curves of the type shown for the 510th hour (Fig. 2) were examined and the work functions of the two faces estimated from them. These estimated work functions are plotted with the corresponding hours of accumulated heat treatment in Fig. 3. An inspection of this graph shows the dependence of the work function on the crystal plane and on the hours of outgassing. The great influence of surface conditions is well exemplified. The problem of obtaining a clean gas free surface is one of the major difficulties encountered in any photoelectric experiment designed to reveal the intrinsic properties of the given substance.

CONCLUSION

The evaporation of metal from the surface constitutes a form of etching. Hence, the outgassing of a single crystal must be carried out at temperatures low enough to prevent evaporation if the original face is to be preserved.

The (111) face assumed a maximum value of approximately 0.73 volt positive with respect to the (100) face after 500 hours of outgassing. This difference is greater than the maximum difference reported by B. A. Rose[2] in his investigation of the contact difference of potential and is of the same sign. The corresponding threshold wavelengths are 2540A for the (111) and 2200A for the (100) faces. The work is being continued with a monochromatic illuminator.

ACKNOWLEDGMENTS

I wish to express my sincere appreciation of the kind supervision and help which Dr. Farnsworth so freely gave. His help and friendly consideration in times of difficulty enabled me to continue. I am indebted to Mr. H. E. Darling for continuing the readings after circumstance made it necessary for me to leave before the outgassing procedure was completed. This work was done while the author was a recipient of a Brown University Fellowship.

LETTERS TO THE EDITOR

Prompt publication of brief reports of important discoveries in physics may be secured by addressing them to this department. Closing dates for this department are, for the first issue of the month, the twentieth of the preceding month; for the second issue, the fifth of the month. The Board of Editors does not hold itself responsible for the opinions expressed by the correspondents.

Induced Radioactivity Using Carbon Targets

In a previous letter[1] we reported observations which showed that at 1000 kv any artificial radioactivity produced in a carbon target when bombarded with protons must be less than one-eight-thousandth of that produced by deuterons, and we concluded, therefore, that any proton-effect comparable to the deuteron-effect, as observed by other workers, must be due to deuterium-contamination.

At the Berkeley meeting Professor Lauritsen presented data obtained by himself and his colleagues showing that the excitation-functions for the two effects were markedly different, and suggested that most of the discrepancy was caused by the fact that the magnitude of their deuterium-effect, given as ten times the proton-effect at 900 kv, would actually correspond to the true value for a considerably lower uniform ion-voltage, due to the rapid decrease in the effectiveness of deuterons with voltage and the fact that the alternating-current ion-beam of their apparatus contains relatively few ions of velocity corresponding to the peak-voltage. This made it possible that their observed proton-effect might be smaller than the experimental limit (one-eight-thousandth of the deuteron-effect) for our proton-determination. Our conclusion based on this large ratio obviously could not apply to effects smaller than the absolute magnitude specified in our report. By increasing our sensitivity we have since observed the proton-effect in question; the ratio of the two effects, however, substantiates our earlier statement. We were thus in error in ascribing the proton-effects announced by the Cambridge and Pasadena groups to deuterium-contamination. This result was reported in the discussion at the International Conference on Physics at London in October, 1934.

Recently we have obtained the excitation-curves for the two effects over the range below 900 kv. These observations are shown plotted on a logarithmic scale in Fig. 1. We have been able to make our intensity-scale entirely comparable to that of the Pasadena workers by using one of Professor Lauritsen's own electroscopes, which he kindly sent us at our request, for this purpose. By measurement, a discharge rate of 4 divisions per minute per microampere on this Lauritsen electroscope corresponds to about 30 counts per minute per microampere on a Geiger tube-counter with a 6-mm diameter window 4 cm from the activated carbon disk. This gives an absolute yield of about one disintegration per 10^{10} incident protons. The voltage-calibration was obtained by assuming a range of 10 mm for 500 kv protons[2] and then adjusting sphere-gap measurements at other voltages proportionately.

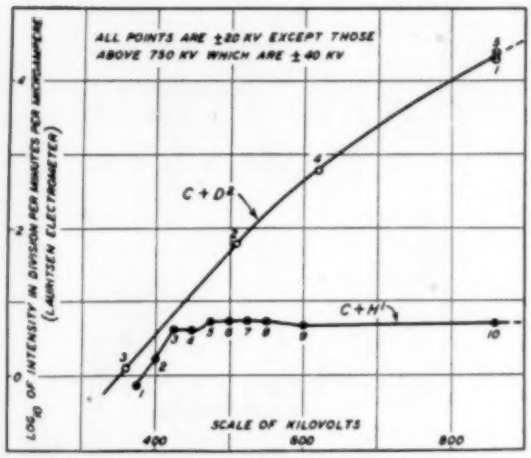
ALL POINTS ARE ±20 KV EXCEPT THOSE ABOVE 750 KV WHICH ARE ±40 KV
LOG10 OF INTENSITY IN DIVISION PER MINUTES PER MICROAMPERE (LAURITSEN ELECTROMETER)
C + D2
C + H1
SCALE OF KILOVOLTS
400
600
800

FIG. 1. Excitation-function for induced radioactivity from carbon.

From Fig. 1, it appears that even at the lowest voltages the effect produced by deuterons is considerably greater than that for protons, in agreement with the latest observations of Cockcroft.[3] The significance of the shape of the proton-curve will be discussed in the letter following.

L. R. HAFSTAD
M. A. TUVE

Department of Terrestrial Magnetism,
Carnegie Institution of Washington,
February 19, 1935.

[1] Hafstad and Tuve, Phys. Rev. **45**, 902 (1934).
[2] Cockcroft and Walton, Nature **129**, 242 (1932); also Blackett and Lees, Proc. Roy. Soc. **134**, 665 (1932).
[3] Cockcroft, Gilbert and Walton, Proc. Roy. Soc. **A148**, 225 (1935).

Resonance Transmutations by Protons

The great difference in the efficiency with which protons and deuterons were found to produce induced radioactivity in carbon, together with the slow rise with voltage of the effect for protons, as reported by Lauritsen at the Berkeley meeting, suggested strongly that the proton-effect might indeed be the infrequent radiative-capture process which was to be expected from theory. This possibility was considered by Breit and Yost[1] who were able to obtain qualitative agreement between theory and experiment insofar as the magnitude of the effect was concerned, but encountered difficulties in reconciling the theoretical excitation function with the available experimental data. During a visit by Professor G. Breit, we accordingly undertook to obtain more accurate observations on the proton-efficiency at various voltages.

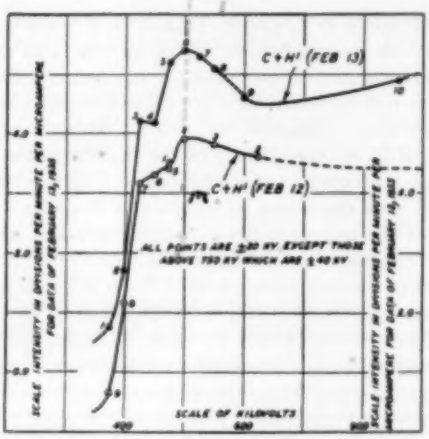

FIG. 1. Excitation-function for induced radioactivity from carbon (thick target).

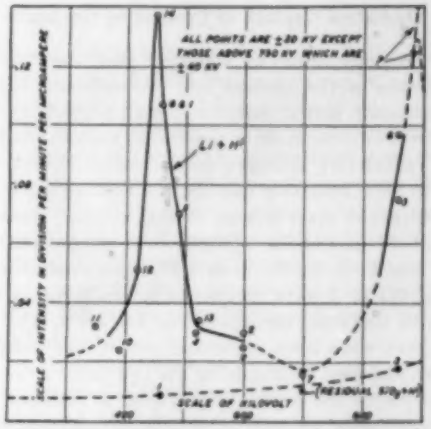

FIG. 3. Excitation-function for gamma-rays from lithium (thin target).

The results obtained for carbon are best summarized by the curves of Fig. 1, which shows the last two of a series of twelve similar observations on both thick and thin targets. The indicated "half-width" of about 15 kv for the 400-kv level is supported by thin-target observations; the width of the second level at about 480 kv has not been carefully examined. Voltage differences in any one sequence are accurate to perhaps 20 kv but the error in the absolute voltage-scale, calibrated as described in our letter above, is probably greater. Fortunately, the existence of sharp voltage-thresholds, such as these, will make it possible to eliminate rapidly any differences in the absolute voltage-scales being used in different laboratories.

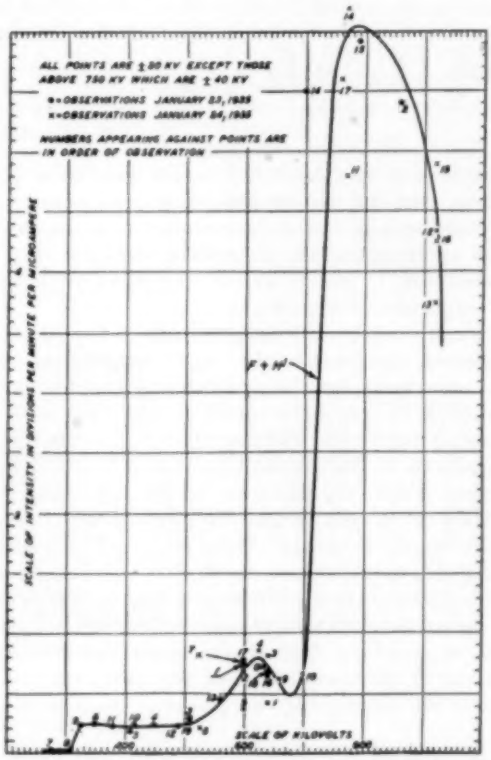
ALL POINTS ARE ±30 KV EXCEPT THOSE ABOVE 750 KV WHICH ARE ±40 KV
NUMBERS APPEARING AGAINST POINTS ARE IN ORDER OF OBSERVATION
F+H'
SCALE OF KILOVOLTS

FIG. 2. Excitation-function for gamma-rays from fluorine (moderately thin target).

In connection with the observations on carbon, it has been convenient to use the Lauritsen electroscope to survey the variation with voltage of gamma-ray emission under proton-bombardment for several elements. The result for fluorine from two days' observations is given in Fig. 2. The three resonance-levels at about 320 kv, 600 kv and 700 kv, suggest among other things, that the gamma-ray emission does not bear a simple relation to a hypothetical short-range group of alpha-particles as has been suggested.

A thin-target curve obtained for lithium is shown in Fig. 3. The sharp resonance at 450 kv supports the suggestion of a resonance at medium voltages made by Professor Lauritsen at the Berkeley meeting. This threshold probably accounts for the failure of Oliphant and Westcott to observe gamma-rays from lithium bombarded by protons, as reported at the London Conference. If the strong indication of a second resonance at 900 kv is verified by future observations showing a decrease at higher voltages, it must follow that the height of the lithium potential-barrier is well in excess of 900 kv in contrast to the indications from alpha-particle emission data.

It is clear that gamma-ray emission is more complex than has been assumed, and that accurate voltage specification is essential in the analysis of gamma-ray components.

We are grateful to Professor Lauritsen for the electroscope he very kindly sent us, which has proved to be exceedingly convenient in this work. We also wish to thank Professors Breit and Gamow for their enthusiastic interest in the problem of radiative capture, and Messrs. Brown and Dahl for invaluable technical assistance.

L. R. HAFSTAD
M. A. TUVE

Department of Terrestrial Magnetism,
Carnegie Institution of Washington,
February 19, 1935.

[1] Breit and Yost, Phys. Rev. **46**, 1110 (L) (1934). (See also letter in this issue.)

Radiative Capture of Protons by Carbon

In a previous note[1] we reported that the "potential well" picture of the nucleus and the ordinary theory of dipole radiation give a sufficiently high probability to the $C^{13}+H^1 \rightarrow N^{13}+\gamma$ to make it possible to explain the formation of radioactive nitrogen under proton bombardment as due to such radiative capture. In the calculations the captured proton state has an orbital angular momentum $L=0$ and the part of the incident wave responsible for the capture has $L=\hbar$. Some numerical errors in substitutions into Eq. (2) of I gave erroneous information as to the position of the first resonance level for $L=\hbar$. The calculations have since been rechecked and it was found that for the model used in preparing the last table a resonance level lies within the experimental range of voltages.

We were kindly supplied with some unpublished data by Crane[2] and Lauritsen which showed a decidedly steeper rise of the yield with voltage than would be expected from the above-mentioned note. Their results indicate resonance at about 600 kv which fits in with the corrected resonance level. The use of alternating current masks the resonance phenomenon somewhat in these experiments. A very clear and indisputable experimental result has been obtained meanwhile independently by Hafstad and Tuve[3] who find by experiments on thick and on thin targets that there are two resonance peaks for the formation of radioactive nitrogen, at 400 kv and at 480 kv, respectively. These data are in approximate agreement with the recently published curve of Cockroft, Gilbert and Walton,[4] who, however, do not definitely speak of the existence of resonance. Because of resonance the theoretically expected yields are much greater with the type of model used than was previously expected. We made calculations using Eq. (2) of I for three values of the nuclear radius R. In each case the depth of the potential well U was adjusted so as to give resonance at about 560 kv. The binding energy of the proton in the captured state and the yield in thick targets were calculated. For $R\times10^{13}=0.33$, 0.41, 0.52 cm the binding energies are 9.7, 6.0, 3.7 mev and the yields are 4×10^{6}, 1.6×10^{6}, 0.6×10^{6} captures per microampere per second while $U=21.4$, 13.4, 8.3 mev. The recoil motion of the C^{13} nucleus was taken into account in these calculations. The computations of the yields involved some numerical integration and are not very accurate.

Experiment gives yields which are about 10^{-3} or 10^{-4} of those calculated and it is significant that changes in the nuclear radius in the limits given above change the yield only by a factor of 7.6 while the combined requirement of correct resonance and binding energies fixes the radius between 0.35×10^{-13} and 0.45×10^{-13} cm. We have thus a definite *contradiction between a model with a constant depth and experiment.*[5]

The calculated yield is not sensitive to exact adjustment of the resonance level to the experimental value. Thus for thick targets on the assumption of the 3/2 power law for variation of range with energy one can express the yield per second of bombardment as

$$\left(\frac{M_1Z_2-M_2Z_1}{M_1+M_2}\right)^2\frac{64\pi^5}{137.2}\frac{c}{v}\frac{N_CN_Pl_0}{(k\lambda)^2k^2}\left|\int\rho\Psi\bar{G}d\rho\right|^2\Big/\left\{\int\left|\bar{G}\right|^2d\rho\cdot\int\Psi^2d\rho\right\},$$

where $\bar{G}/\rho$ is the solution of the radial wave equation for $L=\hbar$ at resonance, N_C is the number of carbon atoms per cm^3, N_P is the number of incident protons per second, l_0 is the range of the protons in carbon at the resonance voltage, Ψ/ρ is the solution of the radial wave equation for $L=0$ and otherwise the notation is as in I. The exponential Gamow factors cancel in this formula because $\bar{G}$ appears to the same power in the numerator and denominator. This expression is not exact theoretically and applies only in cases of sharp resonance for which the upper integration limit of $\int|\bar{G}|^2d\rho$ can be defined without ambiguity as being several times kR. We verified that this expression and Eq. (2) of I give close agreement with results. The penetration through the barrier does not matter much for the final yield, because changes in the width of resonance approximately compensate for changes in $\bar{G}$ at resonance.

The type of change necessary to decrease the theoretically expected yields is that of concentrating the bound proton state inside the N^{13} nucleus so as to decrease its overlapping with $\bar{G}$. This could be accomplished by using a wide and shallow well with an additional deep and narrow sink at very small r. It would seem more likely, however, that the present disagreement between theory and experiment is due to the exclusion principle. A consistent application of the Heisenberg-Majorana or of the Wigner theory of proton neutron interaction will not lead to a simple central field picture.

The half-value breadth is approximately 10 to 20 kv by calculation. The general rise of the Cambridge and Pasadena curves speaks for a larger width while the observations in Washington indicate two peaks each of more nearly the calculated magnitude. The apparent disagreement in the voltage scale of Washington with that of Cambridge and Pasadena is not very significant for the theoretical interpretation of the yield because it does not depend critically on the resonance voltage. There is no real difficulty in finding an explanation for the doublet structure because the vibrations of the α particles with respect to each other and the coupling of their potential valleys can give rise to multiplet structure. Such effects would also give a fine structure of the normal level of N^{13} which may be the cause of the existence of two groups of positrons ejected

by N^{13} according to Cockroft's London conference report. More detailed calculations are necessary in this connection.

If a potential well with variable depth is even a roughly correct picture one should expect similar reactions for heavier elements provided the resonance levels fall in attainable voltage regions.

G. Breit
F. L. Yost

Department of Physics,
University of Wisconsin,
February 18, 1935.

[1] G. Breit and F. L. Yost, Phys. Rev. **46**, 1110 (L) (1934). Referred to as I in the text.
[2] We are very much indebted to Professor Lauritsen for supplying us with these data.
[3] Hafstad and Tuve. See letters in this issue. We are grateful for being informed of the results of these experiments before publication.
[4] J. D. Cockroft, C. W. Gilbert and E. T. S. Walton, Proc. Roy. Soc. **A148**, 225 (1935).
[5] Cf. Henry Margenau, Phys. Rev. **46**, 613 (1934) for evidence of similar breakdown of such a model in heavy nuclei.

Hyperfine Structure of Y II Lines

The yttrium spectrum has been excited in a water-cooled hollow cathode lamp of the vertical type by using argon as the exciting gas. A strong Y II spectrum results. The lines have been examined for hyperfine structure with a Fabry-Perot etalon inserted between the collimating lens and the prisms of a three-prism Steinheil spectrograph. A separation of 3, 4, 5, 8, 10, 12 and 20 mm has been used between the etalon plates. The three lines listed in Table I have shown components.

Table I. *Hyperfine structure in lines of Y II.*

Classification	Int.	λ air A	ν cm^{-1}	$\Delta\nu$ cm^{-}
$4d^2\,{}^3F_3-4d5p\,{}^3D_3$	7	4786.755	20885.15	−0.77
	10	4786.580	20885.92	
$4d^2\,{}^3F_3-4d5p\,{}^3D_2$	10	4900.130	20401.93	+0.15
	7	4900.092	20402.08	
$4d^2\,{}^3F_2-4d5p\,{}^3D_1$	5	4854.089	20591.76	−0.38
	10	4854.870	20592.14	

Since no more than two components have been found for any one line a nuclear moment of $i=\frac{1}{2}$ is indicated A more complete study of the structure is in progress, and the detailed results will be published later.

The writers wish to express their thanks to Professor L. F. Audrieth of the University of Illinois, Chemistry Department, for the supply of Y–Hg alloy which enabled this investigation, and to Professor R. C. Gibbs of Cornell University who has kindly loaned us a pair of Hilger etalon plates.

P. Gerald Kruger
C. N. Challacombe

Physics Department,
University of Illinois,
March 1, 1935.

Ionosphere Studies

The virtual height of the F_2 region of the ionosphere appears to have a definite seasonal variation as shown in the accompanying graph. Over a period of sixteen months, August, 1933 to November, 1934, inclusive, the virtual height, taken near 1200 EST, varies from approximately 250 km in the winter, to 375 km in the summer. The solid curve represents this seasonal effect. The values shown for the individual months are monthly averages of the virtual heights taken over a frequency range from 4500 kilocycles per second up to the particular frequency where the virtual height increases because of the proximity to the critical frequency.

Two possible explanations of such seasonal variation may be offered. (1) In the summer there exists a greater diffusion of the electrons in the F_2 region. If such was the case the wave, having penetrated into the F_2 region, might travel an appreciable distance in the layer before being returned to earth. Because of the greater path traversed at

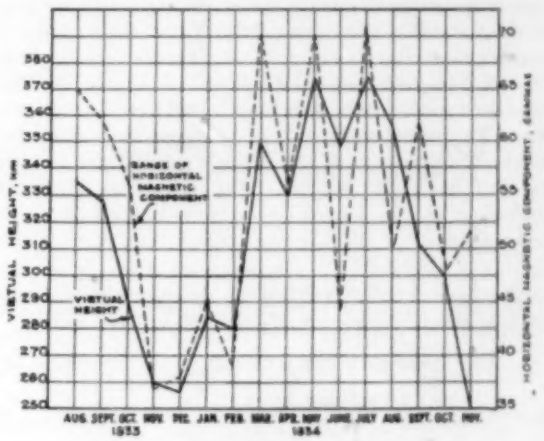
VIRTUAL HEIGHT, KM
HORIZONTAL MAGNETIC COMPONENT, GAMMAS
RANGE OF HORIZONTAL MAGNETIC COMPONENT
VIRTUAL HEIGHT
AUG. SEPT. OCT. NOV. DEC. JAN. FEB. MAR. APR. MAY JUNE JULY AUG. SEPT. OCT. NOV.
1933
1934

Fig. 1.

low group velocity, a greater virtual height would be observed. (2) The F layer is known to separate into two regions, F_1 and F_2, during a summer day. The wave, although returned from the F_2 layer, may have its velocity retarded in traversing the F_1 or any ionized region below the F_2 layer before contacting the latter and again upon leaving it. This would at once indicate a higher virtual height.

It is interesting to note a correlation between the virtual height curve and one for the range of the intensity of the horizontal component of the earth's magnetic field at Cheltenham, for the corresponding period of time. The dashed curve represents an average of the horizontal range for the same days that observations were made on the ionosphere heights.

E. B. Judson

Department of Commerce,
Bureau of Standards,
Washington, D. C.,
February 20, 1935.

Nonelastic Collision Cross Sections for Slow Neutrons

The production of artificial β-active isotopes by neutron impacts, which has been investigated by Fermi and others, shows a considerable increase by sending the neutrons through substances containing hydrogen. It is generally assumed that the effect of these substances is to reduce the velocity of the neutrons to a fairly small fraction of its initial value.

At first it seems very astonishing that the cross sections for these processes as reported by various authors become very much larger than the geometrical cross section of the nuclei in some cases. Chadwick and Goldhaber[1] use this as an argument in assuming that the collision processes are due to forces acting at distances which are large compared with nuclear dimensions. Such a phenomenon would be of very great interest. Indeed Beck and Sitte[2] have pointed out that the radioactive β-decay might possibly take place partially outside the transformed nucleus.

We wish to point out, however, that a very simple quantum-mechanical model sometimes leads to large cross sections and that therefore a definite conclusion cannot be drawn concerning the region in which these processes take place before more detailed evidence is available. We shall consider a small sphere absorbing an incident plane neutron wave. This model is evidently quite independent of detailed assumptions concerning the collision process and accounts for any nonelastic collisions. Let η_0 be the absorption coefficient of the sphere, $k_1=(2\pi/h)(2mE)^{\frac{1}{2}}=2\pi/\lambda_1$ the wave number of the neutrino outside the nucleus, and $k_2=(2\pi/h)[2m(E+U)]^{\frac{1}{2}}$ the same quantity inside the small sphere of radius R. Then the absorption cross section for particles with zero angular momentum becomes

$$Q_0=\frac{\pi}{k_1^2}\left\{1-\frac{\left|i\gamma\dfrac{1-e^{-2\beta}(\cos 2\alpha+i\sin 2\alpha)}{1+e^{-2\beta}(\cos 2\alpha+i\sin 2\alpha)}-i(\alpha+i\beta)\right|^2}{\left|i\gamma\dfrac{1-e^{-2\beta}(\cos 2\alpha+i\sin 2\alpha)}{1+e^{-2\beta}(\cos 2\alpha+i\sin 2\alpha)}+i(\alpha+i\beta)\right|^2}\right\} \qquad (1)$$

$$\alpha=k_2R; \qquad \beta=\eta_0R; \qquad \gamma=k_1R.$$

Under favorable assumptions for $\eta_0(\eta_0R\to 1)$ and for sufficiently small values of k_1 (i.e., for slow neutrons) (1) reduces to the form

$$Q_0\sim R\lambda_1. \qquad (2)$$

Thus, for sufficiently slow neutrons the cross section, Q_0, exceeds the geometrical cross section, $q=\pi R^2$, by a factor $\lambda_1/2\pi R$, which may take values as large as 10,000 provided the neutrons have ordinary temperature velocities.

Though no exactly corresponding phenomenon exists for light, we may regard this result as similar to the well-known fact that in the case of resonance the cross section between atoms and light quanta can become

$$Q\sim\lambda_1^2/4\pi, \qquad (3)$$

which is even of one order higher with respect to λ_1 than (2).

If the velocity of the neutrons decreases, we shall thus generally expect an increase of the cross section (2) up to a lower threshold value of the effective neutron velocities, which of course will be different for various elements and in some cases may be at zero velocity.

Whether this explanation will be sufficient to account entirely for the observed facts cannot be said before more detailed experimental evidence is available.

G. Beck
L. H. Horsley

Department of Physics,
University of Kansas, Lawrence,
February 19, 1935.

[1] Chadwick and Goldhaber, Nature **135**, 65 (1935).
[2] Beck and Sitte, Zeits. f. Physik **86**, 105 (1933).

The Far Ultraviolet Absorption Spectra and Ionization Potentials of Methyl Bromide and Chloride

The absorption spectra of methyl bromide and methyl chloride have been photographed under high dispersion in the region 1800–1000A. The bands in methyl bromide start around 1786A and go to two distinct limits. The strong bands can be arranged in two electronic series. The higher members conform very well to Rydberg formulas and there are only slight deviations in the case of the lower ones. As many as ten series members were observed in each case. The limits of the two series were found to be 85,020 cm^{-1} and 87,590 cm^{-1} corresponding to ionization potentials of 10.488 and 10.805 volts, respectively. The probable error is not greater than 0.002 volt.

In methyl chloride a similar absorption spectrum was found. The strong bands start at about 1400A and go to limits around 1100A. An analysis of the bands showed that they also consist mainly of two electronic series going to the limits 90,520 cm^{-1} and 91,180 cm^{-1} which correspond to the ionization potentials 11.17 and 11.25 volts. On account of the proximity of the two ionization potentials there is a little uncertainty as to the assignment of some of the higher members. However the values given are believed to be correct to 0.01 volt.

Professor R. S. Mulliken has privately informed the author that the difference between the two ionization potentials observed for each of the methyl halides is in each case in excellent agreement with the difference he has calculated on the assumption that the excitation is of a nonbonding $np\pi$ electron.[1] The absence of vibrational pattern accompanying the higher series members is further confirmation that the electrons are of a nonbonding type. However, the actual values of the ionization potentials observed are somewhat lower than those predicted and the author suggests that this may be partly accounted for by the presence of a dipole of about 0.3×10^{-18} e.s.u. in the methyl group.

W. C. Price

Rowland Physical Laboratory,
The Johns Hopkins University,
March 1, 1935.

[1] R. S. Mulliken, Phys. Rev. **47**, 413 (1935).

The Scattering of Protons in Collisions with Neutrons

The scattering of protons and neutrons in their collisions with each other is of importance in connection with one of the most fundamental problems of physics—the nature of the neutron and of the proton, and their relationship to each other and to the negative and the positive electron. The neutron, an atom of zero atomic number,[1] may consist of a proton and a negative electron

$$ {}_0{}^1n_1 \rightarrow {}_1{}^1p_{-1} + {}_{-1}{}^0e_2 $$

as is in agreement with the Harkins[2]-Heisenberg[3] theory of the general composition of atomic nuclei, or a proton may consist of a neutron and a positive electron

$$ {}_1{}^1p_{-1} \rightarrow {}_0{}^1n_1 + {}_1{}^0e_{-2}. $$

On either basis the collision between a proton and a neutron gives a problem similar to that related to H_2^+. There may be scattering, or a deuteron may be formed.

On this basis a neutron-proton exchange reaction is involved, as well as the possibility that in some collisions deuterons are formed.[4] The scattering should be affected by this exchange.

A new neutron source is now being prepared in this laboratory, and this is to be used under conditions which should lead to a better solution of the neutron-proton collision problem. Measurements of the angle θ between the direction of the proton and that of the neutron before impact, have been made for 426 neutron-proton collisions with somewhat larger, and therefore less suitable neutron sources.

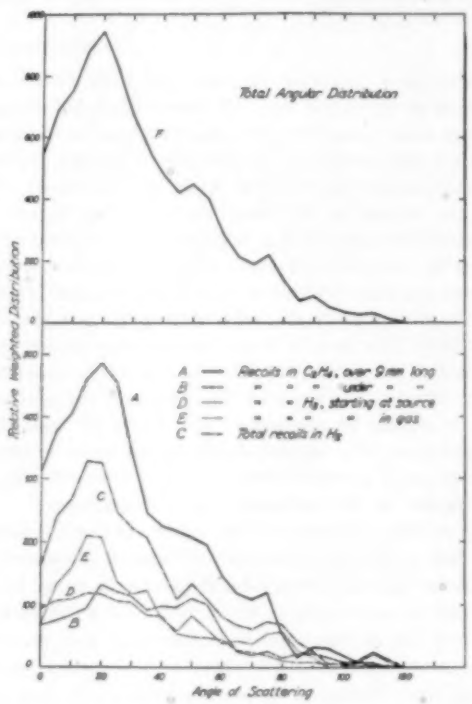
Total Angular Distribution
F
Relative Weighted Distribution
A — Recoils in C_2H_4, over 9 mm long
B — " " " under " "
D — " " H_2, starting at source
E — " " " in gas
C — Total recoils in H_2
Angle of Scattering

FIG. 1.

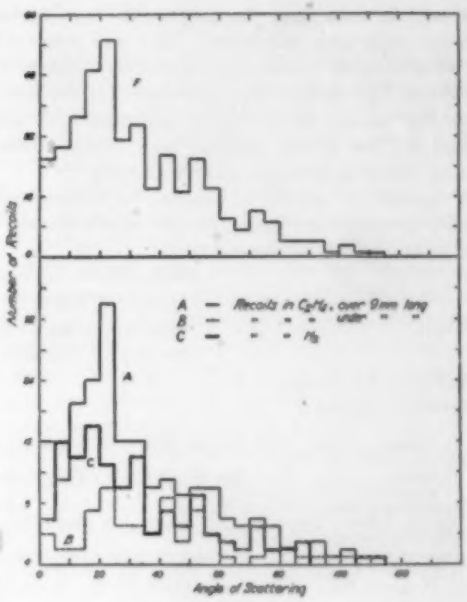

FIG. 2.

For elastic spheres of equal mass the scattering is a maximum at 45°, while Fig. 1 exhibits a maximum at a value of about 20° for θ, the angle between the initial direction of the neutron, and the direction of the proton. For the spheres the distribution is uniform in all directions to an observer at the center of gravity of the system, so that if equal intervals in the value of cos 2θ are taken the number (N) is constant. This is not true for Table I which presents the data of Fig. 1 in this modified form.

TABLE I. *Number (N) of proton tracks per 1000 in each interval of 0.1 in cos 2θ.*
(θ_2 is the value of θ at the end of the interval.)

θ_2	N	θ_2	N	θ_2	N	θ_2	N
12.9	213	33.2	48	47.9	29	63.5	22
18.4	115	36.2	41	50.8	30	67.2	18
22.8	94	39.2	37	53.8	30	71.6	20
26.5	71	42.1	33	56.8	25	77.1	27
30.0	59	45.0	30	60.0	24	90.0	32

To the observer at the center of gravity 770 proton tracks are projected forward and 230 backward. The values of N for the first seven intervals of 0.05 in cos 2θ are 141, 72, 61, 54, 44, 38, 33. Auger[5] and Meitner[6] obtain a scattering which agrees with that for elastic spheres, while that obtained by Kurie[7] is somewhat similar to, though not the same as that found in our experiments.

Fig. 2 gives the number of recoil protons obtained for each interval of 5° in the value of the angle (θ) of scattering.

The values of Fig. 1 were weighted. The neutron source was beryllium mixed with mesothorium for the work in ethylene, and this plus thorium X for that in hydrogen. The diameters of the sources were about 6 mm in ethylene

and 4 mm in hydrogen. To each collision a spread in scattering angle was attributed. This was equal to the angle subtended at the point of impact by a sphere 8 mm in diameter. This makes some allowance for the fact that around the source there was a hemispherical wall of platinum 0.5 cm thick, used to keep x-rays from the chamber, and thus produces some scattering.

The number of points at which the neutron-proton collisions occurred was found to be very nearly proportional to the inverse square of the distance.

WILLIAM D. HARKINS
DAVID M. GANS
MARTIN KAMEN
HENRY W. NEWSON

University of Chicago,
February 25, 1935.

[1] W. D. Harkins, J. Am. Chem. Soc. **42**, 1956 (1920); E. Rutherford, Proc. Roy. Soc. **A97**, 374 (1920).
[2] W. D. Harkins, J. Am. Chem. Soc. **43**, 1038 (1921); W. D. Harkins and S. L. Madorsky, Phys. Rev. **19**, 139 (1922).
[3] W. Heisenberg, Zeits. f. Physik **77**, 1 (1932).
[4] E. Wigner, Zeits. f. Physik **83**, 253 (1933). The writers have discussed this with Professor Guido Beck.
[5] P. Auger and G. Monod-Herzen, Comptes rendus **196**, 1102 (1933).
[6] L. Meitner and K. Philipp, Zeits. f. Physik **87**, 484 (1934).
[7] F. N. D. Kurie, Phys. Rev. **44**, 463 (1933).

The Enhancement of Cosmic-Ray Nuclear Bursts by the Presence of Subsidiary Material

It has been pointed out[1, 2] that cloud-chamber photographs of showers of rays strongly suggest that a shower contains radiation which has the power of creating another shower. Hence it should be possible for the radiation accompanying a shower formed in one body to produce a shower in another body. An experiment to show this phenomenon has been performed. As the first body the water contained in a tank 126 cm in diameter and 150 cm high was employed. Seventy-five centimeters below the tank was placed the second body: a spherical ionization chamber of cast steel of 2.5 cm wall thickness and 14.2 liters capacity, filled with nitrogen to a pressure of 12.5 atmospheres. The number of bursts of ionization greater than 0.45×10^6 ions occurring in the chamber was measured for different thicknesses of water. As the depth of the water was increased, the number of bursts first increased, so that at a thickness of 79 cm of water, the number was about 20 percent greater than at zero thickness. At still greater depths of water, the number of bursts decreased, until, at 136 cm, approximately as many bursts were observed as at zero thickness. This is represented by the center curve of Fig. 1. Some observations were also taken with a slightly higher sensitivity in which bursts greater than 0.35×10^6 ions were measured. The increase between zero and 41 cm of water for these bursts is shown in the upper curve of the figure.

At first glance, the simplest interpretation of these data would seem to be that the additional bursts observed when water was present were bursts of ionizing rays originating in the water and passing through the walls of

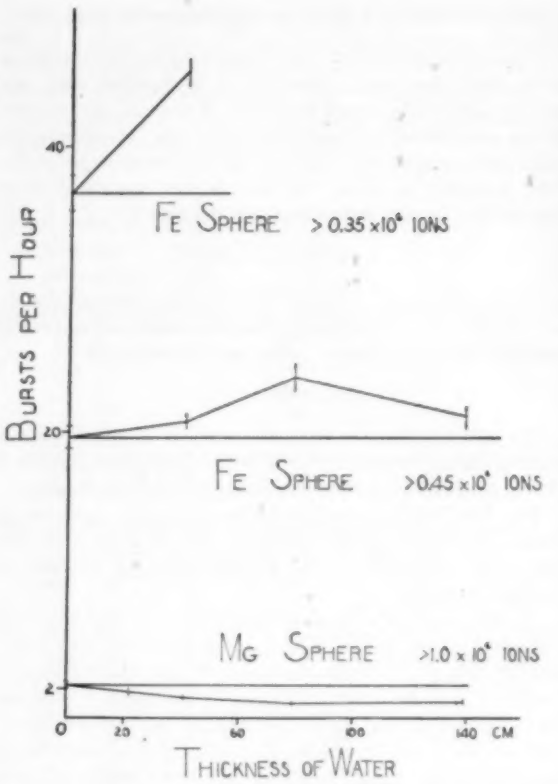

FIG. 1. The rate of occurrence of bursts of ionization in chambers placed below different thicknesses of water. The vertical lines at the observed points represent the standard deviation in the rate computed from the square root of the number of bursts observed.

the ionization chamber despite the large intervening thickness of water and iron. However, when an ionization chamber with one centimeter magnesium walls was substituted for the steel one, the number of bursts decreased uniformly as the depth of the water was increased. These data are shown in the lower curve in the figure. The magnesium chamber had a volume of fifty liters and was filled with nitrogen to a pressure of 14.5 atmospheres. In order to compare its results with those obtained with the steel chamber, bursts of a somewhat larger size should be considered. The size of burst in the magnesium sphere comparable to 0.45×10^6 ions in the steel chamber is 0.78×10^6 ions if we suppose the ionization per centimeter of path should be the same, and 1.84×10^6 ions if the ionization per unit volume should be the same in the two cases. A value between these two, *viz.*, 1.0×10^6 ions, has been chosen for the purposes of this comparison.

The uniform decrease in the number of bursts observed with the magnesium chamber obviously represents the absorption of the primary burst-producing rays. It is of the order of magnitude to be expected from the variation with altitude of the number of bursts in this chamber.[3] There is no evidence of the three or four bursts per hour coming from the water whose occurrence the data taken

with the steel chamber seem to indicate. Thus we must conclude that the additional bursts in the steel chamber originate in its walls, but are occasioned by the presence of the water. The eventual decrease in the number of bursts with increasing thickness of water represents here also the absorption of the primary burst-producing rays.

The initial increase in burst frequency must be produced by some kind of radiation coming from the water. That this radiation is accompanied by a shower of ionizing rays is evidenced by the following experiment. Three Geiger-Müller counters, each of area 109 square centimeters, were placed below the water tank and above the steel sphere in such positions that they would only be simultaneously discharged by at least three ionizing rays. The simultaneous discharges of these three counters were made to light a small lamp which made a trace on the same photographic paper on which was recorded the occurrence of the bursts of ionization. Thus the simultaneous occurrence of a burst and the discharges of the three counters could be recognized. With 41 cm of water in the tank, observations were taken for a period of 10.8 hours. During this time 69 simultaneous discharges of the counters occurred, and 19 of these were coincident with the occurrence of a burst of ionization greater than 0.35×10^6 ions in the steel chamber. Thus the radiation from the water which will produce bursts in the steel chamber walls is accompanied by a shower of ionizing particles.

The authors wish to acknowledge gratefully the financial support of the American Philosophical Society in these experiments.

C. G. MONTGOMERY
D. D. MONTGOMERY
W. F. G. SWANN

Bartol Research Foundation of
The Franklin Institute,
March 4, 1935.

[1] W. F. G. Swann, J. Frank. Inst. **218**, 173 (1934).
[2] C. G. Montgomery, Phys. Rev. **45**, 62 (1934).
[3] C. G. Montgomery and D. D. Montgomery, Phys. Rev. **47**, 429 (1935).

The Liquid State

In the consideration of the application of the third law of thermodynamics to the undercooled liquid state,[1] the writer was impressed by the analogy which holds between the electrons in a metal and the molecules in a liquid. The entropy of a liquid involves a term which depends upon the possibility of the molecules being arranged in different configurations of the same energy. These configurations are in resonance with one another, and the state of the liquid is to be described as a combination of various configurations. The statistics which apply to the molecule are, of course, not the same as for the electron, and the problem of writing the wave functions is even more difficult than in the case of the electron in the metal.

Herzfeld and Mayer[2] have recently discussed the melting of crystals. They consider the impossibility of superheating a crystal to be a unique phenomenon. It is, of course, but the explanation of this behavior is not difficult. The melting point must depend upon the equilibrium between the solid and liquid states, and is, therefore, a measure of the multiplicity of configurations per molecule in the liquid state which correspond to the single configuration in the crystal. Naturally, the entropy of fusion is the greater the more complex the molecule. Superheating does not occur because the heat of activation for fusion is small, presumably no greater than the heat of fusion. In other words, the two states are not separated by a high potential barrier. The situation is quite different with respect to a transition point. Here, for transformation from one crystal form to another, a heat of activation essentially equal to the heat of vaporization is required. If the two crystal forms are brought into intimate contact, the heat of activation is reduced and superheating no longer occurs.

W. H. RODEBUSH

University of Illinois,
February 21, 1935.

[1] W. H. Rodebush, J. Chem. Phys. **2**, 668 (1934).
[2] Herzfeld and Mayer, Phys. Rev. **46**, 995 (1934).

THE AMERICAN INSTITUTE OF PHYSICS

INCORPORATED

GOVERNING BOARD

For The American Physical Society:

KARL T. COMPTON, *Chairman*
Massachusetts Institute of Technology

GEORGE B. PEGRAM, *Secretary*
Columbia University

JOHN T. TATE
University of Minnesota

For The Optical Society of America:

E. C. CRITTENDEN
Bureau of Standards

PAUL D. FOOTE
The Gulf Companies

F. K. RICHTMYER
Cornell University

For The Acoustical Society of America:

HARVEY FLETCHER
Bell Telephone Laboratories

VERN O. KNUDSEN
University of California at Los Angeles

WALLACE WATERFALL
The Celotex Company

For The Society of Rheology:

E. C. BINGHAM
Lafayette College

A. STUART HUNTER
du Pont Rayon Company

S. E. SHEPPARD
Eastman Kodak Company

For The American Association of Physics Teachers:

HOBART L. DODGE
University of Oklahoma

PAUL E. KLOPSTEG
Central Scientific Company

FREDERIC PALMER
Haverford College

ADMINISTRATIVE STAFF

HENRY A. BARTON, *Director* JOHN T. TATE, *Advisor on Publications*

MADELINE M. MITCHELL, *Editorial Secretary*

Office: 11 East 38th Street, New York, New York

JOURNALS

THE PHYSICAL REVIEW

REVIEWS OF MODERN PHYSICS

PHYSICS
JOHN T. TATE, *Editor*
J. W. BUCHTA, *Assistant Editor*
E. C. BINGHAM, *Rheology Editor*

THE JOURNAL OF THE OPTICAL SOCIETY OF AMERICA

THE REVIEW OF SCIENTIFIC INSTRUMENTS WITH PHYSICS NEWS AND VIEWS

F. K. RICHTMYER, *Editor*

JOURNAL OF THE ACOUSTICAL SOCIETY OF AMERICA

F. R. WATSON, *Editor*

THE JOURNAL OF CHEMICAL PHYSICS

HAROLD C. UREY, *Editor*

THE AMERICAN PHYSICS TEACHER

DUANE ROLLER, *Editor*

The American Institute of Physics is a membership corporation of which five societies are the founding members. These five societies are the principal national societies devoted to pure and applied physics in America. Their names, and those of their representatives who form the Governing Board of the Institute, are given above. The principal work of the Institute is the publication of journals sponsored by the societies or by itself. The names and the editors of the journals are also listed above.

The broad purpose of the Institute is to represent, in all matters of wide or common interest, the five thousand or more members and subscribers associated with the Founder Societies and the journals. It aims to advance the science and profession of physics, and to promote cooperation between pure research, the applied sciences and the industries. To achieve these aims, it is greatly in need of an endowment and is empowered by law to administer grants and funds of any kind.

CONTENTS

PHYS. REV. 47 (1935) MARCH 15

Variation with Altitude of the Production of Bursts of Cosmic-Ray Ionization. . . . . C. G. MONTGOMERY AND D. D. MONTGOMERY 429

On the North-South Asymmetry of Cosmic Radiation . . . . . G. LEMAITRE, M. S. VALLARTA AND L. BOUCKAERT 434

Frequency and Magnitude of Cosmic-Ray Bursts as a Function of Elevation. . . . RALPH D. BENNETT, GORDON S. BROWN AND HENRY A. RAHMEL 437

Absorption Spectra of Acetylene, Ethylene and Ethane in the Far Ultraviolet. . . . . W. C. PRICE 444

Artificial Radioactivity Produced by the Deuteron Bombardment of Nitrogen. . . . . EDWIN MCMILLAN AND M. STANLEY LIVINGSTON 452

Note on the Spectrum of Boron Fluoride . . . . . RAYMOND B. DULL 458

Electrical and Impact Phenomena in the Faraday Dark Space . . . . . K. G. EMELEUS AND O. S. DUFFENDACK 460

Probability of Collision for Slow H^+, $(H^2H^1)^+$, $(H^2H^2)^+$, $(H^2H^3)^+$, $(H^3)^+$ and He^+ Ions in Argon . . . . . EDWARD B. JORDAN 467

Radioactivity Produced in Neon and Helium by Irradiation with Their Own Resonance Radiations and the Effect of Foreign Gases on This Conductivity . . . . . R. W. SMITH AND O. S. DUFFENDACK 473

Theory of Electrical Double Layers in Adsorbed Films . . R. W. GURNEY 479

Ionization of Inert Gases by Positive Alkali Ions . . ROBERT N. VARNEY 485

Rotational Energy of Polyatomic Molecules . . . . J. H. VAN VLECK 487

On the Plasticity of Crystals . . . . . POL. DUWEZ 494

Photoelectric Properties of the (100) and (111) Faces of a Single Copper Crystal . . . . . NEWTON UNDERWOOD 502

Letters to the Editor:

Induced Radioactivity Using Carbon Targets . L. R. HAFSTAD AND M. A. TUVE 506

Resonance Transmutations by Protons . . L. R. HAFSTAD AND M. A. TUVE 506

Radiative Capture of Protons by Carbon . . . C. BOCKE AND F. L. YOST 508

Hyperfine Structure of Y II Lines . . . . . P. GERALD KRUGER AND C. N. CHALLACOMBE 509

Ionosphere Studies . . . . . E. B. JUDSON 509

Resonance Collision Cross Sections for Slow Neutrons . . . . . G. BECK AND L. H. HORSLEY 510

The Ultraviolet Absorption Spectra and Ionization Potentials of Methyl Bromide and Chloride . . . . . W. C. PRICE 510

Scattering of Protons in Collisions with Neutrons . . WILLIAM D. HARKINS, DAVID M. GANS, MARTIN KAMEN AND HENRY W. NEWSON 511

Enhancement of Cosmic-Ray Ionization Bursts by the Presence of Subsidiary Material. C. G. MONTGOMERY, D. D. MONTGOMERY AND W. F. G. SWANN 512

Liquid State . . . . . W. H. ROSENBURG 513

LANCASTER PRESS, INC., LANCASTER, PA.